# DINOFLAGELLATE CYSTS FROM THE LATEST MIOCENE THROUGH MIDDLE PLEISTOCENE OF THE CARIBBEAN SEA, ODP SITE 1000: BIOSTRATIGRAPHY, PALEOCEANOGRAPHY, AND SHOALING OF THE CENTRAL AMERICAN SEAWAY

**Masoumeh ("Mehrsa") Mahdavijourshari**

**Department of Earth Sciences**

**A thesis submitted in partial fulfillment of the requirements for the degree of M.Sc. in Earth Sciences**

**Faculty of Mathematics and Science, Brock University**
**St. Catharines, Ontario**

**ABSTRACT**

This is the first detailed study of organic-walled dinoflagellate cysts (dinocysts) and acritarchs for the latest Miocene–Middle Pleistocene of Ocean Drilling Program Site 1000 in the Caribbean Sea. Well-preserved and moderately diverse dinocysts and other palynomorphs reflect the interplay between neritic (carbonate-platform sourced) and oceanic species. The dinocyst biostratigraphy is tied to an existing marine isotope stratigraphy for the interval 5.5–2.2 Ma. For the interval 5.5–3.8 Ma, palynological samples are coupled to published sea-surface temperature estimates based on planktonic foraminiferal Mg/Ca. Changes in dinocyst assemblage composition are noted at ca. 4.6 Ma when shoaling of the Central American Seaway caused a temperature rise in the Caribbean, ca. 3.8–3.6 Ma, during the cold Marine Isotope Stage M2 when pronounced warming occurred, at ca. 2.7 Ma where possible weak cooling may reflect the onset of Northern Hemisphere glaciation, and in the Middle Pleistocene presumably reflecting global cooling and sea-level fall.

**DEDICATION**

This thesis is dedicated to my parents and memory of my loving friend

Dr. Maryam Shakiba

who encouraged me to pursue my studies

**ACKNOWLEDGEMENTS**

The development and completion of this thesis would not have been possible without the input and support of numerous individuals. I would like to express my deepest gratitude and appreciation to my supervisor, Professor Martin J. Head, for his knowledge, guidance and mentorship. He accepted and motivated me with incredible patience and attention when I was going through an extremely difficult and stressful period. He offered me an interesting project and supported me in every step of the work. It has truly been an honour for me to complete my Master's project under his supervision. My sincerest gratitude also to Professor Liette Vasseur for extremely helpful assistance with the statistical analysis; Professor Rick Cheel, for his strong continued support, for which I am eternally grateful; Professor Uwe Brand for his valuable guidance and advice; and Gail Pepper, Joanne Kremble and Charlotte Sheridan (all of the Faculty of Graduate Studies) for administrative support. The Integrated Ocean Drilling Program provided the samples. Financial support was provided by the Department of Earth Sciences and by an NSERC Discovery Grant to Professor Head. Finally, I wish to thank my loving parents and friends for their understanding, encouragement and continuous support during my entire education.

**TABLE OF CONTENTS**

**1. INTRODUCTION** ..... 1

**2. RESEARCH OBJECTIVES** ..... 2

**3. LITERATURE REVIEW** ..... 3

3.1 Atlantic Ocean and North Atlantic thermohaline circulation ..... 3

3.2 Caribbean hydrography and oceanography ..... 7

3.3 Caribbean and eastern Pacific gradients ..... 11

3.4 Tectonic evolution of the CAS ..... 12

3.5 Hypotheses for shoaling and closure of the CAS ..... 15

3.5.1 Vertebrate distribution patterns from North to South America ..... 15

3.5.2 Microfossil assemblages from both sides of the CAS ..... 17

3.5.3 Geochemical proxies ..... 18

3.6 Dinocysts ..... 24

3.7 The Pliocene ..... 25

3.8 Hypotheses for the NHG ..... 27

3.9 Previous dinocyst studies ..... 34

3.9.1 High to mid–latitude North Atlantic region ..... 34

3.9.2 Gulf of Mexico and Caribbean region ..... 35

3.9.3 Europe, North Sea, and Mediterranean Sea ..... 36

3.10 Geological setting of ODP Site 1000 ..... 36

3.11 Age model of ODP Site 1000 ..... 41

**4. MATERIAL AND METHODS** ..... 43

4.1 Sample selection ..... 43

4.2 Palynological processing and counting ..... 44

4.3 Statistical analysis ..... 45

**5. RESULTS** ..... 46

5.1 Composition of palynological assemblages ..... 46

5.1.1 Upper Miocene (Messinian, 5.5–5.4 Ma) ..... 47

5.1.2 Lower Pliocene (Zanclean, 5.3–3.6 Ma) ..... 47

5.1.3 Upper Pliocene (Piacenzian, 3.5–2.6 Ma) ..... 48

5.1.4 Lower and Middle Pleistocene (2.5–0.2Ma) ..... 49

5.2 Results of statistical analysis ..... 53
5.2.1 Dinocyst assemblage biozonation and CCA ..... 55
**6. DISCUSSION** ..... 58
6.1 Biostratigraphy ..... 58
6.1.1 Ecostratigraphy ..... 58
6.1.2 Traditional biostratigraphy ..... 58
6.1.3 Biostratigraphic summary ..... 63
6.2 Paleoenvironmental evolution of Site 1000 ..... 64
**7. SITE 1000 COMPARED WITH OTHER PUBLISHED DINOCYST RECORDS** ..... 69
**8. REGIONAL AND GLOBAL CONTEXT** ..... 70
**9. SUMMARY AND CONCLUSIONS** ..... 75
**REFERENCES** ..... 76

**LIST OF FIGURES**

**Figure 1.** Bathymetry of the Atlantic Ocean; regions less than 3000 m deep are stippled (from Tomczak and Godfrey, 1994)…….. . 4

**Figure 2A.** The Ocean Conveyor Belt, driven by differences in temperature and salinity (from Haug et al., 2004)..... 6

**Figure 2B.** The general surface circulation of the North Atlantic (from Rahmstorf, 2002)……..... 6

**Figure 2C.** Surface and deep water circulation patterns (from Dwyer and Chandler, 2009)…..... 7

**Figure 3.** Overview of the Caribbean Sea (from Wessel & Smith, 1991; Sigurdsson et al., 1997)…….. ..... 9

**Figure 4.** Modern oceanographic configuration of the tropical western Atlantic and eastern Pacific (from Steph et al., 2006)…… ..... 10

**Figure 5.** Modern hydrography in the Caribbean and the east Pacific (from Groeneveld, 2005)……...11

**Figure 6.** A schematic representation of the gradual closure of the CAS from the Late Miocene (~10 Ma) to present (modified from Haug et al., 2004)…….. . ..12

**Figure 7.** Tectonic evolution of the Central American Isthmus (modified from Coates et al., 2004)……...14

**Figure 8.** A schematic illustration of the glacial closure of the Panamanian Gateway (from Webb, 1997)……... 16

**Figure 9.** Southern Central America and northwestern South America in the early Middle Miocene (modified from LIoyd, 1998). ..... 16

**Figure 10.** Sea surface water properties ($SST_{Mg}$/Ca, $\delta^{18}O$ *Globigerinoides sacculifer*, $\delta^{18}O$ water, $\delta^{18}O$ water-gradient, and $\delta^{18}O$ salinity) for the Caribbean (Sites 999 and 1000) and the tropical east Pacific (Site1241) (from Groeneveld, 2005)……...20

**Figure 11.** Locations of ODP Sites from equatorial Atlantic and Pacific (from Billups et al., 1999)..... 22

**Figure 12.** Oxygen isotope data from Caribbean ODP Site 999 and eastern Pacific ODP Site 851 (modified from Haug et al., 2001)…….23

**Figure 13.** Time scale, including palaeomagnetic reversals and the LR04 benthic isotope stack at ODP Site 999 (from De Schepper et al., 2013, and references therein)…… ... 26

**Figure 14.** The closing of CAS, strengtheningof the North Atlantic thermohaline circulation, and development of the NHG (from Haug et al., 2005)……27

**Figure 15.** Timing of key geological events and closure of the Tethyan Seaway (modified from Zhang et al., 2011)……..28

**Figure 16.** Ice-sheet configurations on Greenland (modified from Lunt et al., 2008) ……..29

**Figure 17.** North Atlantic palaeoceanographic proxy records between 3.40 and 3.18 Ma (from De Schepper et al., 2013)……..31

**Figure 18.** Caribbean Sea palaeoceanographic records from ODP Site 999 between 3.40 and 3.18 Ma (from De Schepper et al., 2013 and references therein)…… ..... 32

**Figure 19.** Model for glaciation and deglaciation of the Northern Hemisphere during MIS M2 in the Late Pliocene (from De Schepper et al., 2013)…… 33

**Figure 20.** Location of ODP Site 1000 in the Pedro Channel, Caribbean Sea (modified from Sigurdsson et al., 1997)..... 37

**Figure 21.** Carbonate preservation at Site 1000 compared with other ODP sites in Caribbean Sea (modified from Sigurdsson et al., 1997)..... 37

**Figure 22.** Site 1000 summary column (modified from Sigurdsson et al., 1997 and not updated)…. ..... 39

**Figure 23.** Lithologic units of Site 1000 (Holes 1000A and 1000B) (from Sigurdsson et al., 1997 and not updated)..... 40

**Figure 24.** Benthic $\delta^{18}O$ records of tropical east Pacific (Tiedemann et al., 2006) and western Atlantic (Bickert et al., 1997; Tiedemann and Franz, 1997; Shackleton and Hall, 1997) correlated to benthic $\delta^{18}O$ records from Caribbean (Haug and Tiedemann, 1998) (from Steph et al., 2006)……...42

**Figure 25.** Planktonic foraminiferal Mg/Ca results for ODP Site 1000 for the time interval 5.6 Ma to 3.9 Ma, allowing reconstructing of SST and Sea Surface Salinity (SSS). (from Groeneveld et al., 2008)……..... 43

**Figure 26.** Ratios of pollen+spore/dinocyst, oceanic/total dinocysts and heterotrophic/autotrophic dinocysts throughout the studied interval (5.5–0.2 Ma)…….51

**Figure 27.** Relative abundances of dinocyst taxa recovered in this study……..52

**Figure 28.** Relative abundances of acritarch taxa recovered in this study (based on percentage of totalacritarchs)……53

**Figure 29.** Selected dinocyst taxa (as percentage of total palynomorphs) compared with the Mg/Ca-based SST from the Upper Miocene to Lower Pliocene (5.6–3.9 Ma)……..……54

**Figure 30.** Six dinocyst (DAZ 1–6) assemblage biozones identified using constrained cluster analysis (dinocyst taxa only)……...57

**Figure 31.** Correlation between the marine isotope stages (Steph et al., 2006) and samples (this study) from Site 1000 for the interval 5.5–2.2 Ma.…… 74

## LIST OF TABLES

**Table 1.** Astronomical age estimates of calcareous nannofossil biohorizons and ages of stage boundaries in the interval 1.8–0.2 Ma (from Raffi et al, 2006 and references therein)……. ...41

**Table 2.** Foraminiferal data (from Groeneveld et al., 2008)…….44

**Table 3.** Stratigraphic distributions of dinocysts, acritarchs and other palynomorphs recorded in the ODP Site 1000 from the latest Miocene–Middle Pleistocene (this study)……118

## APPENDIXES

**Appendix 1.** List of recorded dinocysts and acritarchs from ODP Site 1000 ..... 103

**Appendix 2.** Taxonomy of new dinocysts and achritarchs from ODP Site 1000..... 105

**Appendix 3.** Plates ..... 108

## LIST OF ABBREVIATIONS

AABW: Antarctic Bottom Water

AAIW: Antarctic Intermediate Water

CAS: Central American Seaway

CCA: Constrained cluster analysis

DSDP: Deep Sea Drilling Project

IODP: Integrated Ocean Drilling Program

mbsf: metres below sea-floor

MIS: Marine Isotope Stage

NADW: North Atlantic Deep Water

NHG: North Hemisphere Glaciation

ODP: Ocean Drilling Program

SST: Sea-Surface Temperature

SSS: Sea-Surface Salinity

## 1. INTRODUCTION

Considering the ongoing threat of global warming to modern life, it is essential to understand the causes of climate change and shifts in ocean dynamics. The Late Cenozoic provides a basis for interpreting the process of changing global climate from that of a greenhouse to icehouse world. The Neogene Period, commencing 23.03 Ma, was followed by the Quaternary period at 2.58 Ma (Head et al., 2008; Gibbard and Head, 2010), which broadly represents the transition to a glacially dominated climate. The Pliocene Epoch (5.33–2.58 Ma) is considered a "Time of Change" (Wrenn et al., 1999) and can be viewed as a transition from a warm "El Niño-like state" to a cold "La Niña-dominated state".

The early Late Pliocene (Early Piacenzian, 3.6–3.0 Ma) is the most recent interval in Earth's history when global climate was warmer than today. The Mid–Piacenzian warm period (ca. 3.3–3.0 Ma) is considered a possible near future analog (e.g., Chandler et al., 1994; Dowsett et al., 2009; De Schepper et al., 2013) whereby we are shifting towards a Mid-Piacenzian overall pattern of North Atlantic surface paleoceanography. The warm stable climate of the Early Piacenzian was suspended by a brief, intense global glaciation (3.305–3.285 Ma) during marine isotope stage (MIS) M2 (e.g., De Schepper et al., 2009; 2013). The gradual shoaling and closure of the Central American Seaway (CAS) during the Pliocene has been linked to dramatic changes in North Atlantic paleoceanography and North Hemisphere Glaciation (NHG) and has left a profound signature at Ocean Drilling Program (ODP) Leg 165 Site 1000, Caribbean Sea. However, the influence of the gradual shoaling (e.g., Groeneveld et al., 2008) and closure (e.g., Haug et al., 2004) of the CAS on the Pliocene NHG is still under debate (e.g., Bartoli et al., 2005; Lunt et al., 2008; De Schepper et al., 2013).

Dinoflagellate cysts (hereafter "dinocysts") are sensitive paleoceanographic and paleoclimatic tracers for the Pliocene. However, the stratigraphic record of Late Cenozoic dinocysts at low latitudes is not well known. This research explores these microfossils and their response to paleoceanographic changes at ODP Site 1000, Caribbean Sea, an important location for understanding the development of North Atlantic ocean circulation and climate change during the Late Miocene–Middle Pleistocene (5.5–0.2 Ma). The site, characterized by periplatform carbonates, has the advantage of an independent chronostratigraphy tied to marine isotope stratigraphy, and a record of foraminiferal Mg/Ca paleotemperatures to complement paleoenvironmental interpretations based on the dinocyst analyses.

## 2. RESEARCH OBJECTIVES

The goal of this research is to improve insight in the following domains:

- Paleoceanography. Upper Miocene–Middle Pleistocene deposits from the Caribbean Sea ODP Site 1000 have been analysed palynologically, with focus on the dinocysts, to explore paleoceanographic changes and their link to the closure of the CAS.
- Biogeography. This study documents in detail the Upper Miocene–Middle Pleistocene dinocyst record of the Caribbean Sea, as a contribution to the relatively understudied field of Neogene low-latitude dinocyst research. This will help close an important gap in our understanding of the latitudinal control on assemblages.
- Biostratigraphy. Site 1000 has a marine isotope stratigraphy for the interval 5.5–2.2 Ma (Steph et al., 2006) and nannofossils control for the interval 1.8–0.2 Ma (Kameo and Sato, 2000; Raffi et al., 2006) which potentially allowing the construction of an independently-calibrated biostratigraphy for the Caribbean Sea based on dinocysts.
- Paleoecology. The samples are coupled to foraminiferal Mg/Ca paleotemperature study for this site up to 3.8 Ma (Groeneveld et al., 2008), providing an opportunity to link palynological assemblages quantitatively to a reliable proxy for SST, and gain insights into the paleoecology of tropical dinocysts. Geochemical and palynological results, including the statistical analysis of dinocysts taxa, are discussed.
- Taxonomy. This study documents the assemblages taxonomically and informally describes several new dinocyst and acritarch species.

## 3. LITERATURE REVIEW

### 3.1 Atlantic Ocean and North Atlantic thermohaline circulation

Initiated during the Jurassic (www.Scotese.com), the Atlantic Ocean (Figure 1) is the second largest ocean in the world covering approximately 22% of Earth's surface. The Atlantic Ocean has an average depth of 3300 m, somewhat shallower than the Pacific and Indian oceans. It is divided by the Mid-Atlantic Ridge where the depth rises to less than 2000 m and consequently has a strong impact on deep layer circulation (e.g., Schnitker, 1980; Tomczak and Godfrey, 1994). The North Atlantic Ocean is characterized by two gyres, the subtropical gyre and the subpolar gyre between which flows the North Atlantic Current.

The ocean propagates in a nonlinear global thermohaline circulation, driven by wind and differences in water-mass density that convey heat and moisture around the entire planet. This circulation is also referred to as the Great Ocean Conveyor Belt or the Meridional Overturning Circulation (Figure 2A, 2B, e.g., Broecker and Denton, 1989; Haug et al., 2004). Present-day thermohaline circulation comprises warm, saline surface water from the Caribbean, the Gulf of Mexico, and the equatorial Atlantic, which then flows into the North Atlantic Ocean. This northward surface current originates with the Florida Current, which flows between the Florida Straits and Cape Hatteras. Thereafter, the current diverts from the continental shelf, becomes the Gulf Stream, and continues as the North Atlantic Current (Williams et al., 2008; Meinen et al., 2009). The major warm surface currents in the North Atlantic are the Gulf Stream, North Atlantic Current, and Continental Slope Currents which make the northeastern Atlantic warmer than comparable latitudes in the northern Pacific. The North Atlantic Current is the largest and most well-known of the western boundary currents. It flows northeastwards along the east side of the Grand Banks and plays a significant role in the transport of warm and saline tropical waters to the higher latitudes; thus controlling the growth of ice sheets and influencing global climate (e.g., Hansen and Østerhus, 2000). These waters are cooled by contact with cold air masses near Iceland and the Labrador Sea, with heat and moisture being recruited into the atmosphere. The result is a cold, salty and thus dense, water mass that sinks to the ocean floor. The major hydrology of the North Atlantic Ocean is affected by the formation and recirculation of North Atlantic Deep Water (Figure 2C) that is characterized by high salinity, a low nutrient content, and high $^{13}C/^{12}C$ values, creating a southward flow in the Atlantic at a depth of 2–4 km. When North Atlantic Deep Water reaches Antarctica, it is diverted to the east by the Antarctic Circumpolar Current and joins the Antarctic Bottom Water. The deep-water current eventually returns to the surface in the Indian and Pacific oceans because of mixing with warmer waters and upward wind-

driven circulation gyres, and finally flows back into the Atlantic Ocean to complete the circulation loop (Ruddiman, 2008).

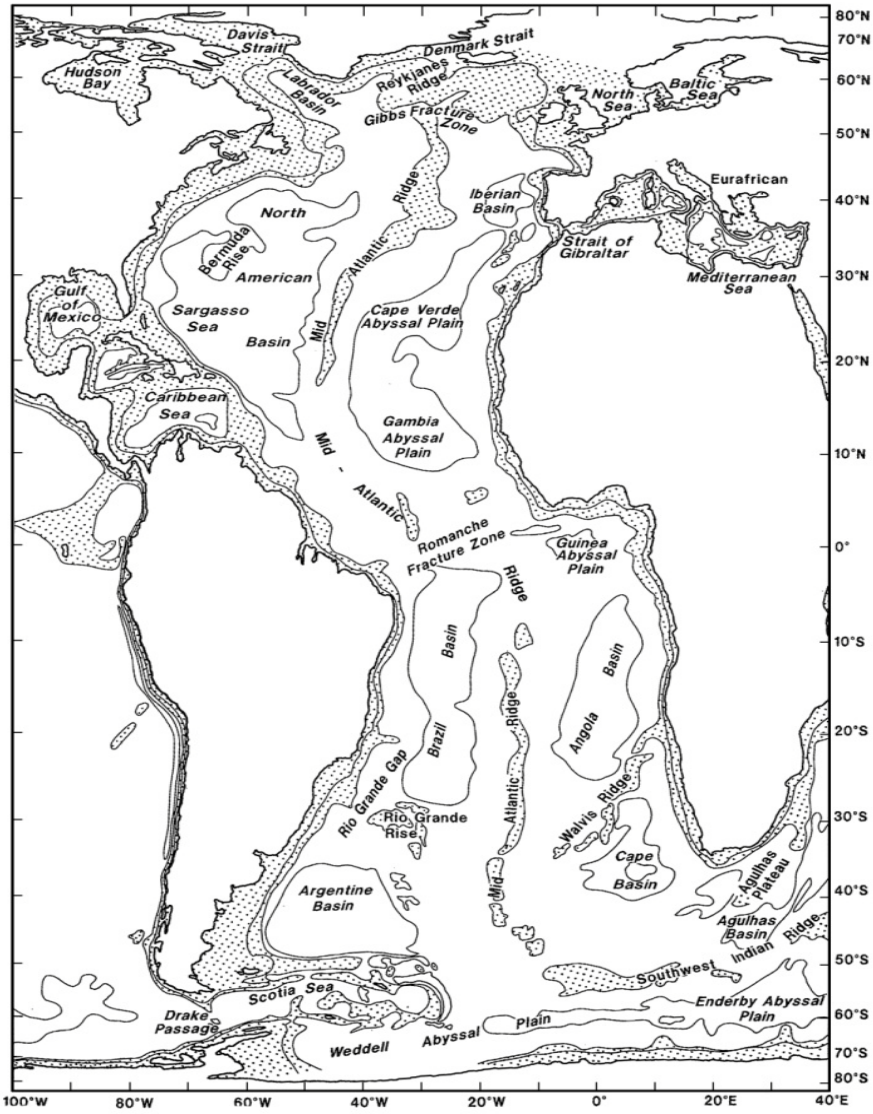


**Figure 1.** Bathymetry of the Atlantic Ocean; regions less than 3000 m deep are stippled (from Tomczak and Godfrey, 1994).

Antarctic Bottom Water has a somewhat similar origin to that of North Atlantic Deep Water; it results from sea water freezing and the formation of sea ice in the Weddell Sea, causing cold, dense water to descend to the ocean floor. This water travels far into the North Pacific and Atlantic at depths of about 2–5 km and competes with southward-penetrating North Atlantic Deep Water. This circulation pattern is driven by the difference in salinity and temperature between the Atlantic and Pacific oceans (Renterghem, 2012). Evaporation in the tropical Atlantic results in elevated salinities, and the transport of fresh water to the Pacific by the Trade Winds

causes the Pacific to become fresher than the Atlantic Ocean. Surface waters in the Atlantic are, on average, one salinity unit more saline than those in the Pacific Ocean, and have a temperature difference of +3–4°C. This density contrast is critical for deep water formation; while temperatures of about +2°C are sufficient for dense Atlantic Ocean water to sink to the bottom; Pacific waters are required to be cooled below freezing point just to penetrate a few hundred meters before their buoyancy limit is reached (Broecker, 1991; Broecker and Denton, 1989). Therefore, deep-water formation in the Pacific is severely limited.

Coupled ocean–circulation models have been applied to demonstrate that thermohaline circulation is the major factor responsible for North Atlantic warming. A dynamic conveyor belt induces a temperature rise of up to 5°C. These results suggest that during glacial periods the ocean conveyor belt was weakened or even switched off. However, dilution of dense surface North Atlantic water through ice melting, precipitation and continental runoff imposes a severe threat to the conveyor belt (e.g., Manabe and Stauffer, 1988; Broeker, 1991; Steph et al., 2006; De Schepper et al., 2009; Rayner et al., 2011; De Schepper et al., 2013).

The North Atlantic Ocean has experienced dramatic changes to its cryosphere and is considered to be the World's most climatically sensitive region (e.g., Stein et al., 2006). The major hydrology of the North Atlantic Ocean is affected by the formation and recirculation of North Atlantic Deep Water. Today, the arctic domain is considered the main region where North Atlantic deep water is formed (e.g., Pflaumann et al., 2003).

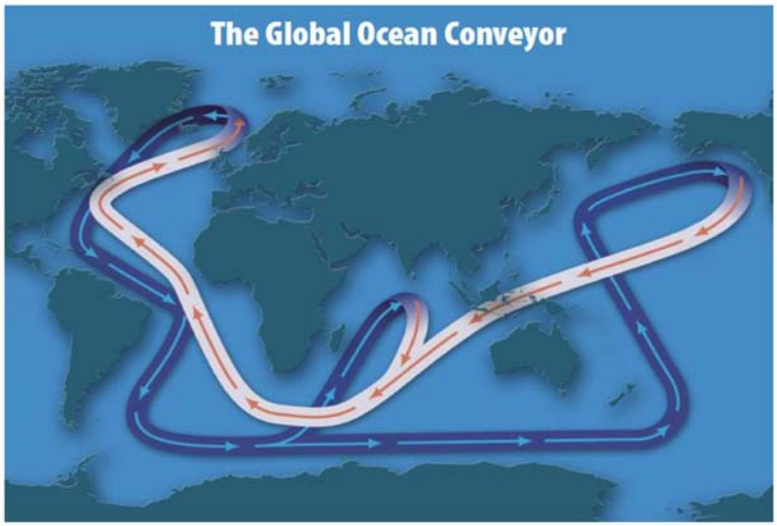


**Figure 2A)** The Ocean Conveyor Belt, driven by differences in temperature and salinity (from Haug et al., 2004).

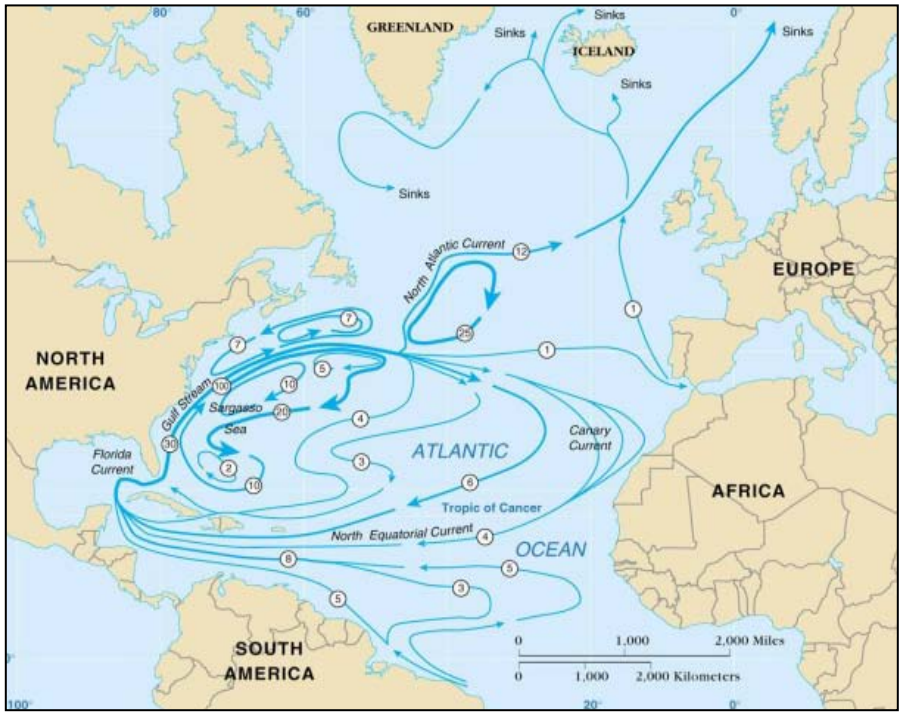


**Figure 2B)** The general surface circulation of the North Atlantic. The numbers indicate flow rate in sverdrups (1 sv =1 million) cubic meters of water per second (from Rahmstorf, 2002).

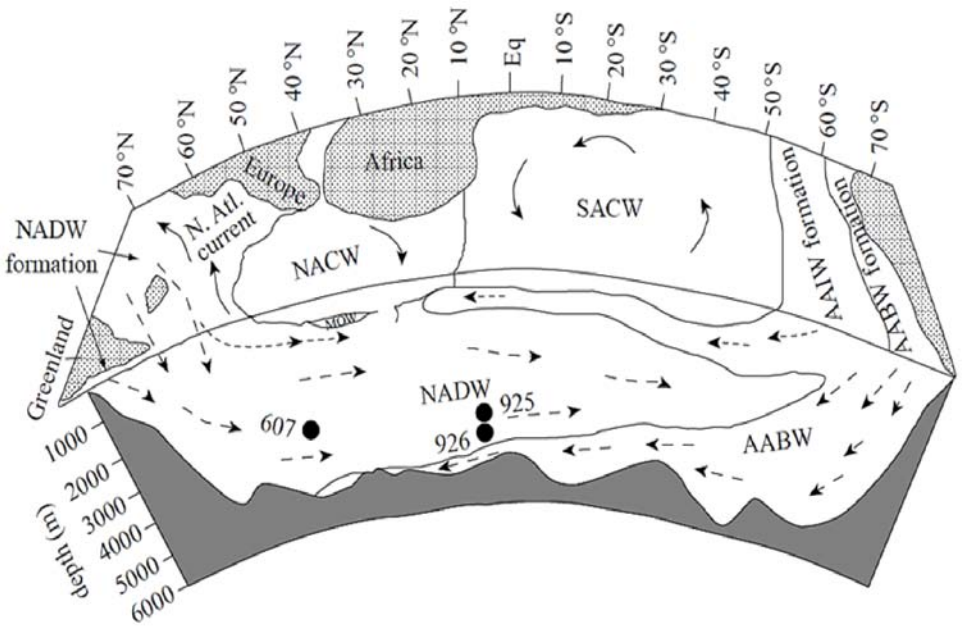


**Figure 2C)** Surface and deep water circulation patterns. Abbreviations are NADW: North Atlantic Deep Water, NACW: North Atlantic Central Water, MOW: Mediterranean Outflow Water, SACW: South Atlantic Central Water, AAIW: Antarctic Intermediate Water, and AABW: Antarctic Bottom Water (from Dwyer and Chandler, 2009).

### 3.2 Caribbean hydrography and oceanography

The Caribbean Sea is important for studying a wide array of geological questions due to its relatively uncertain plate tectonic evolution and important role in global ocean circulation and climate change. The Caribbean is a large igneous province forming multi-layer thick oceanic crust stretching from across the Colombian Basin, Venezuelan Basin, and to the Beata Ridge where it reaches its thickest point (Diebold, 2009).With the exception of Deep Sea Drilling Project (DSDP) Site 502, the Caribbean had not been targetted by the DSDP or ODP for more than two decades when ODP Leg 165 commenced. Drilling at five ODP sites (Figure 3) provided an excellent opportunity to analyze nearly 90 myr of Earth's record. These locations include the Cayman Rise ODP Site 998, Colombian Basin ODP Site 999, Nicaraguan Rise ODP Site 1000, lower Nicaraguan Rise ODP Site 1001, and Cariaco Basin ODP Site 1002 (Sigurdsson et al., 1997). The late Neogene ocean circulation and climate change are intimately linked to the tectonic history of the Caribbean and closure of the CAS (e.g., Duque-Caro, 1990).

The Caribbean Sea is a major source region for the Western Boundary Current and performs an important role in the net export of heat and salt into high northern latitudes. In the modern Caribbean Sea (Figure 4), the uppermost part of the water column in the southern Caribbean consists of relatively fresh (<35.5‰) Caribbean Water (0–80 m) and highly saline (>37‰) Subtropical Under Water (80–180 m) which forms the permanent Caribbean thermocline

(Wüst, 1964). Caribbean Water comprises a mixture of Amazon and Orinoco river outflow and equatorial Atlantic surface water that mostly enters the Caribbean via the Guyana Current through the Lesser Antilles Passages. The highly saline Subtropical Under Water, formed by excess evaporation in the subtropical gyre, enters the Caribbean mostly via the North Equatorial Current through the Greater Antilles Passages (Windward and Mona passages) (Wüst, 1964; Johns et al., 2002). The above mentioned water masses make up the Caribbean Current that passes through the Yucatan Channel and the Florida Straits, where it combines with the Antilles Current to form the Western Boundary Current (Steph et al., 2006). As part of the Tropical Western Hemisphere Warm Pool, together with the Gulf of Mexico and the western tropical Atlantic, modern Caribbean annual mean SSTs reach at least 28.5°C (Wang and Enfield, 2001; Wang and Lee, 2007). High solar radiation fluxes and a closed basin setting where warm water can be collected are responsible for the formation of this warm water body.

Considerable quantities of Amazon freshwater are passed northwestward and can be traced into the central Caribbean Sea to about 70°W (Hellweger and Gordon, 2002). However, the largest river discharging directly into the western Caribbean is the Magdalena River, but its absolute volume is trivial in comparison with the freshwater provided by the Orinoco and Amazon rivers. Moreover, adding to the influence of the Amazon and Orinoco rivers, Caribbean sea surface salinity (SSS) is controlled by various factors including the seasonal position of the tropical rain belt that follows the Intertropical Convergence Zone and controls the seasonal evaporation/precipitation ratio (Hellweger and Gordon, 2002).

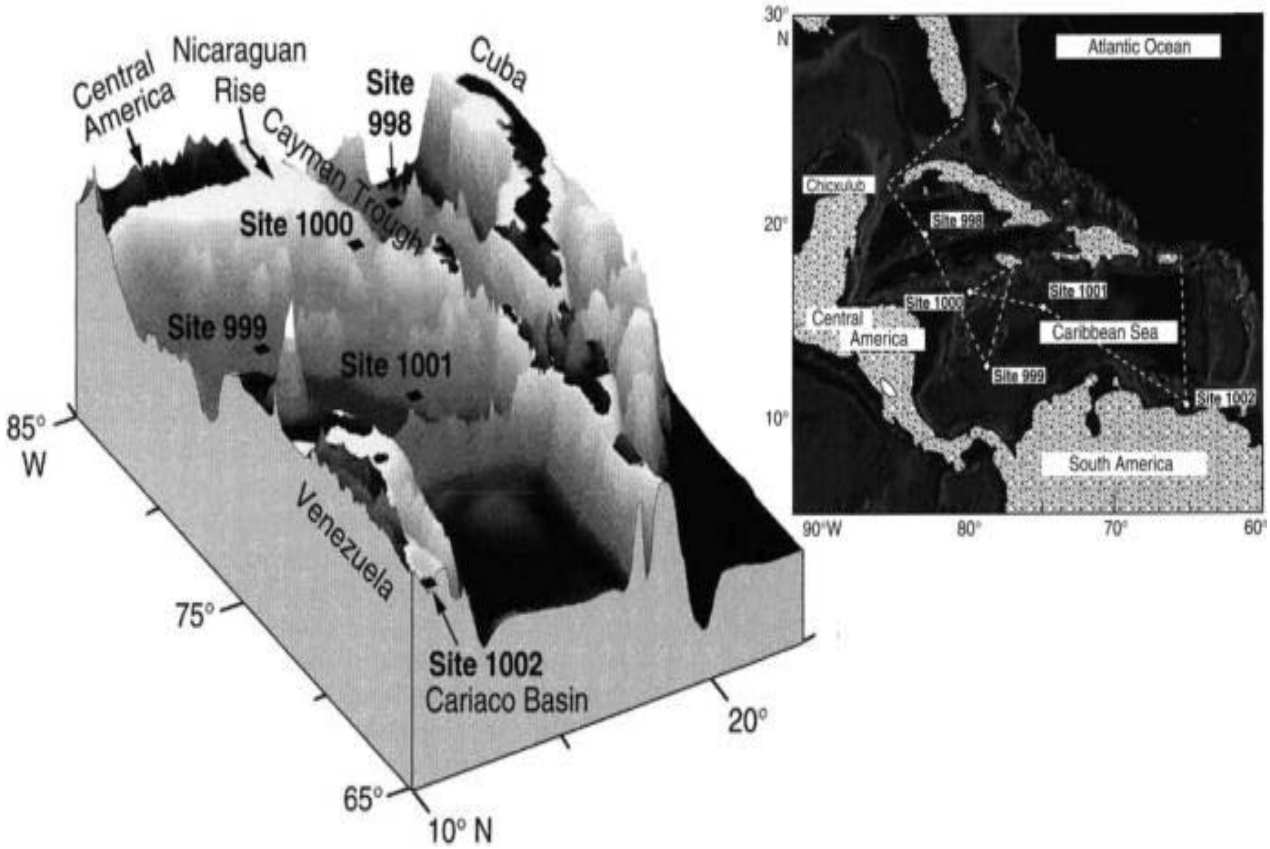


**Figure 3.** Overview of the Caribbean Sea and location map of ODP Leg 165 sites (from Wessel & Smith, 1991; Sigurdsson et al., 1997).

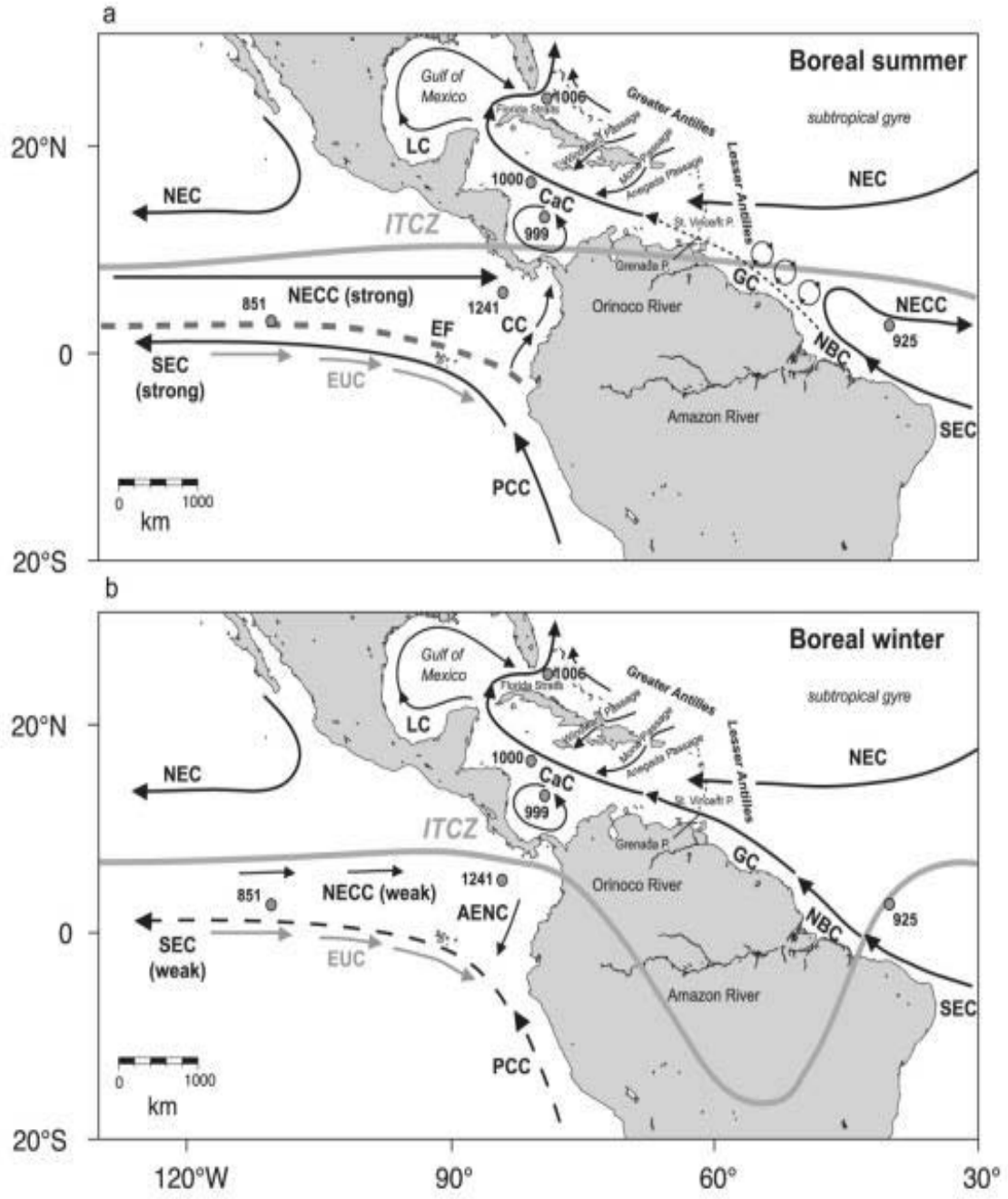


**Figure 4.** Modern oceanographic configuration of the tropical western Atlantic and eastern Pacific displaying surface currents (from Steph et al., 2006). **a)** Scenario during boreal summer with the ITCZ at its northernmost position. The Atlantic SEC is retroflected toward the east. **b)** Scenario during boreal winter with the ITCZ at its southern position. The Atlantic GC enters the Caribbean via the Lesser Antilles Passages. Abbreviations are NEC, North Equatorial Current; NECC, North Equatorial Counter Current; SEC, South Equatorial Current; NBC, North Brazil Coastal Current; GC, Guyana Current; CaC, Caribbean Current; LC, Loop Current; PCC, Peru-Chile Current; CC, Colombia Current; EUC, Equatorial Undercurrent; AENC, Annual El Ninõ Current; EF, Equatorial Front; and ITCZ, Intertropical Convergence Zone.

### 3.3 Caribbean and eastern Pacific gradients

The restricted exchange of sea surface waters has led to the establishment of the modern Atlantic/Pacific SST and SSS, a reflection of the North Atlantic Ocean as a warmer and more saline region (Figure 5). The eastern Pacific and Caribbean are characterized by distinctly increasing salinity and temperature gradients with depth (Figure 5). Upwelling along the Peruvian coast and the Equator, caused by Southeastern Trade Winds (Figure 6), forms the Pacific Cold Tongue, which reduces the Pacific thermocline depth to less than 50 m (Mitchell and Wallace, 1992). Accordingly, the temperature contrast between both basins at this depth is around 5°C, while surface temperature differences remain similar (Levitus and Boyer, 1994a, 1994b). A salinity difference of more than 1‰ exists between the Atlantic and the eastern Pacific, caused by an excessive evaporation in the Caribbean. This water vapour is subsequently transported into the Pacific via the prevailing Easterly Trade Winds, hence creating a salinity gradient either side of Central America (Broecker and Denton, 1989).

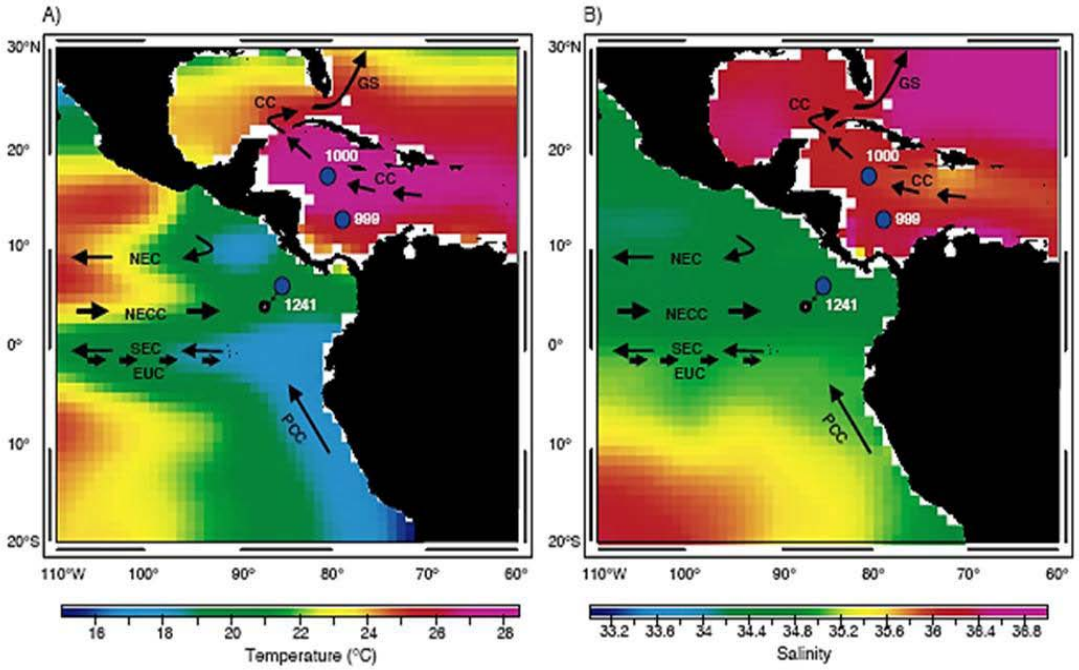


**Figure 5.** Modern hydrography in the Caribbean and the east Pacific, showing annual average sea water temperatures **(A)** and salinities **(B)** at a water depth of 50 m (from Levitus and Boyer, 1994), corresponding to the assumed habitat depth of *G. sacculifer* (30–80 m). Blue dots indicate locations of ODP Sites 999, 1000, and 1241 and the tectonic backtrack for Site 1241 (open black dot) (from Mix et al., 2003). Major current directions are indicated with arrows: GS: Gulfstream; CC: Caribbean Current; NEC: North Equatorial Current; NECC: North Equatorial Counter Current; SEC: South Equatorial Current; EUC: Equatorial Under Current; PCC: Peru/Chile Current (from Groeneveld, 2005).

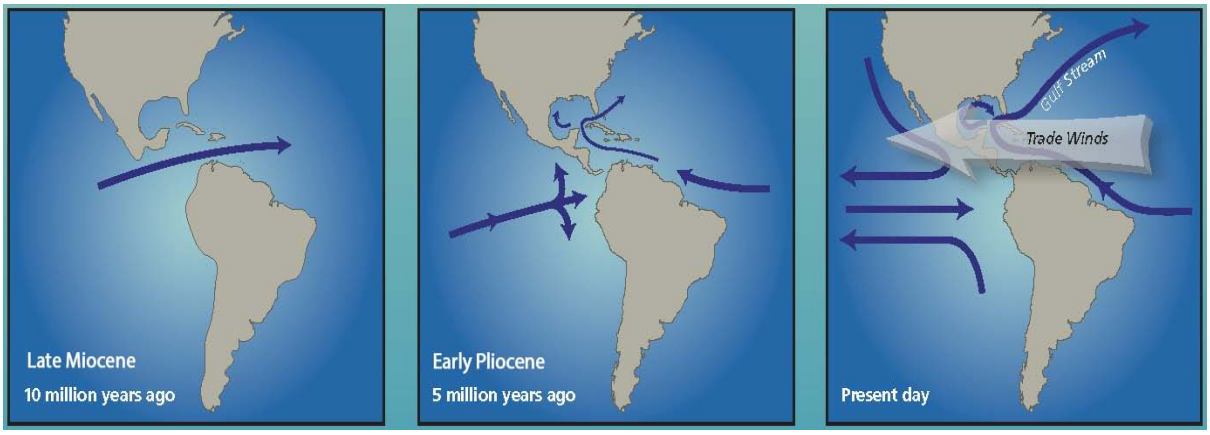


**Figure 6.** A schematic representation of the gradual closure of the CAS from the late Miocene (~10 Ma) to present (modified from Haug et al., 2004).

### 3.4 Tectonic evolution of the CAS

Sea level changes are considered the dominant factor in causing shoaling/closure and reopening of the CAS throughout the Neogene–Quaternary. However, its tectonic evolution is still the primary controlling factor on the emergence of the seaway. The North and South Atlantic oceans during Early Cretaceous assisted in the formation of the Caribbean tectonic history. Divergence between the westward motion of the North and South American plates resulted in the formation of the Caribbean Plate (Burke, 1988).

Regarding the tectonic evolution, there are three main stages that subsequently determined the configuration of the land bridge (Figure 7). The first stage occurred during the Late Cretaceous, when a volcanic arc (with several fore- and back-arc basins) formed as a result of subduction of the Farrallon Plate, and in a later phase the Cocos and Nazca plates, underneath the Caribbean Plate (e.g., Dengo, 1985; Burke, 1988; Coates and Obando, 1996; Hoernle et al., 2002). Different movements and subduction rates at the western margin, influencing volcanism and basin development, were a cause of large variations along the entire arc.

The second stage, which resulted in an initial uplift phase, was the collision of the eastward moving Southern Central American Volcanic Arc with the South American Plate during the Middle Miocene (Coates et al., 2004). The detailed lithostratigraphic and biostratigraphic analyses by Coates et al. (2004) placed this episode during 12.8–9.5 Ma. However, they noted the onset of tectonic evolution had already occurred around 16 Ma and collision with South America was completed by 7.1 Ma.

The third and most important phase includes the subduction of the 15-km-thick oceanic Cocos Ridge. This resulted in strong deformation and uplift of the volcanic arc with pervasive

effects over a distance of 400 km along the isthmus (Coates and Obando, 1996). The Panama Arc then still lay to the west of South America (Coates et al., 2004). Underthrusting of the Cocos Ridge dramatically elevated the land brige, and caused the final closure of the Central American Seaway. The suggested initiation of this process ranges from 1 Ma (Corrigan et al., 1990) to more than 3.6 Ma (Collins et al., 1995), or to 5 Ma (de Boer et al., 1995). Nevertheless, from the Pliocene onwards marine sedimentation in the different basins along the arc is rare or absent (Coates et al., 2004).

To summarize, major tectonic processes from 16 Ma onwards controlled the evolution of the Central American Volcanic Arc. Deep-water exchange between the Atlantic and Pacific oceans terminated around 7 Ma, although sea-surface water exchange was able to continue until the end of the Pliocene (Molnar, 2008).

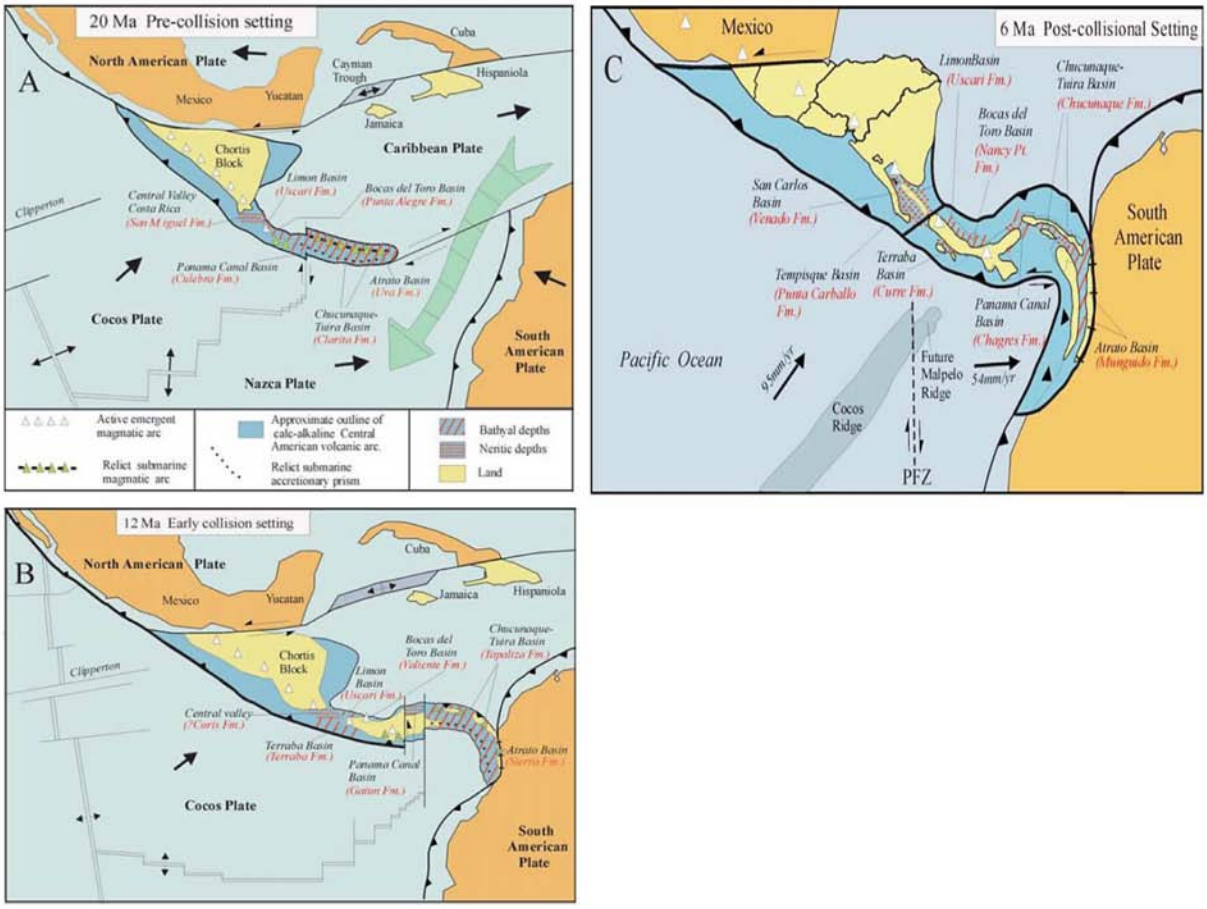


**Figure 7.** Tectonic evolution of the Central American Isthmus. **A)** A volcanic arc accompanied by several back-arc and fore-arc basins already developed since the Late Cretaceous because of the subduction of the Farallon, Cocos and Nazca plates. **B)** Uplifting during the Middle Miocene caused by collision with the South American Plate. **C)** Subduction of the Cocos Ridge finally caused the complete closure of the CAS during the Pliocene (modified from Coates et al., 2004).

Nonetheless, a recent study by Montes et al. (2012a; 2012b) challenges the hypothesis of a Late Pliocene closure of the CAS. Palaeogeographic restoration of the deformed Panamanian Belt showed that the space for the seaway narrowed at 25 Ma and completely disappeared by about 15 Ma. They postulated that water exchange had been eliminated significantly from that point onwards.

### 3.5 Hypotheses for shoaling and closure of the CAS

In this section, several hypotheses are examined that use faunal distributions and oceanographic characteristics either sides of the isthmus to reconstruct the gradual shoaling and closure of the Central American Seaway.

#### 3.5.1 Vertebrate distribution patterns from North to South America

The detailed investigations into land mammal exchange (Figure 8) between North and South America, known as the Great American Interchange, record the final and most pronounced emergence of the Panamanian Land Bridge (Webb, 1976). The presence of Miocene mammal fossils of Northern American affinity in Panama (Lloyd, 1963; Jacobs et al., 1963) points to the conclusion that Central America was attached to North America by ca. 10 Ma. The disappearance of the Bolivar Seaway (Figure 9) or the Antilles Archipelago before 3 Ma led to the exchange of a few land mammals and oak trees between North and South America, although, large-scale exchange took place only from 2.7 Ma onwards (Stehli and Webb, 1985; Marshall, 1988).

Although the emergence of the land bridge (a combination of tectonics and sea level dynamics) was a necessary precondition for large-scale migration, this exchange was impossible without climate change (Savin and Douglas, 1985). Mammal migration could not take place until savanna-like environments developed in Central and South America. The Great American Interchange is presently dated around 2.7 Ma and represents the final and complete closure of the Central American Seaway, caused by the onset of the NHG (e.g., Molnar, 2008; De Shepper et al., 2013).

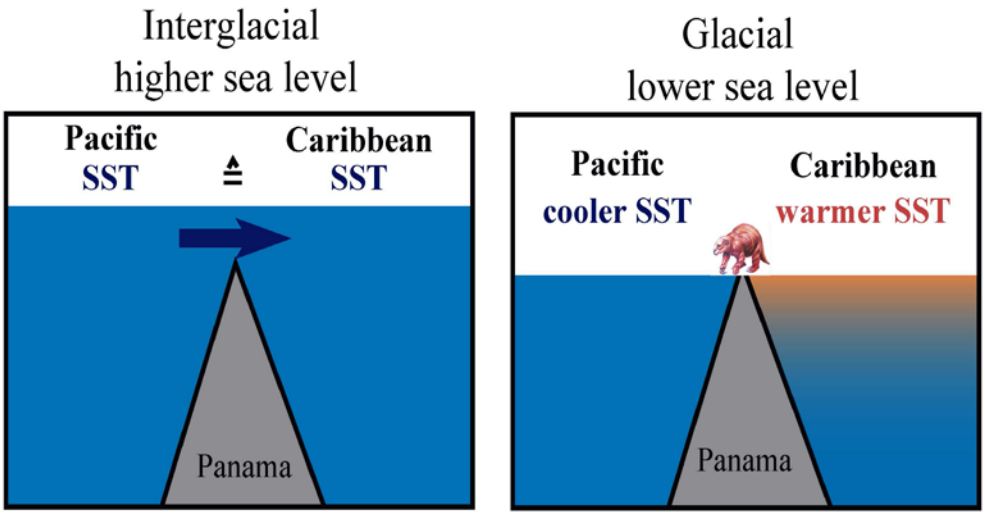


**Figure 8.** A schematic illustration of the glacial closure of the Panamanian Gateway. During glacial intervals (MIS 96, 98, and 100) sea level dropped causing the land bridge to become exposed and leading to a considerable warming of Caribbean surface water masses and allowing vertebrates to migrate from North to South America and vice versa (from Webb, 1997).

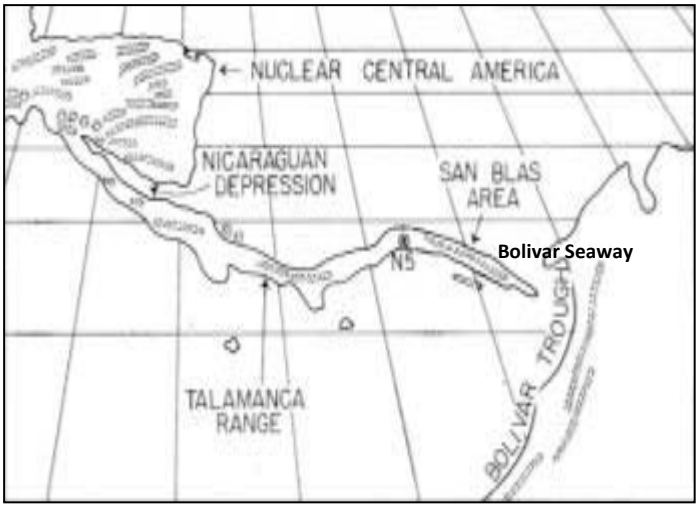


**Figure 9.** Southern Central America and northwestern South America in the early Middle Miocene. N5; Cucaracha Miocene mammal site (modified from LIoyd, 1998).

### 3.5.2 Microfossil assemblages from both sides of the CAS

Detailed microfossil and nannofossil studies provide strong evidence for the shoaling and final closure of the CAS. Studies by Keller et al. (1989) based on planktonic foraminiferal records from sites in the equatorial Pacific and Atlantic distinguished three major events in the history of Panama. Microfossil assemblages in the Caribbean Sea and the eastern Pacific were similar prior to 6.2 Ma, implying an unrestricted flow between both basins. Between 6.2 and 4.2 Ma, however, Caribbean samples are characterized by high abundances of the common high-latitude species *Neogloboquadrina pachyderma*, which is nearly absent from Pacific samples. Its presence in the tropical Caribbean is remarkable and is probably the result of upwelling of cool waters, deflected against a rising sill.

Between 4.2 and 2.4 Ma the first changes between Caribbean and eastern Pacific surface waters appear. Caribbean surface waters became gradually enriched in the salinity-tolerant species *Globigerinoides sacculifer* that suggests a restricted surface exchange through the gateway. The most prominent change occurred at 2.4 Ma. Caribbean assemblages became dominated by the high-salinity-tolerant species *Globigerinoides ruber*. Keller et al. (1989) suggested that a cessation of surface currents occurred at that point. However, they noted that the final divergence between surface- and intermediate-dwelling species only started from 1.8 Ma onwards, and therefore small-scale leakages between both basins were still possible before then.

The first evidence for the existence of a deep-water barrier was provided by Duque-Caro (1990) who showed that distinct benthic foraminiferal faunas developed between the Caribbean and the east Pacific at around 12.9–11.8 Ma. An analysis by McDougall (1996) based on different benthic foraminifera from the same deep sea cores as Keller (1989) suggested that a restricted deep-water exchange between the North Atlantic and eastern Pacific developed between 6.7 and 6.4 Ma. From 3.4 Ma, benthic foraminifera indicated the establishment of cooler, Antarctic-dominated bottom water in the Caribbean until 2.0 Ma. McDougall (1996) correlated this event to global climate change and local sill depth changes between the Caribbean and Atlantic, rather than shoaling and closure of CAS.

Kameo and Sato (2000) studied the biogeography of Neogene calcareous nannofossils from the Caribbean and eastern equatorial Pacific using principal component analysis. Emphasis was specifically placed on general assemblage distribution and not on the paleoecology of individual species. Floral assemblages significantly changed during the Late Pliocene at 2.76 Ma, with complete divergence between Caribbean and Pacific samples.

On the other hand, assemblages from ODP 998 and 999 within the Caribbean became very similar. Kameo and Sato (2000) argued that between 3.65 and 2.76 Ma the Central American barrier prevented exchange between the Caribbean and the Pacific, deflecting the Circum-Tropical Current and creating the northward intra-Caribbean current. According to their interpretation, a gradual closure of the Central Amercian Seaway took place during the Late Pliocene with complete basin separation by 2.76 Ma.

### 3.5.3 Geochemical proxies

The main geochemical analyses include measurements of $\delta^{18}O$, Mg/Ca and $\delta^{13}C$ ratio on planktonic and benthic foraminifera.

Oxygen isotopic values in planktonic foraminifera are sensitive to surface water temperatures and salinities, and can thus be used as proxies reflecting sea-water temperatures, evaporation rates, and salinity (Dwyer and Chandler, 2009; Molnar, 2008). They are therefore useful for reconstructing water-mass properties on both sides of the Panamanian Isthmus (Haug et al., 2001).

Measuring Mg/Ca in the calcareous tests of planktonic foraminifera, and to a lesser extent in benthic foraminifera, is a relatively new method compared to oxygen isotopes, alkenone unsaturation ratios, and transfer functions, each with their own limitations to estimate palaeothermometry (Dekens et al., 2002). However, biological and dissolution effects bias the temperature estimates severely. Therefore, the optimal use of Mg/Ca as a palaeotemperature proxy requires precise calibrations for different species and dissolution grades (Dekens et al., 2002). As an independent palaeothermometer, this method is appealing since it can be measured on the same species as $\delta^{18}O$ thereby allowing the temperature and water $\delta^{18}O$ signal to be separated (Dekens et al., 2002; De Schepper et al., 2009).

$\delta^{13}C$ values from benthic foraminifera are used to distinguish the influence of different water masses, and can be considered a proxy for deep water ventilation. At subtropical Atlantic latitudes, surface waters are enriched in $^{13}C$ because of enhanced photosynthesis in this region. Subsequently, these waters move north to higher, even more productive, latitudes where they sink to the bottom as North Atlantic Deep Water. In this case, North Atlantic Deep Water is characterized by positive $\delta^{13}C$ values and low nutrient concentrations. In the Antarctic region on the other hand, fractionation of carbon isotopes is incomplete because of limited photosynthesis. This results in Antarctic Bottom Water having negative $\delta^{13}C$ values and high nutrient concentrations (Ruddiman, 2008). Because the Caribbean basin is characterized by a mixture of North Atlantic Deep Water and Antarctic Bottom Water, their relative pervasive strengths provide information about the closure of the gateway.

The $\delta^{18}O$ and Mg/Ca records based on the planktonic foraminifera *Globigerinoides sacculifer* were used (Figure 10) to reconstruct the sea-surface temperatures and salinity for the Caribbean ODP Sites 999 (12°44'N, 78°44'W, 2828 m water depth) and 1000 (16°33.222'N, 79°52.044'W, 916 m water depth) and equatorial Pacific Site 1241 (5°50□'N, 86°26'W, 2027 m water depth) (Groeneveld, 2005; Steph et al., 2006; Groeneveld et al., 2008). Comparison of the two proxies illustrates a divergence in temperature and salinity records from 5.6 to 4.4 Ma; the northern part of the Caribbean (Site 1000) was ca. 3°C warmer than the southern Caribbean and the adjacent Pacific (24–27°C). Shoaling of the Seaway by <100 m (ca. 4.5 Ma) led to the development of the WAWP and hence to the strengthening of the Gulf Stream/NAC by introducing warm and saline water to northern latitudes. This event was marked by the divergence in SST and SSS between Caribbean and Pacific sites. Increases in SST of 2°C (29°C) and 1% in SSS were recorded at Site 1000. This trend is not reflected in the Gateway region (Sites 999 and 1241), which suggests that the more northerly Site 1000 unlike Site 999 in the Caribbean Sea was less affected by Pacific inflow after 5.6 Ma.

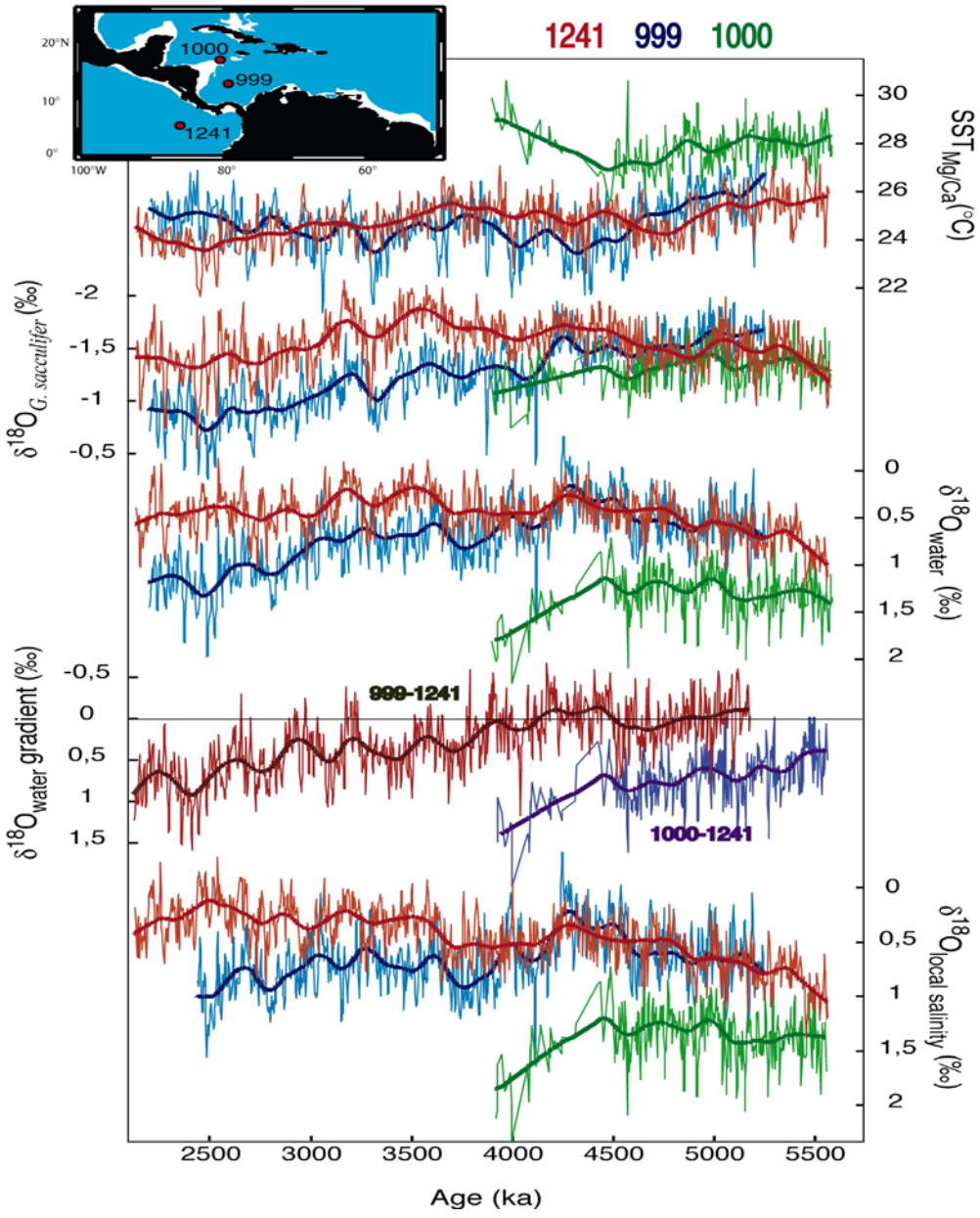


**Figure 10.** Sea surface water properties ($SST_{Mg}$/Ca, $\delta^{18}O$ *Globigerinoides sacculifer*, $\delta^{18}O$ water, $\delta^{18}O$ water-gradient, and $\delta^{18}O$ salinity) for the Caribbean (Sites 999 and 1000) and the tropical east Pacific (Site1241). Analyses were performed on the planktonic foraminifer *G. sacculifer*. Coloured numbers 999, 1000, and 1241 indicate the proxy data for the respective sites. Inlet shows the locations of ODP Sites 999, 1000, and 1241 (from Groeneveld, 2005).

Changes in the North Atlantic THC strengthened deep-water formation in the Labrador Sea at ca. 4.4 Ma, as indicated by increased NADW ventilation and carbonate preservation owing to displacement of AABW (Figure 11) (e.g., Billups et al., 1999). The influx of NADW is seen through measurements on the benthic foraminifera *Cibicidoides wuellerstorfi* from sites in the Atlantic Ocean compared with results from the western and eastern tropical Pacific. The large $\delta^{18}O$ values at the shallower sites of the Atlantic Ocean compared to the deeper sites is indicative of warmer and more saline NADW conditions at ca. 4.4 Ma. Despite this evidence, several modeling studies (e.g., Groeneveld et al., 2005) have suggested that northward transport of warm and saline waters was not efficient enough until the latest Pliocene (ca. 2.7 Ma) to generate intensified NADW. However, results based on planktonic foraminiferal oxygen isotopes indicate a southward shift of the Intertropical Convergence Zone during the Early Pliocene (ca. 4.4 Ma). This permitted an increase in the transport of warm and saline water into the subtropics, thereby contributing to NADW formation in the North Atlantic. It has been suggested that this shift may have been triggered by a variety of factors such as the restriction of surface water flow through the CAS (e.g., Billups et al., 1999). Benthic oxygen isotope ratios from sites in the Atlantic and Pacific suggest a change in oceanography during ca. 3.330–3.283 Ma caused by a brief suspension of the North Atlantic thermohaline circulation, and can be correlated to the global cooling event (ca. 2–3°C) of MIS M2.

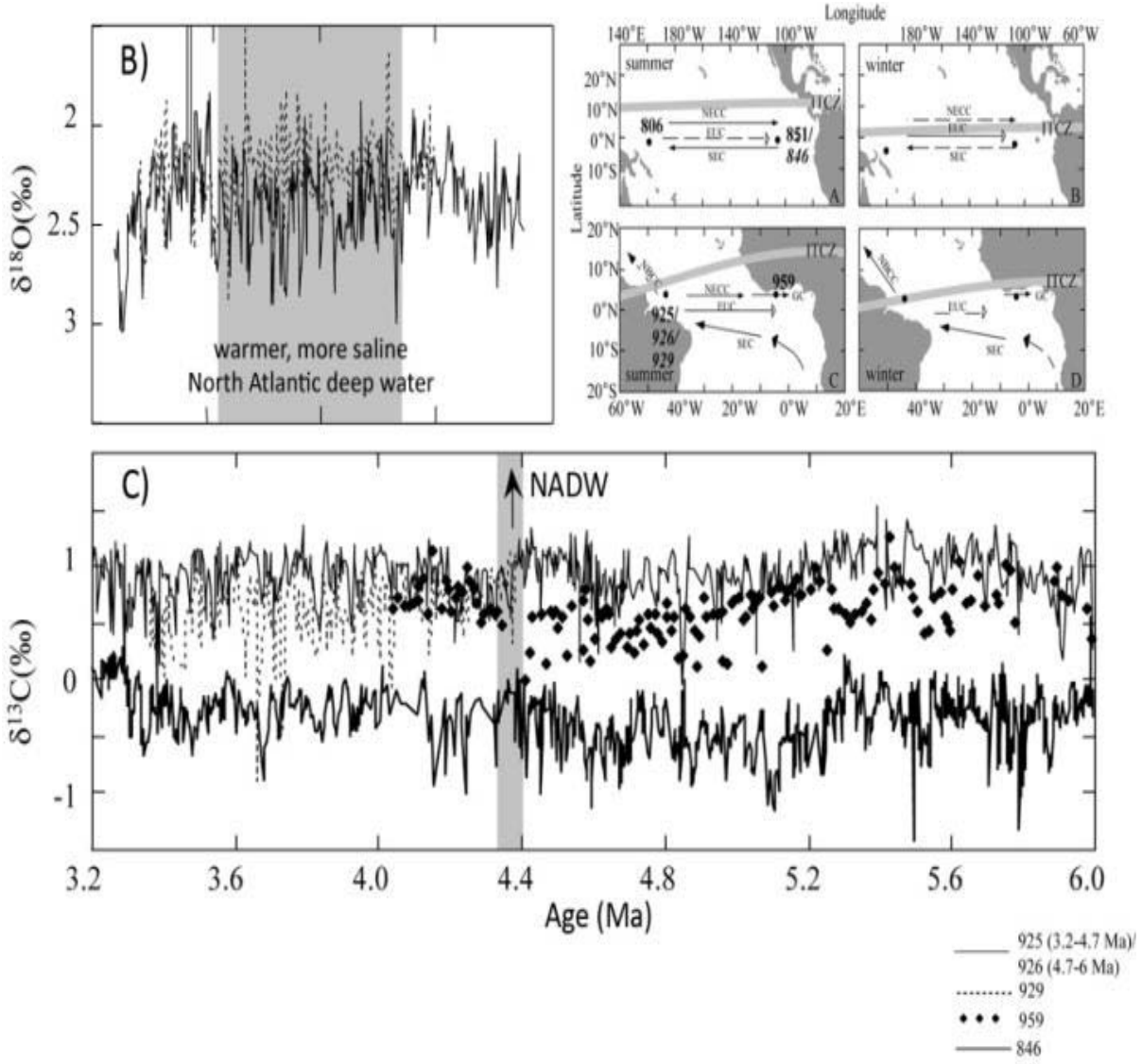


**Figure 11 A)** Locations of ODP Sites. Surface currents are; South Equatorial Current (SEC), North Equatorial Counter Current (NECC), Equatorial Undercurrent (EUC), North Brazil Coastal Current (NBCC), Guinea Current (GC), Intertropical Convergence Zone (ITCZ). Dashed arrows show relatively weak and solid arrows indicate relatively strong transport of surface water. **B)** Early Pliocene benthic (*Cibicidoides*) $\delta^{18}O$ records from Ceara Rise ODP Sites 925 and 929 illustrating relatively high $\delta^{18}O$ values at Site 925 in comparison to Site 929 between 4.3 and 3.7 Ma. **C)** Late Miocene–Early Pliocene $\delta^{13}C$ records from equatorial Atlantic and Pacific illustrating increase in Site 959 $\delta^{13}C$ values at 4.3–4.4 Ma (from Billups et al., 1999).

Planktonic (*Globigerinoides sacculifer*) oxygen isotope records from Caribbean ODP Site 999 and Pacific Site 851 were used to determine the timing of surface water separation between these realms (Haug et al., 2001; Figure 12). Results indicate that before 4.7 Ma, East Pacific $\delta^{18}O$ values were similar to, or even higher, than those of the western Atlantic. At about 4.7 Ma, the Caribbean record became enriched in $\delta^{18}O$, and a salinity difference of 0.5‰ was established at 4.2 Ma which gradually increased further to the modern day differential of 1‰. Haug et al. (2001) interpreted these variations as a response to the gradual shoaling of the CAS to depths less than 100 m since 4.2 Ma. A difference of 0.5‰ between both basins roughly corresponds to a SSS difference of 1‰ and a 2.5°C temperature offset (Zahn and Mix, 1987). As the Early Pliocene was a warm interval, it is unlikely that SSTs in the Caribbean dropped by 2.5°C. The difference in $\delta^{18}O$ values is in this case best explained by an increase in Caribbean surface salinity as a result of the net transport of water vapour to the eastern Pacific. Therefore, Haug et al. (2001) interpreted these results as reflections of the formation of the CAS since 4.7 Ma. Pacific flow into the Caribbean, as a result of the density contrast between both basins, initially tried to attenuate this contrast, but because of further shoaling this mechanism also failed. These findings were confirmed by Steph (2005) and Steph et al. (2006) who evaluated $\delta^{18}O$ records from the Caribbean (Sites 999 and 1000), western Atlantic (Sites 851 and 1241) and tropical East Pacific (Sites 851 and 1241).

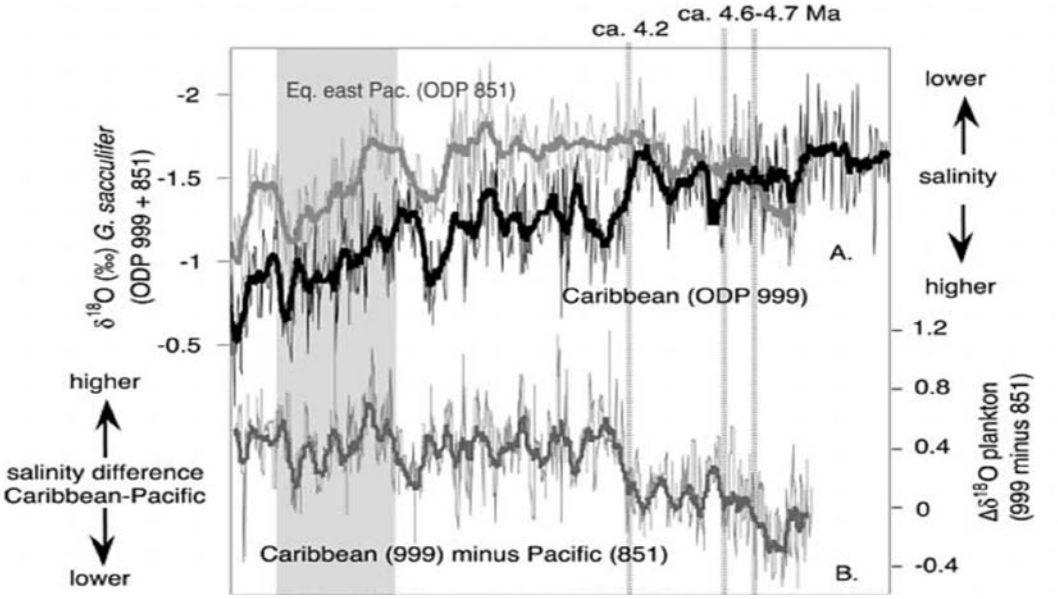


**Figure 12.** Oxygen isotope data from Caribbean ODP Site 999 and eastern Pacific ODP Site 851. **A)** $\delta^{18}O$ record from the planktonic foraminifer species *Globigerinoides sacculifer*. **B)** Gradient in foraminiferal $\delta^{18}O$ between the Caribbean and the Pacific (modified from Haug et al., 2001).

Studies by Haug et al. (2005) based on alkenone saturation ratios and oxygen isotopes in diatoms from sites in the North Pacific suggested that the late Pliocene (ca. 2.7 Ma) saw increased evaporation in the North Pacific, followed by transportation of moisture across northern North America. This finally led to snowfall over the Greenland ice sheet, initiating NHG. The increase of the northern hemisphere ice sheet lowered sea level which hastened the final closure of the CAS.

The aforementioned results suggest that the final closure of the CAS was not formed until 2.7–2.2 Ma, which resulted in separation between both nannofossil assemblages and foraminiferal $SST_{Mg/Ca}$ from the Caribbean and the eastern Pacific.

**3.6 Dinocysts**

Dinoflagellates are a diverse group of protists characterized by two dissimilar flagella and a distinctive nucleus. They occupy a wide range of habitats across the marine and freshwater realms, and have various feeding strategies including autotrophy, heterotrophy, mixotrophy, and parasitism (e.g., Taylor, 1987; Schnepf and Elbrächter, 1992; Fensome et al., 1993, Fensome et al., 1996b). The term 'cyst' in dinocysts is generally adopted for a non-motile cell that lacks flagella and therefore mobility. Resting cysts are usually assumed to represent hypnozygotes and their walls are made of organic, calcareous or siliceous substances with high preservation potential. They can survive harsh environments, and remain in quiescence or dormancy until improved environmental conditions induce germination. Although molecular phylogenetic and biochemical evidence suggests a Late Precambrian origin for the dinocysts lineage (e.g., Stover et al., 1996; Fensome et al., 1996a, 1999), definitive evidence from fossil organic-walled dinocysts is known only from the Late Triassic onwards.

The sensitivity of dinocysts to their environment allows the record of their cysts to serve as a excellent detectors of subtle as well as extreme environmental fluctuations. Cyst distributions in the sedimentary record are useful proxies for reconstructing upper water-column conditions (e.g., temperature, salinity and nutrient availability) and have been considered as valuable tools in palaeoecology, palaeoclimatology, palaeoceanography and biostratigraphy (e.g., Evitt, 1963; 1985; Wall, 1967; Versteegh, 1995; Fensome et al., 1996; Head and Westphal 1999; Sluijs et al., 2005; De Schepper et al., 2009, 2011, 2013).

### 3.7 The Pliocene

The Neogene Period, commencing 23.03 Ma, was followed by the Quaternary Period at 2.58 Ma (Head et al., 2008; Gibbard and Head, 2010) that broadly represents the transition to a glacially dominated climate. The Pliocene Epoch (5.33–2.58 Ma, Figure 13) includes the mid-Piacenzian Warm Period (3.3–3.0 Ma) which is considered a possible near future analog (e.g., Chandler et al., 1994; Haywood et al., 2000; Jiang et al., 2005; De Schepper et al., 2013). This interval is marked by ca. 3°C warmer global temperatures, 10–40 m higher global sea levels, reduced continental ice sheets, and an Atlantic meridional overturning circulation comparable to or stronger than preindustrial levels. Atmospheric $CO_2$ concentrations were higher than preindustrial values, and likely as high as modern anthropogenic values of ca. 400 ppm (De Schepper et al., 2013). However, Zhang et al. (2013) suggested at high latitude mid-Pliocene warming can not be explained as a direct response to an intensification of AMOC and related increase in northward ocean heat transport by the Atlantic.

Early Piacenzian warmth was interrupted between 3.305 and 3.285 Ma by an abrupt cooling event within MIS M2, with benthic foraminiferal $\delta^{18}O$ values reaching levels characteristic of Early Quaternary glaciations. It is estimated that the Antarctic and Northern Hemisphere ice sheets expanded to volumes larger than today, and that sea level fell to more than 10 m and perhaps as much as 65 m below present (De Schepper et al., 2013). MIS M2 maybe a failed attempt of the climate system to reach the intensity of glaciation characterising the Quaternary, and initiated in the latest Pliocene at around 2.7 Ma.

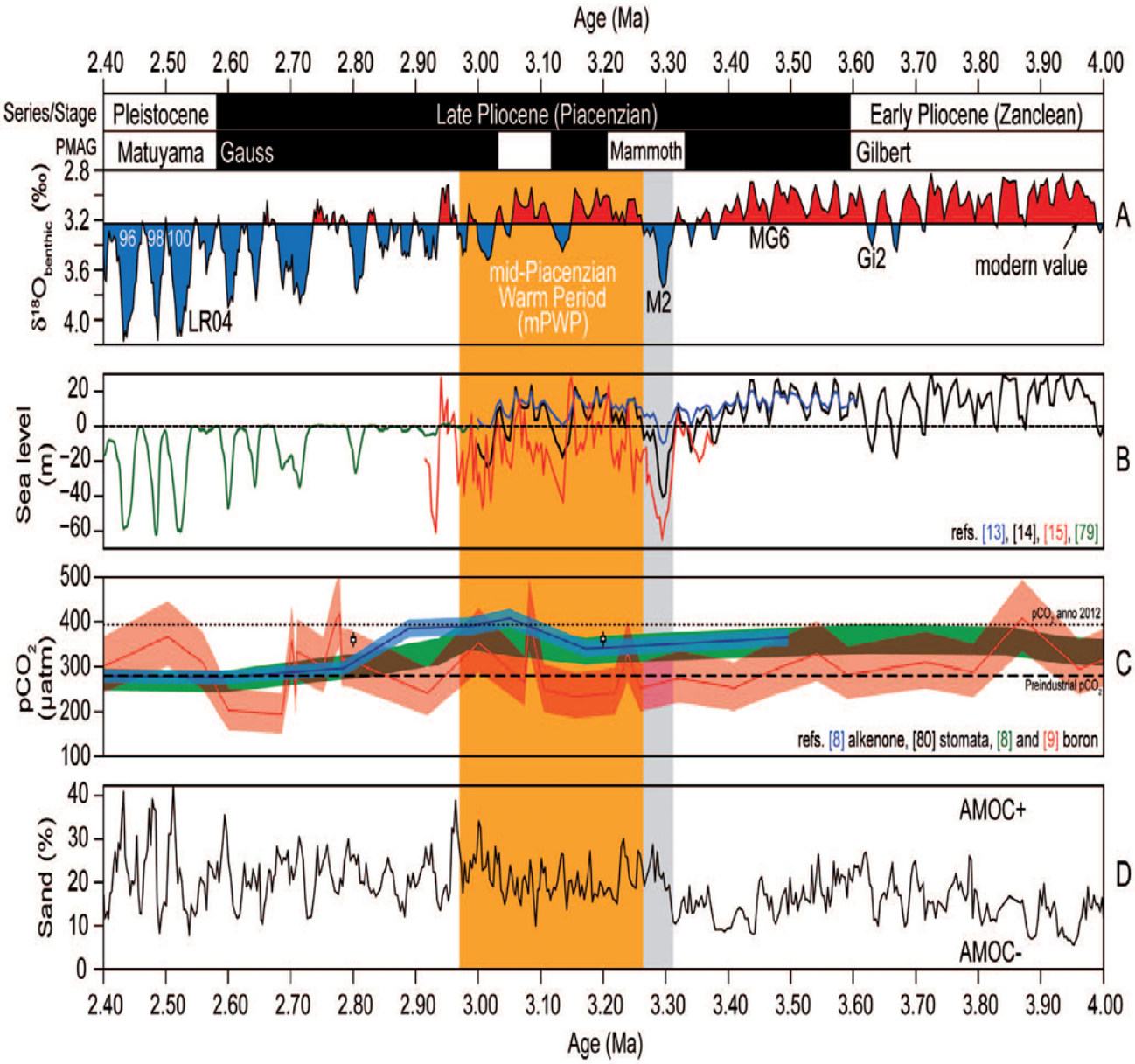


**Figure 13 A)** Time scale, including palaeomagnetic reversals and the LR04 benthic isotope stack, orange shading shows mid-Piacenzian Warm Period, grey shading shows marine isotope stage MIS M2**. B)** Sea level estimates for the Pliocene to Pleistocene**. C)** Late Pliocene atmospheric carbon dioxide concentrations based on boron, alkenones and leaf stomata**. D)** long-term carbonate-sand record at ODP Site 999 as an indicator of Pacific water flow through the CAS into the Atlantic and AMOC (from De Schepper et al., 2013, and references therein).

### 3.8 Hypotheses for the Northern Hemisphere Glaciation

The Late Cenozoic witnessed major palaeoceanographic changes that culminated in the NHG. Numerous mechanisms have been invoked to explain the onset of NHG, including: 1) the opening or closure of oceanic seaways (e.g., Ruddiman et al., 1989; Wright and Miller, 1996, Cane and Molnar, 2001; Gladenkov et al., 2002; Haug et al., 2001; 2004; 2005; Bartoli et al. 2005, Poore et al. 2006; Lunt et al., 2008; Ruddiman, 2008; De Schepper et al., 2009; Naafs et al., 2010, Zhang et al., 2011); 2) orbital forcing (e.g., Berger, 1989; Maslin et al., 1998); 3) mountain range uplift (e.g. Raymo and Ruddiman, 1992; Raymo et al., 1988; Foster et al. 2009); and 4) changes in atmospheric $CO_2$ input (e.g. Raymo et al., 1996). However, conflicting opinions suggest that no one hypothesis explains all aspects of the NHG. Results of three aforementioned hypotheses are summarized in Figures 14, 15 and 16.

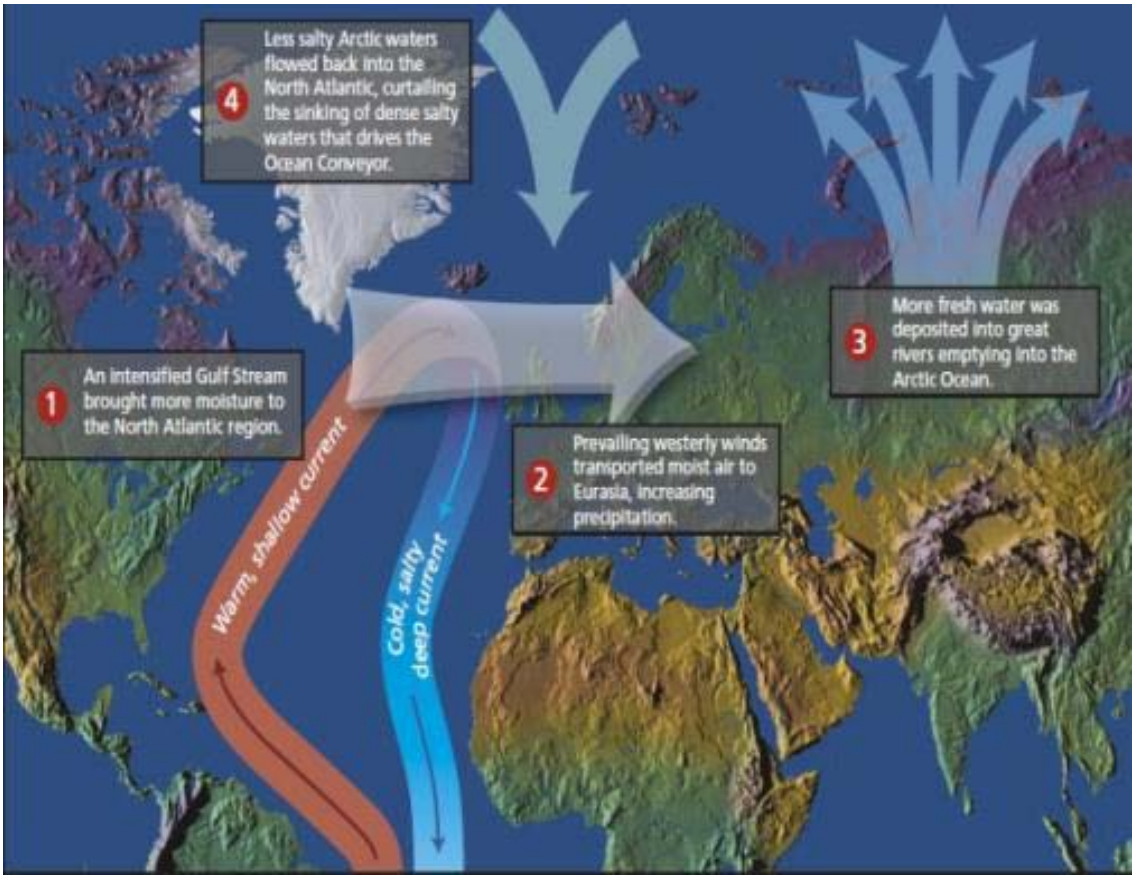


**Figure 14.** The closing of CAS, strengthening of the North Atlantic thermohaline circulation, and development of the NHG (Haug et al., 2005).

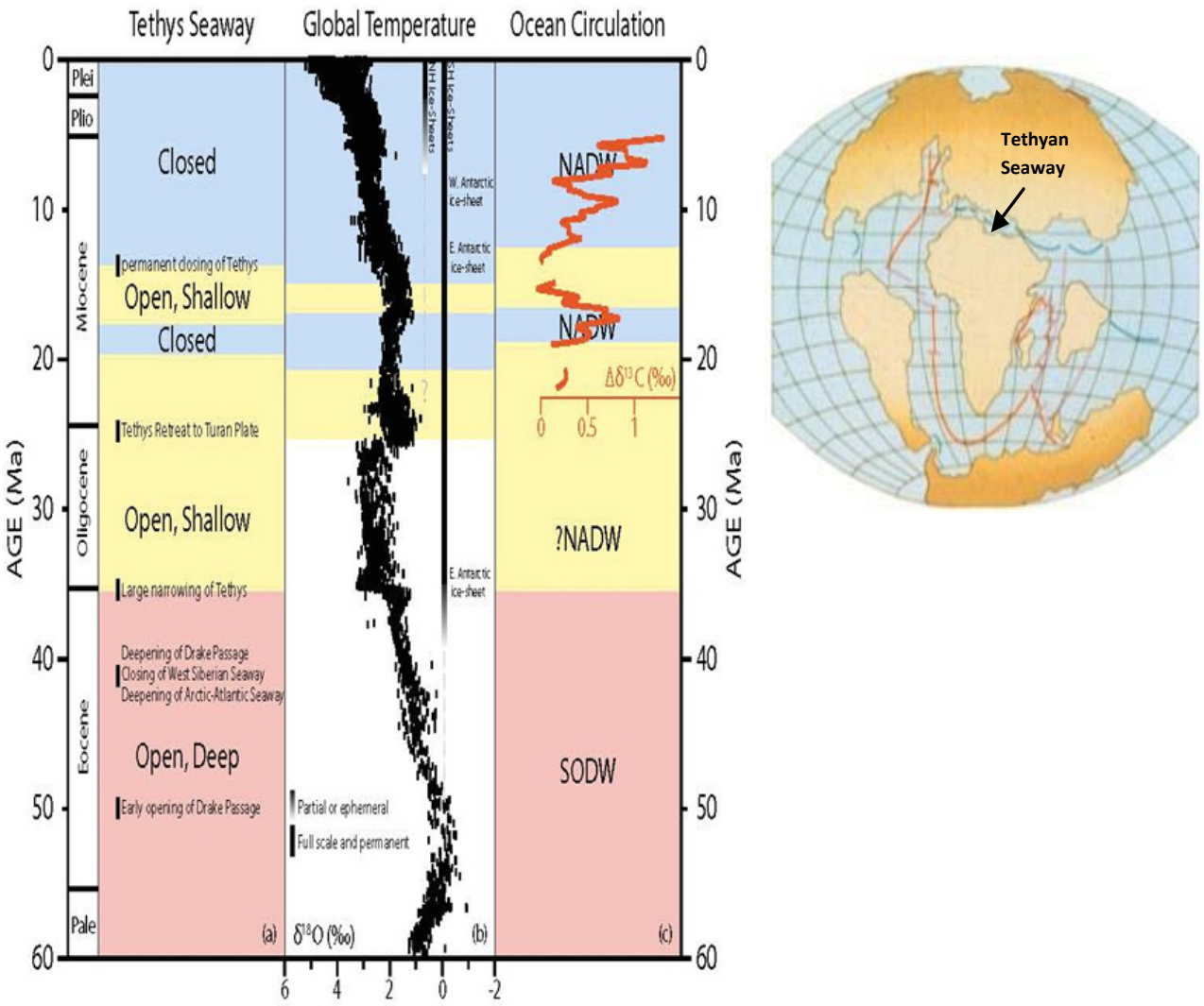


**Figure 15.** Timing of key geological events and closure of the Tethyan Seaway. The red line shows the NADW index based on benthic carbon isotopes (from Wright et al., 1992). The high value of $\delta^{13}C$ indicates active NADW, and the low value indicates inactive NADW (modified from Zhang et al., 2011 and references therein).

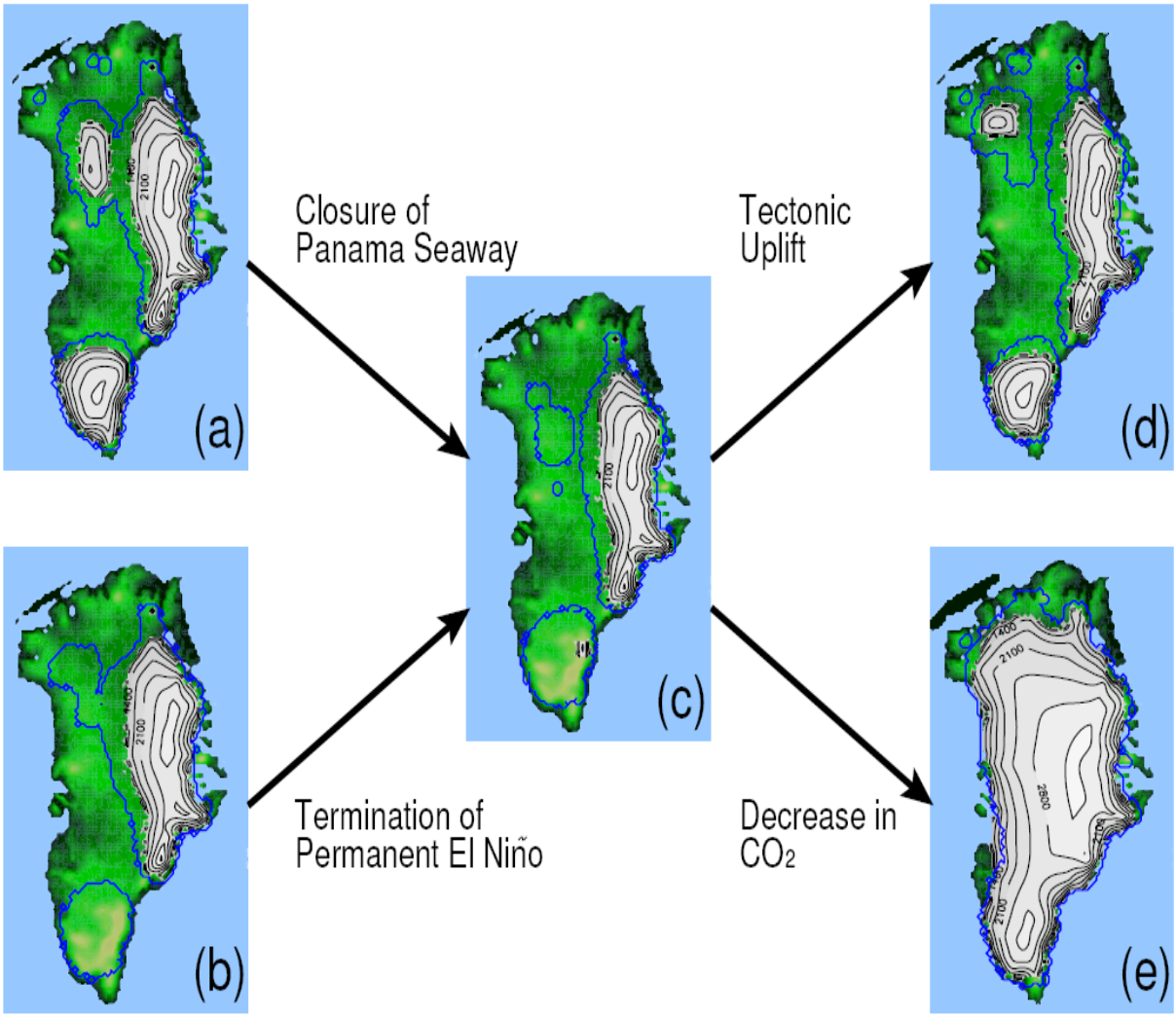


**Figure 16.** Ice-sheet configurations on Greenland; a–e Pliocene ice-sheet configuration with open seaway (a) permanent EN (b) closed seaway, dynamic ENSO, low orography and high $CO_2$ (the Pliocene control) (c) high orography (d) and low $CO_2$ (e) the blue line represents the extent of the ice sheet under orbital conditions favorable for inception. The arrows represent the direction of geological time (modified from Lunt et al., 2008).

Several studies have suggested that an increase in northward transport of warm and saline water was necessary to supply the Greenland ice sheet with the moisture it needed to expand (e.g., Haug and Tiedemann, 1998; Bartoli et al., 2005). In contrast, De Schepper et al. (2009) using dinocysts and foraminiferal Mg/Ca and $\delta^{18}O$ from sites in the North Atlantic Ocean suggested a southward shift or decrease of NAC before and during the earlier MIS M2. This, in conjunction with climate modeling studies, is believed to support the occurrence of increased ice sheet growth over Greenland (e.g., Klocker et al., 2005; Lunt et al., 2008). Dinocyst analysis has shown a drop below 10% in abundance of *Operculodinium centrocarpum* sensu Wall and Dale between ca. 3.330 and 3.283 Ma, this species having been abundant before and after MIS M2 with values often exceeding 50%. Today, high abundances of *O. centrocarpum* in the North Atlantic are strongly controlled by the presence of the NAC, prompting its use as a NAC indicator in the past. De Schepper et al. (2009) concluded that a sudden decrease or interruption of the NAC was related to a brief reopening of CAS during the MIS M2.

A recent study of MIS M2 by De Schepper et al. (2013) incorporating additional sites in the North Atlantic and Caribbean Sea suggests an open CAS as the trigger for NHG. The glacio-eustatic closure of the CAS during MIS M2 eventually re-established northward heat transport in the North Atlantic, causing the Greenland ice sheet to diminish. Results of their study are summarized in Figures 17, 18 and 19.

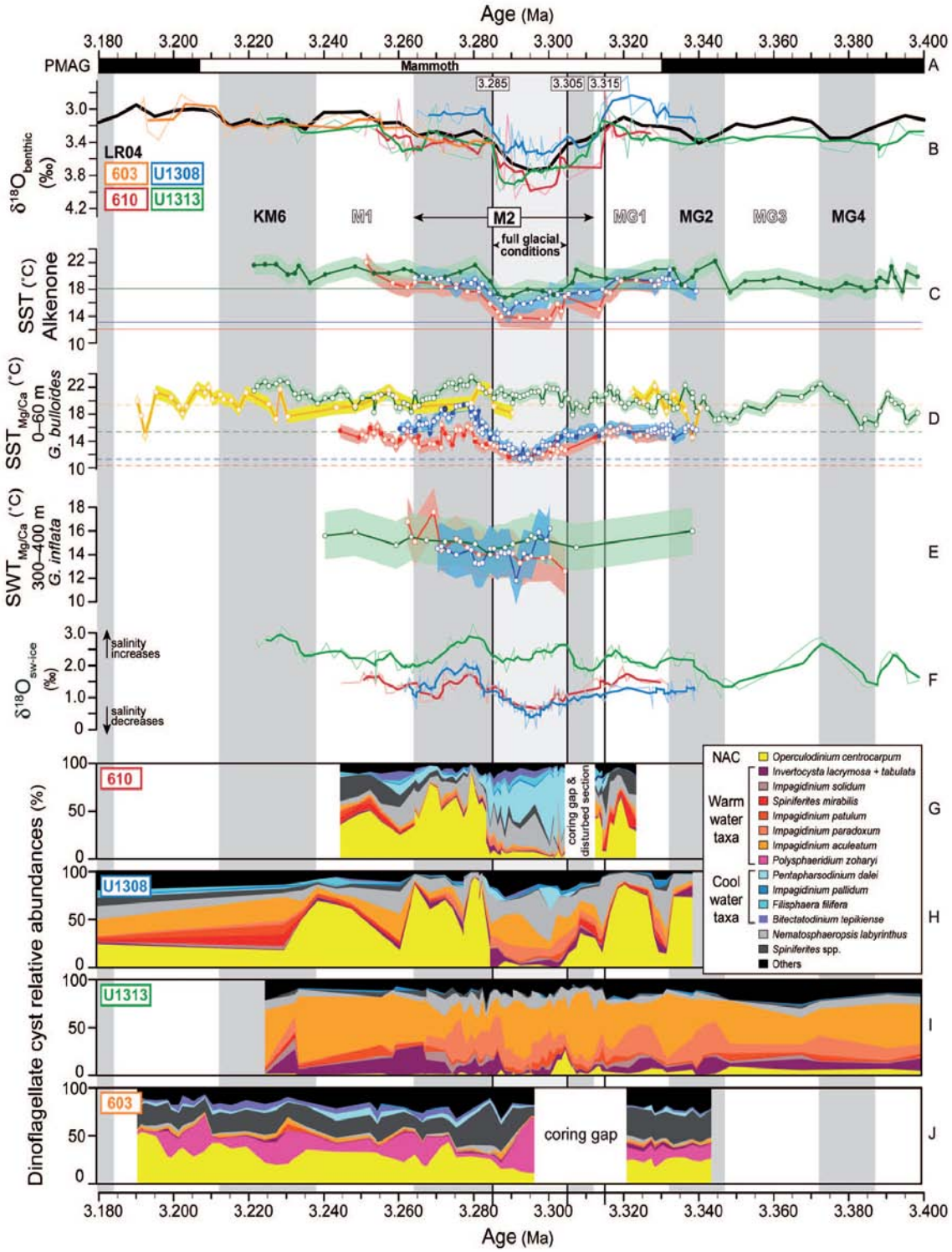


**Figure 17.** North Atlantic palaeoceanographic proxy records between 3.40 and 3.18 Ma (from De Schepper et al., 2013).

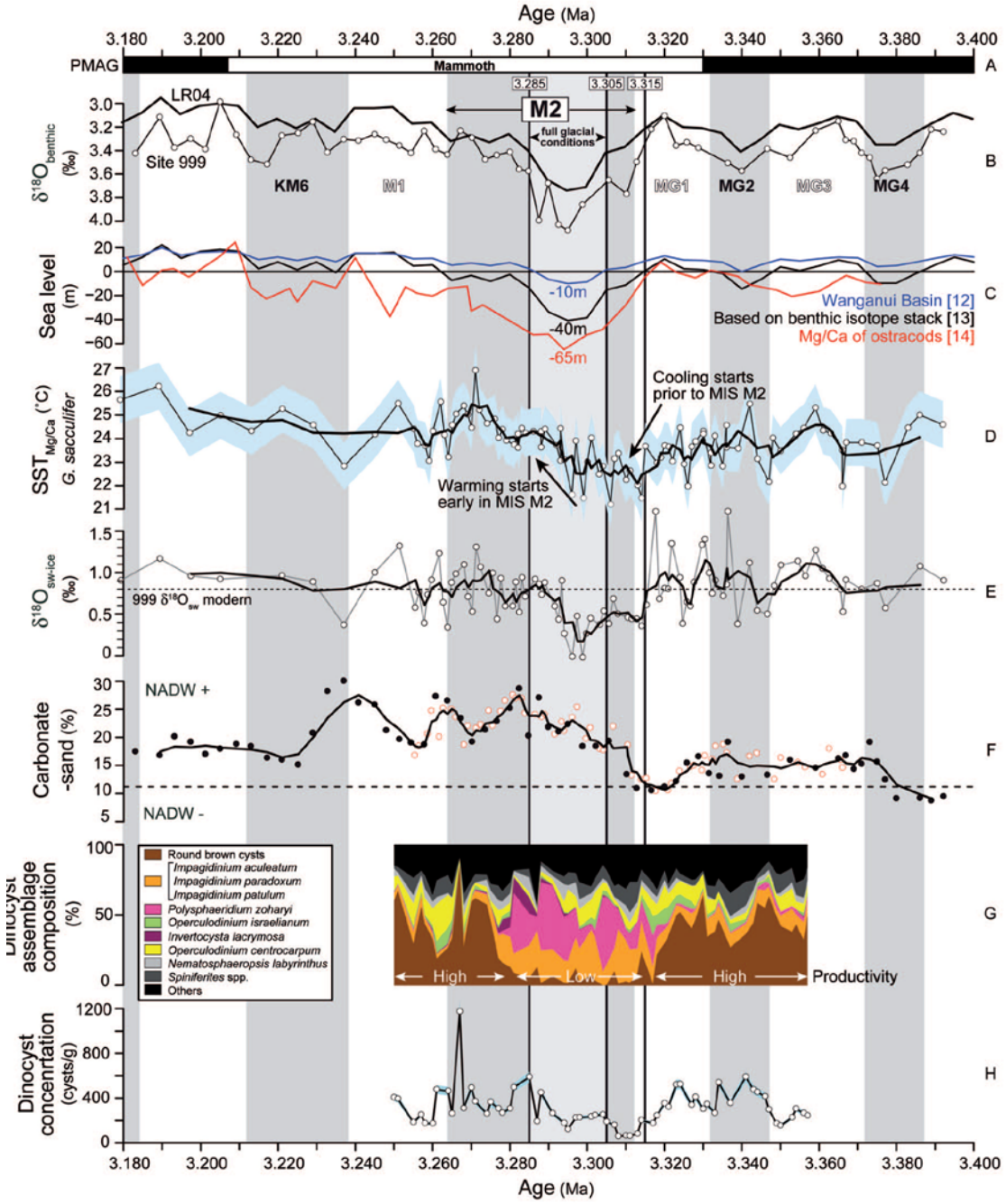


**Figure 18.** Caribbean Sea palaeoceanographic records from ODP Site 999 between 3.40 and 3.18 Ma (from De Schepper et al., 2013 and references therein).

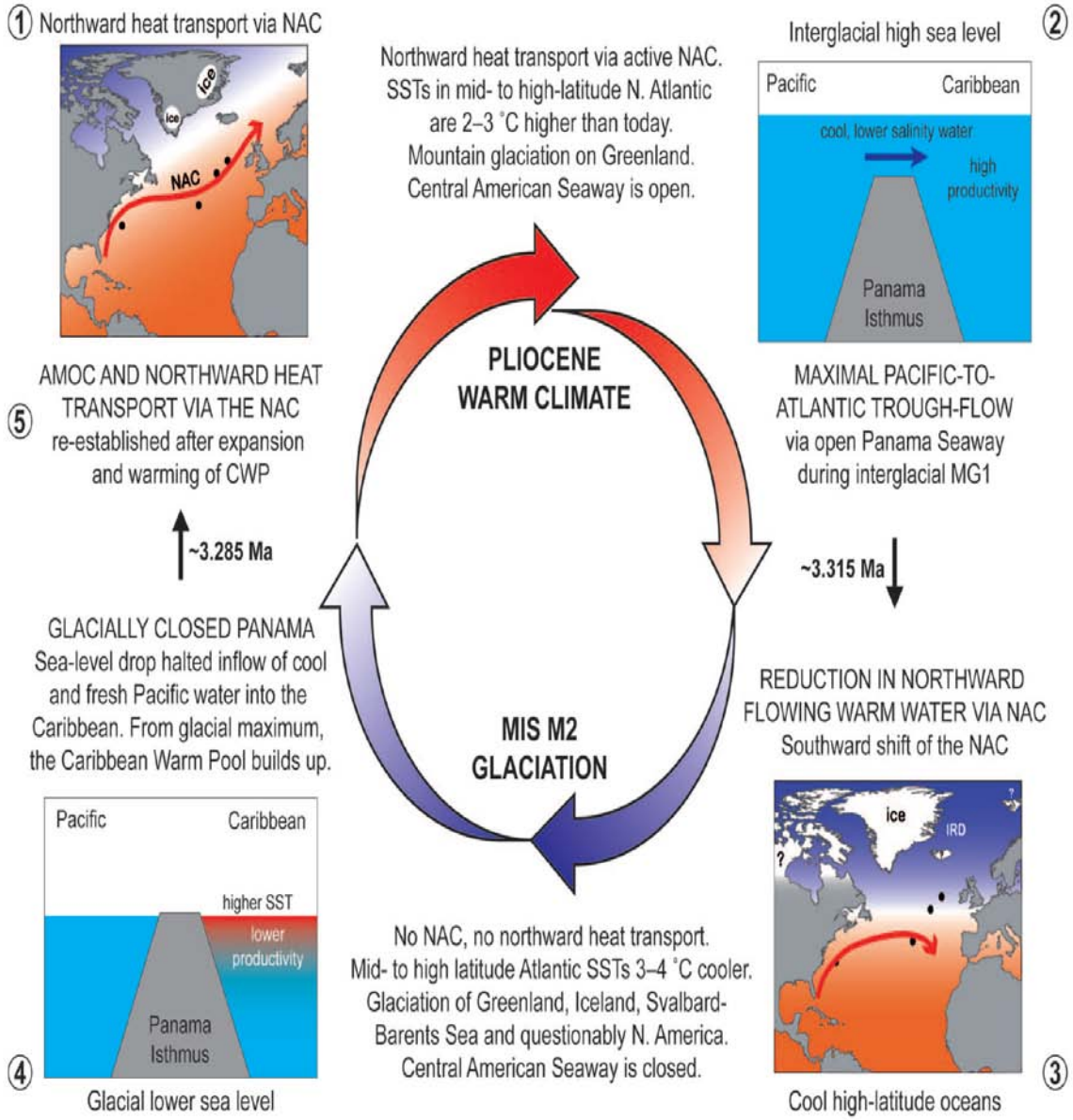


**Figure 19.** Model for glaciation and deglaciation of the Northern Hemisphere during MIS M2 in the Late Pliocene (from De Schepper et al., 2013).

### 3.9 Previous dinocyst studies

The North Atlantic Ocean has been the setting for numerous dinocyst studies addressing oceanic responses to climatic fluctuations and regional tectonics. Most Late Cenozoic dinocyst studies have focused on the high-latitude North Atlantic Ocean and adjacent seas, as these exhibit high species diversity compared with lower latitudes. In contrast, poorer knowledge of the low-latitude dinocyst record hampers detailed marine palaeoenvironmental reconstructions for these latitudes. The following overview, while not comprehensive, describes some of the more important studies of Neogene and Lower Pleistocene dinocysts in the North Atlantic region.

#### 3.9.1 High- to mid-latitude North Atlantic region

The earliest detailed stratigraphic study of Neogene dinocysts was from offshore eastern Canada by Williams (1975). Dinocysts from the Mid–Miocene to Quaternay of the Bay of Biscay were studied by Harland (1979) to interpret paleoceanographic changes and establish an informal dinocyst zonation. Edwards (1984) documented the stratigraphic ranges of important dinocyst species in the Miocene of the eastern North Atlantic Ocean.

Mudie (1987) recorded well-preserved dinocysts throughout the Upper Miocene–Pleistocene of the central and northern North Atlantic and showed that their stratigraphic distribution was influenced by latitude. Additional oceanic sites in the Norwegian Sea (Mudie, 1989), Labrador Sea and Baffin Bay (de Vernal et al., 1989a, b; Head et al., 1989a,b,c), and Norwegian Sea (Manum et al. 1989) greatly improved understanding of the biostratigraphy and taxonomy of Neogene–Quaternary dinocysts at high northern latitudes. Edwards et al. (1991) used quantative methods on Pliocene–Pleistocene dinocyst assemblages to evaluate the potential of this group for interpreting paleotemperature and paleoceanographic patterns in the North Atlantic (see also Edwards, 1992).

Versteegh and Zonneveld (1994) used statistical methods on Upper Pliocene–Pleistocene dinocyst assemblages to determine the ecological preferences of individual species. Neogene studies by Versteegh and Zevenboom (1995) revealed new dinocyst genera and species from the North Atlantic and Mediterranean. Versteegh (1996) compared the impact of Late Pliocene–Early Pleistocene NHG on dinocyst and acritarch distibutions in southern Italy and the eastern North Atlantic. De Verteuil and Norris (1996) demonstrated the utility of Miocene dinocysts for stratigraphic subdivision of the eastern USA continental shelf.

Assemblages documented by Piasecki (2003) from offshore West Greenland showed the highest species diversity in the Miocene, decreasing through the Lower Pliocene, to a minimum in the Upper Pliocene, with fluctuations reflecting paleoceanographic changes.

The Pliocene and Pleistocene deposits in the eastern North Atlantic were studied both biostratigraphically (De Schepper and Head, 2008, 2009) and taxonomically (De Schepper and Head, 2008b, 2014), leading to the establishment of several new dinocyst and acritarch taxa.

Detailed multiproxy studies incorporating dinocysts and focusing on early Late Pliocene MIS M2 in several holes in the North Atlantic were conducted by De Schepper et al. (2009, 2013). Results of these studies have been summarized in the introduction. De Schepper et al. (2011) used these and other multiproxy studies to calibrate Pliocene and Pleistocene dinocysts to their respective paleotemperatures based on same-sample foraminiferal Mg/Ca analyses, thereby establishing quantitative temperature tolerances for extinct Plio–Pleistocene dinocyst species for the first time.

Fischer (2011) studied dinocyst assemblages and foraminiferal geochemistry from the Lower Pleistocene of the western North Atlantic to reconstract paleoceanography, paleosea-surface temperatures, and the paleoecological affinities of individual dinocyst species.

Many of the above studies are based on deposits with poor independent chronological control. Notable dinocyst studies directly calibrated to magnetostratigraphy are the Pliocene–Lower Pleistocene of eastern North Atlantic DSDP Hole 610A (De Schepper and Head, 2008, 2009), Lower through Middle Miocene of eastern North Atlantic (Porcupine Basin) ODP Site 1318 (Louwye et al., 2007), and Middle Miocene through Upper Pliocene of Iceland Sea ODP Hole 907A (Schreck et al., 2012a,b).

### 3.9.2 Gulf of Mexico and Caribbean region

Duffield and Stein (1986), Lenoir and Hart (1986), and Wrenn and Kokinos (1986) all reported rich Neogene dinocysts from the continental slope of the Gulf of Mexico. A study of the Pliocene and Pleistocene of the Bahama carbonate platform by Head and Westphal (1999) revealed paleoenvironmental fluctuations on the platform and allowed the establishment of several new dinocyst species (see also Head, 1998). Palynological and foraminiferal Mg/Ca analysis of MIS M2 at 3.3 Ma at Caribbean ODP Site 999 (Renterghem, 2012) demonstrated the applicability and sensitivity of dinocysts for documenting paleoceanographic changes at low latitudes.

### 3.9.3 Europe, North Sea, and Mediterranean Sea

Studies of the Lower Pleistocene of southwestern England (Head (1993) and Pliocene–Lower Pleistocene of eastern England (Head, 1994, 1996, 1997, 1998) revealed insights into dinocyst assemblages of the neritic realm, and led to the description of several new dinocyst and acritarch species (Head, 1996, 1997, 1999; De Schepper and Head, 2014). From onshore Belgium representing the southeastern margin of the southern North Sea basin, Louwye et al. (2004), Louwye and Laga (2008), De Schepper et al. (2008), and Louwye and

Louwye and De Schepper (2010) recorded diverse and well-preserved Middle Miocene through Pliocene dinocyst assemblages, applying dinocyst biostratigraphy to test sequence stratigraphic concepts.

## 3.10 Geological setting of ODP Site 1000

Site 1000 was cored during ODP Leg 165 on the Nicaraguan Rise (Pedro Channel) (16°33.222'N, 79°52.044'W, Figure 20). The Nicaraguan Rise is a major NE–SW trending structural feature on the northwestern part of the Caribbean Plate on which carbonate platforms have been formed on basement highs (Arden, 1975; Duncan et al., 1999). Site 1000 is located at 927.2 m water depth in the Pedro Channel along the northern Nicaraguan Rise, which is surrounded by the Cayman Trough to the north, and the southern Nicaraguan Rise and Colombian Basin to the south. The Pedro Channel is the widest (ca. 150 km) and deepest (ca. 1350–1450 m) channel along the east-northeast trending Nicaraguan Rise. It is bounded by shallow-water (30 m) carbonate banks on three sides, which include the Pedro Bank to the east, the Rosalind Bank to the west, and the Serranilla Bank, Alice Shoal, and Banco Nuevo to the south. Carbonate preservation is excellent at Site 1000 compared to other ODP sites because of its shallow location far above the lysocline (Figure 21).

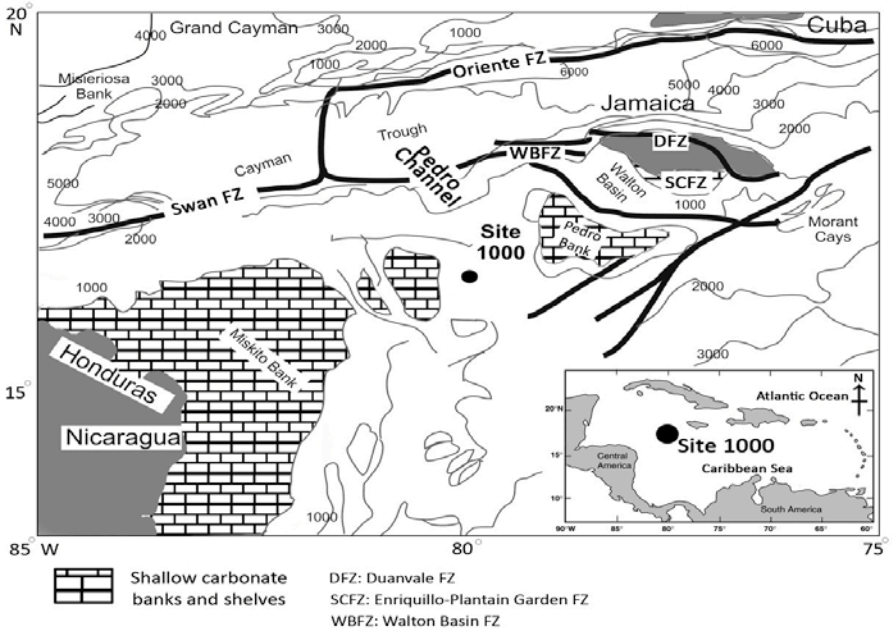


**Figure 20.** Location of ODP Site 1000 in the Pedro Channel, Caribbean Sea (modified from Sigurdsson et al., 1997)

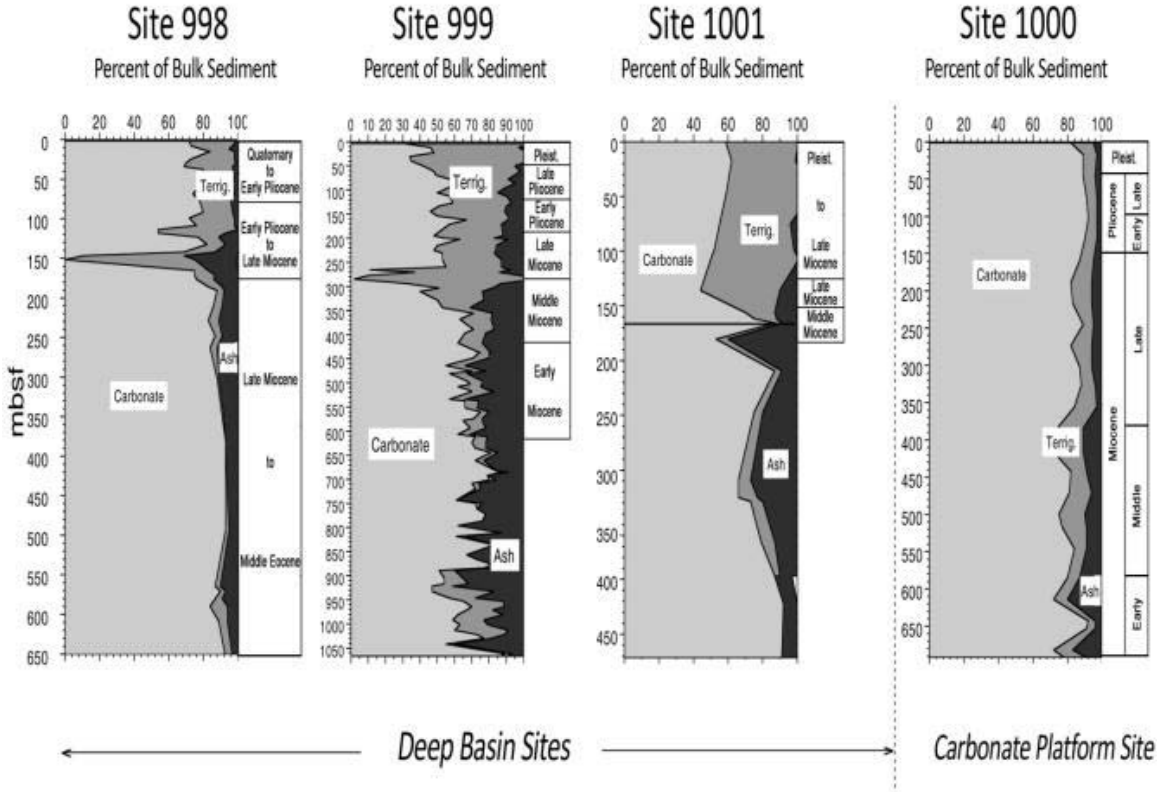


**Figure 21.** Carbonate preservation at Site 1000 compared with other ODP sites in Caribbean Sea (modified from Sigurdsson et al., 1997).

A detailed lithologic description of the studied interval at Site 1000 and its subdivision into lithological units is summarized in Figures 22 and 23. An approximately 695 m thick, continuous Lower Miocene to present-day sedimentary sequence was drilled at Site 1000. This sequence mainly consists of nannofossil micritic oozes, chalks, limestones with intermittent foraminifers, and clays, deposited at relatively constant sedimentation rates of 3.41 cm/kyr. The uppermost Miocene and the basal Pliocene correspond to a time of relatively low carbonate accumulation rates. The later part of the Pliocene and the Pleistocene are characterized by the lowest carbonate accumulation (Sigurdsson et al., 1997).

Two holes (1000A and 1000B) were drilled. Hole 1000A ultimated in Middle Miocene calcareous limestone with nannofossils after coring mainly periplatform oozes and chalks. It was cored with the advanced hydraulic piston corer to a depth of 312.9 mbsf (Middle Miocene) with 103.5% recovery, and then cored with an extended core barrel to a depth of 553.2 mbsf with 89.2% recovery.

Hole 1000B was terminated in Lower Miocene limestone at a depth of 695.9 mbsf with recovery averaging 67.6% over the cored interval which recovered two cores in oozes above 117 mbsf before the hole was drilled ahead to a depth of 503.5 m with the RCB system (Sigurdsson et al., 1997).

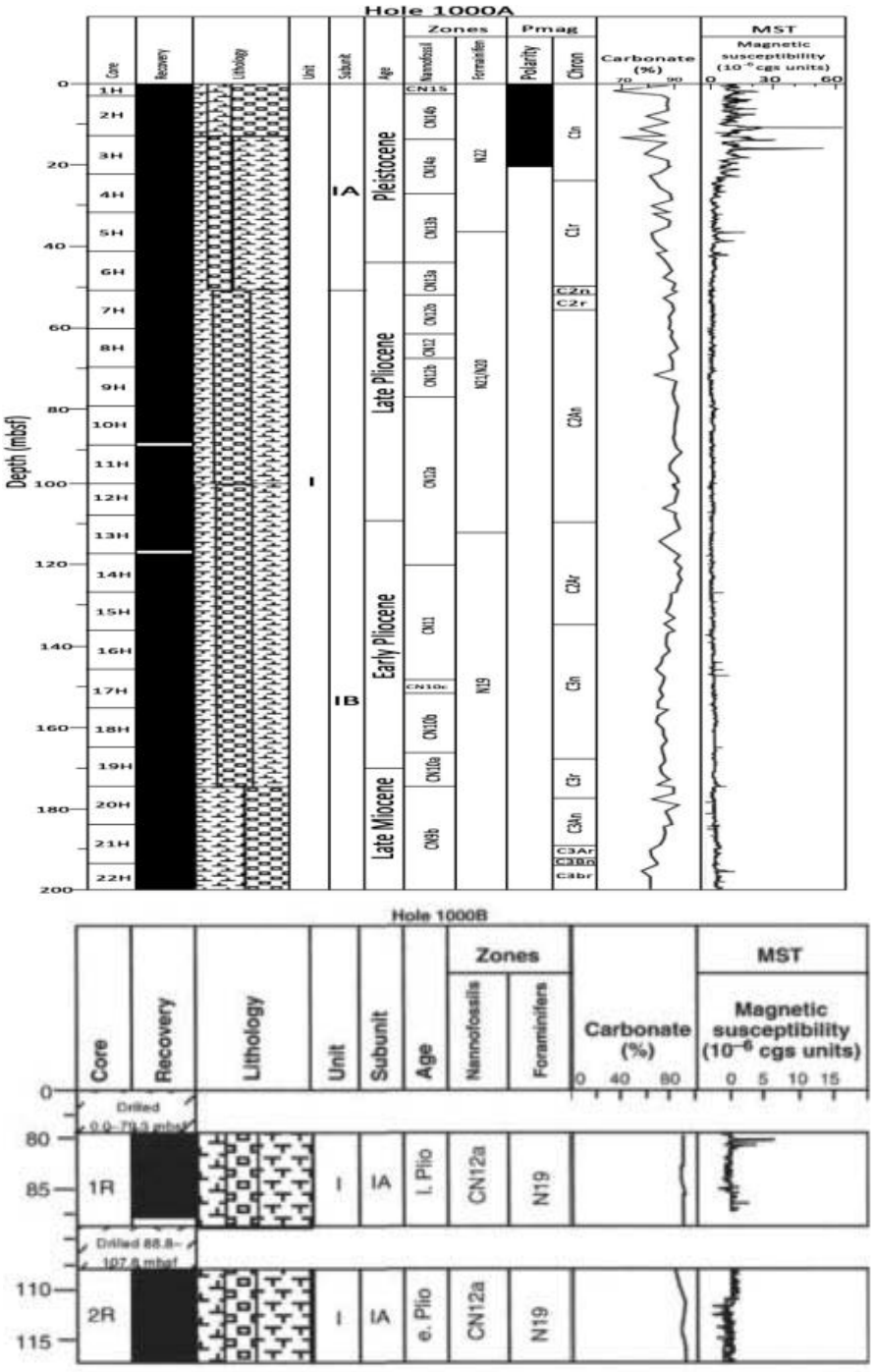


**Figure 22.** Site 1000 summary column for core recovery, lithology, volcanic ash layer occurrence, lithologic unit and subunit boundaries, ages, nannofossil and foraminiferal datum boundaries, magnetic reversal boundaries, carbonate percentages, MST magnetic susceptibilities (modified from Sigurdsson et al., 1997 and not updated).

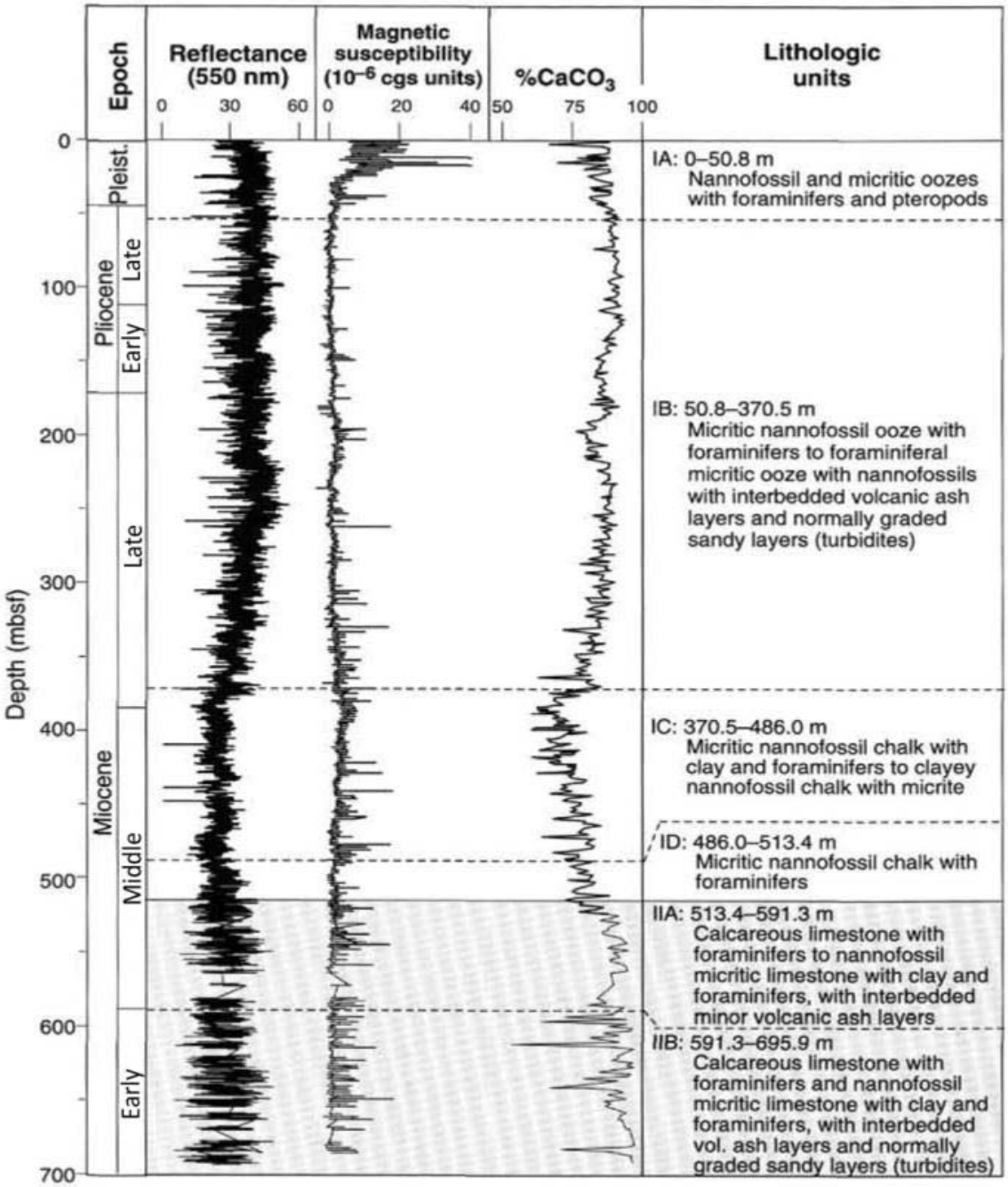


**Figure 23.** Lithologic units of Site 1000 (Holes 1000A and 1000B) and their relationship to down core variations in color reflectance, magnetic susceptibility, and %$CaCO_3$ (from Sigurdsson et al., 1997 and not updated).

### 3.11 Age model of ODP Site 1000

The age model for Site 1000 is primarily based on isotope stratigraphy using the benthic foraminifer *Cibicidoides wuellerstorfi* and on biostratigraphy (Steph et al., 2006). A preliminary age model for Site 1000 was constructed by determining major $\delta^{18}O$ isotopic stages according to the nomenclature of Shackleton et al. (1995) and using the age model and the $\delta^{18}O$ reference record from ODP Site 925/926 from Ceara Rise (Bickert et al., 1997; Tiedemann and Franz, 1997; Shackleton and Hall, 1997). The initial age model suggested the presence of stratigraphic gaps (up to 70 kyr) due to core breaks. A relatively large gap between 3.6 Ma and 3.8 Ma represents drilling-disturbed intervals of overlapping cores 1000A-13H and 1000B-2R that were not sampled. The final age model (Figure 24) exposed the presence of dominant precession cycles in the planktonic $\delta^{18}O$ record, which were then used to further tune the age model from Site 1000 (see Steph et al., 2006 for details). The entire orbitally–tuned $\delta^{18}O$ record extends from 5.5 Ma (Messinian) to 2.2 Ma (Early Pleistocene). Above this level, datums based on the calcareous nannofossil biostratigraphy of Raffi et al. (2006; ODP Sites 925, 926) were used to estimate, by linear interpolation, the ages of samples from Sample 6-4 to the top of the examined sequence (Sample 1-1). Data used in these parts of the age–depth model are given in Table 1.

| Biohorizon | Zone/subzone (transition) | Age (Ma) |
|---|---|---|
| LO *Emiliania huxleyi* | CN14b–CN15, NN20–NN21 | 0.2 |
| HO *Pseudoemiliania lacunosa* | CN14a–CN14b, NN19–NN20 | 0.4 |
| HCO *Reticulofenestra asanoi* | CN13bD–CN14a | 0.8 |
| HO large *Gephyrocapsa* (45.5 mm) | CN13bC–CN13bD | 1.2 |
| LCO large *Gephyrocapsa* (45.5 mm) | CN13bB–CN13bC | 1.4 |
| LO medium *Gephyrocapsa* (>3.5 mm) | CN13a–CN13bA | 1.6 |
| HO *Discoaster brouweri* | CN12d–CN13a | 1.8 |

**Table 1.** Astronomical age estimates of calcareous nannofossil biohorizons and ages of stage boundaries in the interval 1.8–0.2 Ma (from Raffi et al, 2006 and references therein).

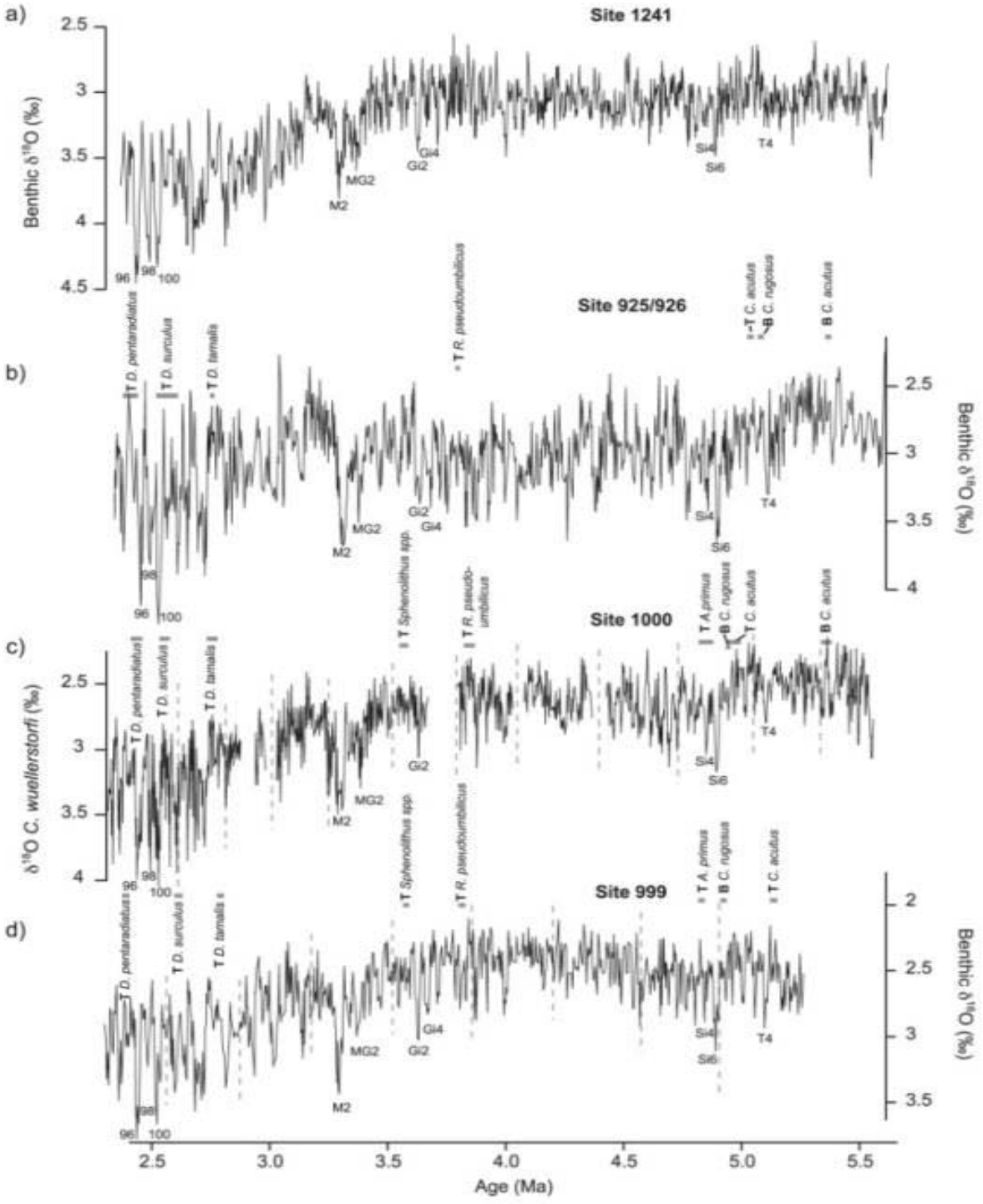


**Figure 24.** Benthic $\delta^{18}O$ records of (a) tropical east Pacific Site 1241 (Tiedemann et al., 2006) and (b) western Atlantic Sites 925/926 (Bickert et al., 1997; Tiedemann and Franz, 1997; Shackleton and Hall, 1997) correlated to benthic $\delta^{18}O$ records from Caribbean Sites (c) 1000 (d) 999 (Haug and Tiedemann, 1998). Dashed lines indicate core breaks at Caribbean Sites (from Steph et al., 2006).

## 4. MATERIAL AND METHODS

### 4.1 Sample selection

A total of 70 analyzed samples span the uppermost Miocene (Messinian) through Middle Pleistocene (5.5–0.2 Ma) of ODP Site 1000. They are primarily from Hole 1000A (65 samples), but are supplemented by five samples from cores 1R and 2R of Hole 1000B to stratigraphically splice across drilling-disturbed intervals of Cores 1000A-10H and 1000A-13H, respectively. Samples were taken with an average spacing of 2.62 m representing an average duration of 80 kyr. However, five closely-spaced samples between 103.33 and 100.93 mbsf were analysed to examine MIS M2 in the Lower Piacenzian.

A published high-resolution Mg/Ca record based on the planktonic foraminifer *Globigerinoides sacculifer* from the latest Miocene to Early Pliocene (5.5–3.8 Ma) at Site 1000 provided a reconstruction of SST, and had been combined with $\delta^{18}O$ to estimate relative changes in SSS resulting from the shoaling of the CAS (Groeneveld et al., 2008; Figure 25). Samples in the present study were chosen from the same and as close a position as possible (average 1.79 cm, 1792 kyr) to the level at which samples (Table 2) were taken by Groeneveld et al. (2008) (Figure 25) in order to compare the foraminiferal Mg/Ca paleotemperature and salinity estimate with each dinocyst assemblage.

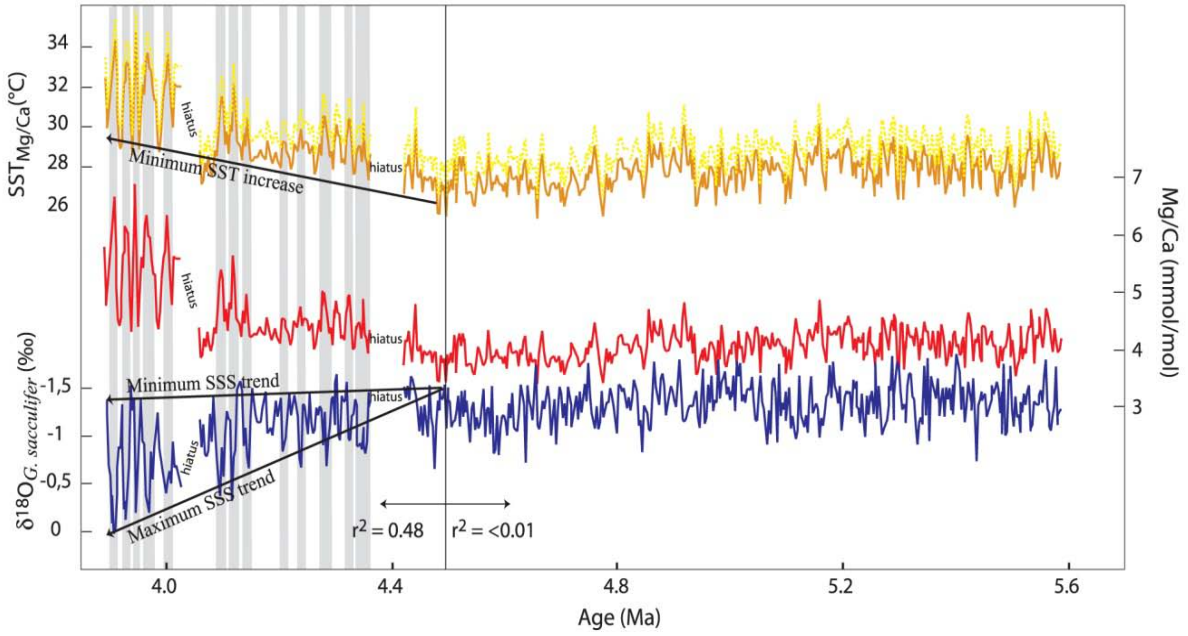


**Figure 25.** Planktonic foraminiferal Mg/Ca results for ODP Site 1000 for the time interval 5.6 Ma to 3.9 Ma, allowing reconstructing of SST and SSS. Arrow in Mg/Ca indicates the paleoceanographically reliable trend, solely based on those samples which do not contain any indications for secondary influences on Mg/Ca, associated with the restriction of upper ocean water masses between the Pacific and the Caribbean since 4.5 Ma (from Groeneveld et al., 2008).

| Palynological sample code | Palynological sample depth (mbsf) | Age (Ma) | Foraminiferal Mg/Ca depth (mbsf) | Depth differences (cm) | Duration of depth difference (kyr) | SST $_{Mg/Ca}$ (°C) | $\delta^{18}O$ ‰ | $\delta^{13}C$ ‰ |
|---|---|---|---|---|---|---|---|---|
| 24 | 120.53 | 3.800 | 120.55 | 2.00 | 2000.00 | 34.2 | 0.0442 | 1.8048 |
| 23 | 122.73 | 3.900 | 122.75 | 2.00 | 2000.00 | 33.5 | 0.0305 | 1.7929 |
| 22 | 124.56 | 3.900 | 124.55 | 1.00 | 1000.00 | 34.7 | -0.1868 | 2.0027 |
| 21 | 126.00 | 3.900 | 126.05 | 5.00 | 5000.00 | 29.7 | -0.741 | 2.1175 |
| 20 | 127.83 | 4.000 | 127.85 | 2.00 | 2000.00 | 28.5 | -0.7569 | 2.0117 |
| 19 | 128.87 | 4.100 | 128.85 | 2.00 | 2000.00 | 32.1 | -0.7691 | 2.0552 |
| 18 | 133.83 | 4.200 | 133.85 | 2.00 | 2000.00 | 27.8 | -1.4058 | 1.5642 |
| 17 | 135.03 | 4.300 | 135.05 | 2.00 | 2000.00 | 30.4 | -0.947 | 1.7213 |
| 16 | 137.93 | 4.400 | 137.95 | 3.00 | 3000.00 | 27.4 | -0.6466 | 1.5735 |
| 15 | 139.93 | 4.500 | 139.95 | 2.00 | 2000.00 | 28.5 | -1.1981 | 1.9429 |
| 14 | 142.77 | 4.600 | 142.75 | 2.00 | 2000.00 | 28.0 | -1.1792 | 1.8533 |
| 13 | 145.53 | 4.700 | 145.55 | 2.00 | 2000.00 | 26.9 | -1.1798 | 1.9327 |
| 12 | 147.73 | 4.800 | 147.75 | 2.00 | 2000.00 | 27.3 | -1.0224 | 2.2455 |
| 11 | 151.13 | 4.900 | 151.15 | 2.00 | 2000.00 | 30.1 | -1.1417 | 1.7202 |
| 10 | 155.53 | 5.000 | 155.55 | 2.00 | 2000.00 | 28.4 | -1.3489 | 1.4519 |
| 9 | 158.77 | 5.100 | 158.75 | 2.00 | 2000.00 | 28.5 | -1.2734 | 1.6391 |
| 8 | 161.93 | 5.200 | 161.95 | 2.00 | 2000.00 | 28.8 | -1.424 | 1.9456 |
| 7 | 164.15 | 5.300 | 164.15 | 0.00 | 0.00 | 26.4 | -1.5326 | 1.981 |
| 6 | 167.85 | 5.400 | 167.85 | 0.00 | 0.00 | 27.8 | -1.4674 | 1.9631 |
| 5 | 171.43 | 5.500 | 171.45 | 2.00 | 2000.00 | 27.2 | -1.0954 | 1.739 |
| 4 | 174.44 | 5.500 | 174.44 | 0.00 | 0.00 | 30.7 | -1.04 | 2.05 |
| 3 | 176.43 | 5.500 | 176.44 | 1.00 | 1000.00 | 30.0 | -0.88 | 1.57 |
| 2 | 178.43 | 5.500 | 178.44 | 1.00 | 1000.00 | 27.9 | -0.71 | 1.80 |
| 1 | 183.46 | 5.500 | 183.44 | 2.00 | 2000.00 | 27.2 | -1.03 | 2.15 |

**Table 2.** Foraminifera data (from Groeneveld et al., 2008) and sample codes (this study).

### 4.2 Palynological processing and counting

Dry carbonate samples from the uppermost Miocene–Lower Pleistocene were weighed (average 24.5 g) and processed in the Department of Earth Sciences at Brock University using standard procedures involving cold HCl (20% conc.) and cold HF (48%). The least amount of chemical and mechanical treatment was employed, with no oxidation or alkali treatments being used. Two *Lycopodium clavatum* spore tablets (batch number 1031), containing an estimated 41697±2186 spores (20848 per tablet) were then added to the residue in each centrifuge tube with a little HCl as necessary to dissolve the tablets. These enabled the estimation of palynomorph concentrations (Stockmarr, 1971; Maher, 1981; Mertens et al., 2009; Table 3).

After thorough homogenization, the organic residue was sieved using a Nitex 10-μm nylon screen (discarded after each sample), then mixed with glycerine jelly and strew mounted onto at least four microscope slides in order to count the palynomorphs. Additional residues of all samples were stained with safranin-o and re-sieved at 20 μm before mounting with glycerine jelly. These slides were used for identifying larger dinocysts, searching for rare taxa, and photographing important species. No ultrasound was used on any residues, as they did not contain large amounts of obscuring amorphous organic material. Counting was performed at 400x and 1000x magnification using a Leica DM 2500 transmitted light microscope. Around 300 cysts were counted per sample, although six samples were not rich enough to count a minimum of 200 specimens. After reaching 300 cysts, the remainders of the 20 μm slides were scanned at 400x and 1000x objective for rare taxa not seen during counting. The following additional palynomorph groups were also counted: acritarchs, copepod fragments, foraminiferal linings, angiosperm pollen, bisaccate pollen, fern and bryophyte spores, and fungal spores and hyphae.

An England Finder reference follows the sample and slide number for each specimen illustrated. Detailed morphological analysis of dinocysts and acritarch species was performed using a 100x oil objective. All photographs were taken with a Leica DMR microscope with a Leica DFC490 digital camera (Plates 1–8). All counts are given in Table 3.

### 4.3 Statistical analysis

To allow comparison with other studies, only the dinocyst data were used in the constrained cluster analysis (CCA), and because of low counts recorded in the two highest samples only 68 samples were used in the statistical analyses (see Results section).

CCA combines individual samples into larger groups by agglomerating them with similar features while constraining the stratigraphic position of samples (e.g., Dale and Dale, 2002a). The statistical package PAST (Ryan et al., 1995; Hammer et al., 2009) was applied.

## 5. RESULTS

### 5.1 Composition of palynological assemblages

Of the palynomorph groups represented, both marine (dinocysts, acritarchs, copepods, invertebrate remains) and transported terrestrial groups (including angiosperm and bisaccate pollen, embryophyte spores, fungal spores, and freshwater palynomorphs) were distinguished. Abundances are shown in alphabetical order in Table 3, although only the dinocysts and acritarchs were classified to species level, where possible. A total of 49 dinocyst and 11 acritarch taxa were recorded that were abundant and generally well-preseved with no indication of obvious reworking. Marine palynomorphs consist mostly of gonyaulacacean dinocysts (0–39%), while the terrestrial palynomorphs mainly comprise angiosperm pollen and fern and bryophyte spores (0–3%) and bissacate pollen (mostly *Pinus* spp., *Picea* spp. and *Abies* spp., 1–2 %) showing variable degrees of preservation. All percentages are based on the total count including all palynomorphs groups.

The dinocysts are mainly neritic gonyaulacaceans, with low percentages of outer neritic–oceanic taxa (1–3%) and protoperidinioid species (0–4%). Cosmopolitan neritic species such as *Achomosphaera*/*Spiniferite*s spp. indet. (14–39%) are abundant and mostly well-preserved. *Operculodinium* species (23–33%) are mainly represented by *O. centrocarpum–israelianum* and *O. bahamense*. Moreover, *Polysphaeridium zoharyi* (1–12%), *Dapsilidinium pseudocolligerum* (0–3%) and *Lingulodinium machaerophorum* (1–2.5%) were documented. Typical outer neritic–oceanic species are registered by *Amiculosphaera umbraculum*, *Edwardsiella sexispinosa*, *Impagidinium* spp., and *Nematosphaeropsis* spp. Protoperidinioid dinocysts are mainly represented by *Brigantedinium* spp. indet., and partial oxidation has caused the separation of wall layers in some specimens (e.g., *Lejeunecysta* spp. indet.). In addition, acritarchs (0–2%), foraminiferal linings (only those with six or more chambers were counted, 5.5–19%; see Traverse and Ginsburg, 1966; Head and Westphal, 1999), unidentified invertebrate remains and copepod appendages (0.2–7%), and sporadic occurrences of the green alga *Pediastrum* spp. were registered (see Table 3).

Additional components based on qualitative observations include brown to dark brown structured and unstructured (cuticle and tracheid) partially pyritized wood particles with variable amounts of black debris. Charcoal particles and non-charcoalified black debris were not distinguished. Low to high percentages of amorphous organic matter (AOM) with brownish, fluffy, granular and partly pyritized characteristics were recorded.

Eleven dinocyst and five acritarch taxa are treated informally in the present study and listed in Table 3. They are apparently new to science and described in Appendix 2. An alphabetical list of palynomorph assemblages is given in Appendix 1.

The overall assemblage characteristics for each stage and/or subseries are given below.

**5.1.1 Upper Miocene (Messinian, 5.5–5.4 Ma)**

Dinocysts assemblages are dominated by gonyaulacacean cysts and neritic taxa, particularly *Polysphaeridium zoharyi* (8–19%), *Achomosphaera/Spiniferites* spp. indet. (12–18%), *Operculodinium* species including the *O. centrocarpum–israelianum* complex (12–17.5%), *O. bahamense* (6–17%), *Operculodinium* sp. A (1–4), *O. longispinigerum* (0.2–1.5%), *O. janduchenei* (0–1.5%), cf. *Batiacasphaera hirsuta* (1–3%), *Dapsilidinium pseudocolligerum* (0.2–3%), *Batiacasphaera* spp. indet. (0–3%), *Lingulodinium machaerophorum* (0–2%), *Hystrichokolpoma rigaudiae* (0–1%), linings of calcareous dinocysts (0–1%), *Spiniferites mirabilis* (0–0.4%), and *Tuberculodinium vancampoae* (0–0.2%). *Ataxiodinium*? spp. and cf. *Blysmatodinium* sp. were recorded in sample numbers 20-3 and 19-3 respectively, Dinocyst sp. A (0.2%) in sample numbers 19-3 and 19-5, and *Pyxidinopsis* sp. A (0.2%) in sample number 19-3 (Table 4). Outer neritic–oceanic species are represented by *Nematosphaeropsis labyrinthus* (0.2–1%) and the genus *Impagidinium*, which is mostly represented by *I. patulum* (0–2%). Heterotrophic dinocysts are generally scarce, being mainly represented by *Selenopemphix quanta* (1–6%), *Brigantedinium*? spp. indet. (1–6%), *Lejeunecysta* spp. indet. (1–2%) and *Selenopemphix nephroides* (0–1%).

Acritarchs are mainly represented by *Cyclopsiella elliptica/granosa* (1–3%), leiospheres (0.6–1%), *Paralecaniella indentata* (0.4–1%), *Cymatiosphaera latisepta* (0–0.5%), *Cymatiosphaera* sp. A (0.2%), *Nannobarbophora walldalei* (0.2% in sample number 19-3) and Acritarch sp. A (0.2%, in sample number 20-7). Other marine palynomorphs are generally represented by foraminiferal linings (5–10%), and copepods and other invertebrate remains (1–7%).

Terrestrial palynomorphs are mostly angiosperm pollen, fern and bryophyte spores, fungal spores and hyphae (0–6%) and bisaccate pollen (0–0.2%).

**5.1.2 Lower Pliocene (Zanclean, 5.3–3.6 Ma)**

Assemblages are characterized by *Operculodinium* species including the *O. centrocarpum–israelianum* complex (9–30%), *O. bahamense* (6–22%), *O. janduchenei* (0–2.5%), *O. longispinigerum* (0–1%), *Operculodinium* sp. A (0–2%), *Achomosphaera/Spiniferites* spp. indet. (13–25%), *Polysphaeridium zoharyi* (1–25%), *Dapsilidinium pseudocolligerum* (0–13%), *Lingulodinium machaerophorum* (0–4%), *Tuberculodinium vancampoae* (0–4%), cf.

*Batiacasphaera hirsuta* (0–2%), *Hystrichokolpoma rigaudiae* (0–2%), and calcareous dinocyst linings (0–1.5%). Outer neritic–oceanic species chiefly consist of *Nematosphaeropsis labyrinthus* (0–8%) and *Impagidinium* spp. of which most are *Impagidinium plicatum* (0–5%), *I. velorum* (0.2% in sample number 14-1), *Edwardsiella sexispinosa* (0–0.5%), and *Amiculosphaera umbraculum* (0.2% in sample number 17-4). There are also sparse occurrences of cf. *Blysmatodinium* sp., Dinocyst sp. A, Dinocyst sp. B, *Impagidinium* sp. B, *Habibacysta tectata*, *Operculodinium* sp. B, *Pentapharsodinium dalei*, *Pyxidinopsis reticulata, Pyxidinopsis* sp. A, *Spiniferites rhizophorus* and *S. mirabilis* (Figure 27). Heterotrophic dinocysts are mostly represented by *Brigantedinium*? spp. indet. (1–6.5%), *Selenopemphix nephroides* (0–4%), and *Lejeunecysta* spp. indet. (0–3.5%).

Other marine palynomorphs are mainly represented by foraminiferal linings (3–15.8%), Acritarch sp. D (0–6.5%), *Cyclopsiella elliptica/granosa* (0–3%), leiospheres (0–1.5%), *Paralecaniella indentata* (0–1.5%), *Nannobarbophora walldalei* (0–1%), *Cymatiosphaera latisepta* (0–0.2%), and copepods and other invertebrate remains (0–5%). There are sparse occurrences of Acritach sp. B, Acritach spp. C, Acritach spp. D and *Cymatiosphaera* spp. A (Table 4).

Terrestrial palynomorphs comprise angiosperm pollen, fern and bryophyte spores, fungal spores and hyphae (0–4%) and bisaccate pollen (0–1%).

**5.1.3 Upper Pliocene (Piacenzian, 3.5–2.6 Ma)**

This interval is characterized by *Operculodinium* species including *O. centrocarpum–israelianum* (10–43%), *O. bahamense* (0–7%), *O. longispinigerum* (1.1%, sample number 12-2), *O. janduchenei* (0–0.3%), *Achomosphaera/Spiniferites* spp. indet. (15–40%), *Polysphaeridium zoharyi* (0–42%), *Lingulodinium machaerophorum* (0–7%), linings of calcareous dinocysts (0–7%), *Dapsilidinium pseudocolligerum* (0–6%), *Hystrichokolpoma rigaudiae* (0–0.5%), and *Tuberculodinium vancampoae* (0–0.5%). Outer neritic–oceanic species are mainly *Edwardsiella sexispinosa* (0.5% in sample number 1-4), *Nematosphaeropsis lativittata* (0.5% in sample number 11-2), *N.* cf. *rigida* (0–0.2%), *N. labyrinthus* (0–0.2%) and *Impagidinium* spp. (0–3%) of which most are *I. patulum*. Also recorded were sporadic occurrences of *Ataxiodinium choane*, cf. *Corrudinium harlandii*, Dinocyst sp. A, *Impagidinium* sp. A, *Impagidinium* sp. B, *Spiniferites mirabilis, Operculodinium* sp. A, *Pentapharsodinium dalei* and *Pyxidinopsis* sp. A (Figure 27). Heterotrophic dinocysts are mainly represented by *Brigantedinium*? spp. (0–7%). *Selenopemphix* cf. *undulata* (1%) was recorded in a sample (2R-3).

Other marine palynomorphs present are foraminiferal linings (0–37%), copepods and other invertebrate remains (0–7%), leiospheres (0–9%), *Cyclopsiella elliptica/granosa* (0–1.5%),

Acritarch sp. D (0–1%), *Nannobarbophora walldalei* (0–1%), Acritarch spp. A, and Acritarch spp. C in some intervals.

Terrestrial palynomorphs mainly comprise angiosperm pollen, fern and bryophyte spores, fungal spores and hyphae (0–3%) and bisaccate pollen (0–0.5%).

### 5.1.4 Lower and Middle Pleistocene (2.5–0.2 Ma)

#### Gelasian (2.5–2.2 Ma)

This interval is characterized by *Polysphaeridium zoharyi* (0–39%), *Achomosphaera/Spiniferites* spp. (10–35%), *Operculodinium* species including *O. centrocarpum–israelianum* (10–34%), *O. bahamense* (0.5–3%), *Operculodinium* sp. A (0.5%, in sample number 8-2), *O. longispinigerum* (0.2%, in sample number 8-6) and *O. janduchenei* (0.2%, in sample number 5-3), *Lingulodinium machaerophorum* (0–6%), calcareous dinocysts (0–3%), *Dapsilidinium pseudocolligerum* (0–2%), *Hystrichokolpoma rigaudiae* (0–0.5%), *Tuberculodinium vancampoae* (0–0.5%) and *Pyxidinopsis* sp. A (0.1%, in sample number 8-3). Outer neritic–oceanic species mainly consist of *Nematosphaeropsis labyrinthus* (0–1%), and *Impagidinium* spp. (0–2%) which are mainly represented by *I. patulum.* Sporadic occurrences of *Nematosphaeropsis* cf. *rigida*, *Pentapharsodinium dalei* and *Spiniferites mirabilis* were also recorded (Figure 27). Heterotrophic dinocysts were mainly represented by *Brigantedinium* spp. (0–5%).

Acritarchs are mainly represented by leiospheres (0–3%), *Cyclopsiella elliptica/granosa* (0–2%), *Nannobarbophora walldalei* (0–1%), Acritarch sp. D (0–0.4), and *Cymatiosphaera latisepta* (0.1%, in sample number 8-3).

Also present are foraminiferal linings (6.5–31%), copepods and other invertebrate remains (0–10%). Terrestrial palynomorphs mainly consist of angiosperm pollen, and fern and bryophyte spores, fungal spores and hyphae (0–3%) and bisaccate pollen (0.5%, in sample number 8-1).

#### Calabrian (1.8–0.8 Ma)

This interval is characterized by *Achomosphaera/Spiniferites* spp. (15–56.5%), *Polysphaeridium zoharyi* (0–14%), *Operculodinium* species including the *O. centrocarpum–israelianum* complex (19–43%), *O. bahamense* (0–1.2%), and *Operculodinium* sp. A (0.5%, in sample number 5-3), *Lingulodinium machaerophorum* (0–4.7%), *Hystrichokolpoma rigaudiae* (0–2.2%), calcareous dinocysts (0–0.8%), and *Pentapharsodinium dalei* (0.5%, in sample number 5-7). Outer neritic–oceanic species are mainly represented by *Nematosphaeropsis labyrinthus* (0–1), *N. lativittata* (0.4%, in sample number 6-2), and *Impagidinium* spp. (0–2%) of which most are

*I. strialatum* (Figure 27). Heterotrophic dinocysts are mainly represented by *Brigantedinium* spp. (13.8%, in sample number 4-2).

Acritarchs are mainly represented by *Paralacaniella indentata* (3%, in sample number 4-2), Acritarch spp. D (0–2.2), and *Cyclopsiella elliptica/granosa* (0.88%, in sample number 6-2). Also present are foraminiferal linings (0–15%) and copepods and invertebrate remains (0–2.5%). Terrestrial palynomorphs mainly comprise angiosperm pollen, fern and bryophyte spores, fungal spores and hyphae (0–5%) and bisaccate pollen (0–4.7%).

**Middle Pleistocene (0.4–0.2 Ma)**

This interval is characterized by *Achomosphaera/Spiniferites* spp. indet. (32–66.6%), *Operculodinium* species including the *O. centrocarpum–israelianum* complex (8.6–30%) and *O. janduchenei* (0–4%), *Lingulodinium machaerophorum* (2 %, in sample number 3-2), *Polysphaeridium zoharyi* (1.8%, in sample number 3-2). Outer neritic–oceanic species mainly comprise *Nematosphaeropsis* cf. *rigida* (1%, in sample number 3-2), and *Impagidinium* spp. of which most are *I. strialatum* (0–4%).

Acritarchs are represented by *Cyclopsiella elliptica/granosa* (3.5%, in sample number 1-1) and Acritarch spp. C (0.5%, in sample 3-2). Also present are foraminiferal linings (24%, in sample number 1-1) and copepods and other invertebrate remains (0–10%). Terrestrial palynomorphs mainly comprise angiosperm pollen, and fern and bryophyte spores, fungal spores and hyphae (0–8.6%) and bisaccate pollen (1.5%, in sample number 1-1).

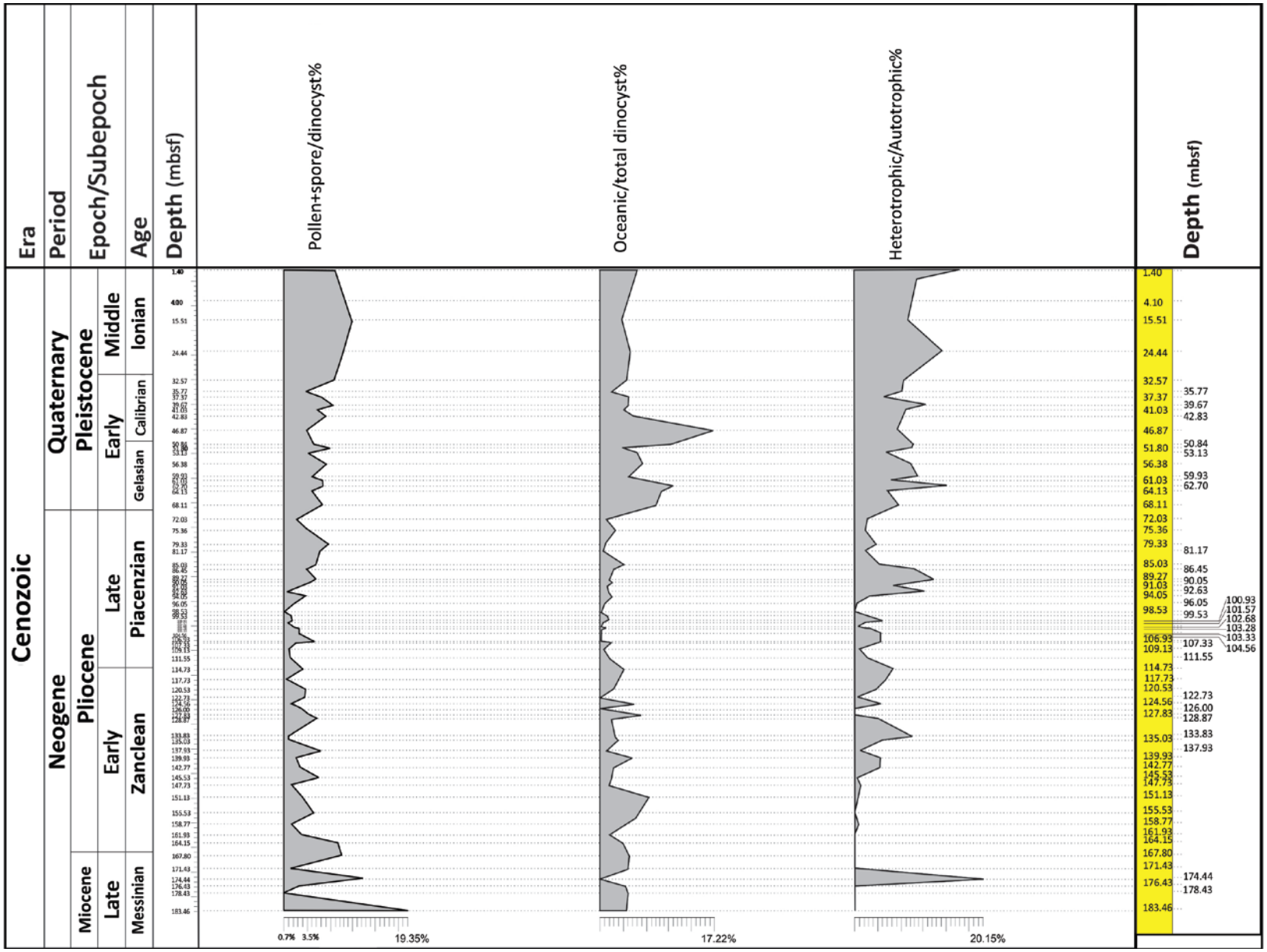


**Figure 26.** Ratios of pollen+spore/dinocyst, oceanic/total dinocysts and heterotrophic/autotrophic dinocysts throughout the studied interval (5.5–0.2 Ma).

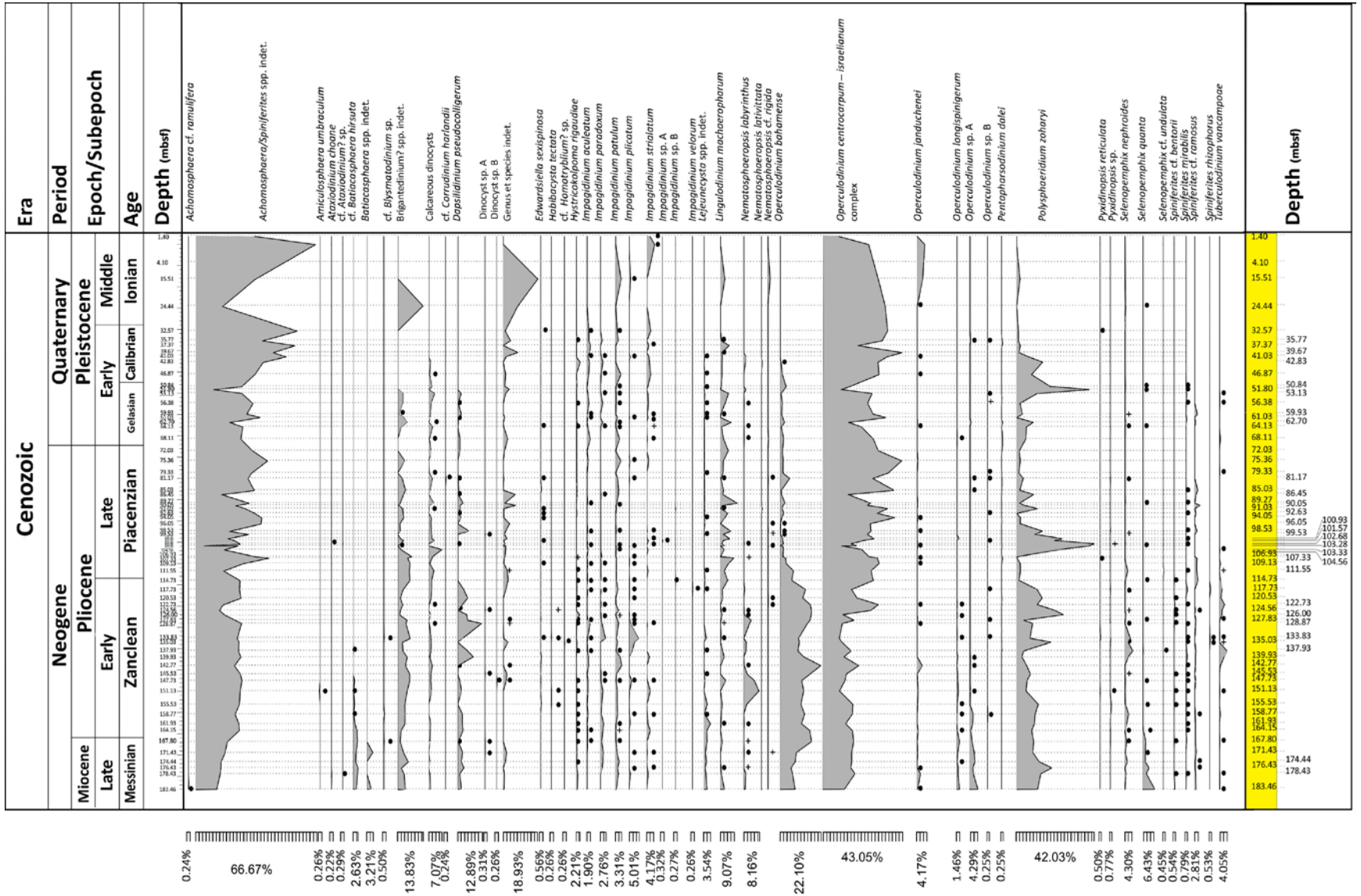


**Figure 27.** Relative abundances of dinocysts cyst taxa recovered in this study. A cross (+) indicates rare occurrences of taxa recorded outside of the counts. A solid dot indicates taxa recorded in the counts with frequencies below 1%.

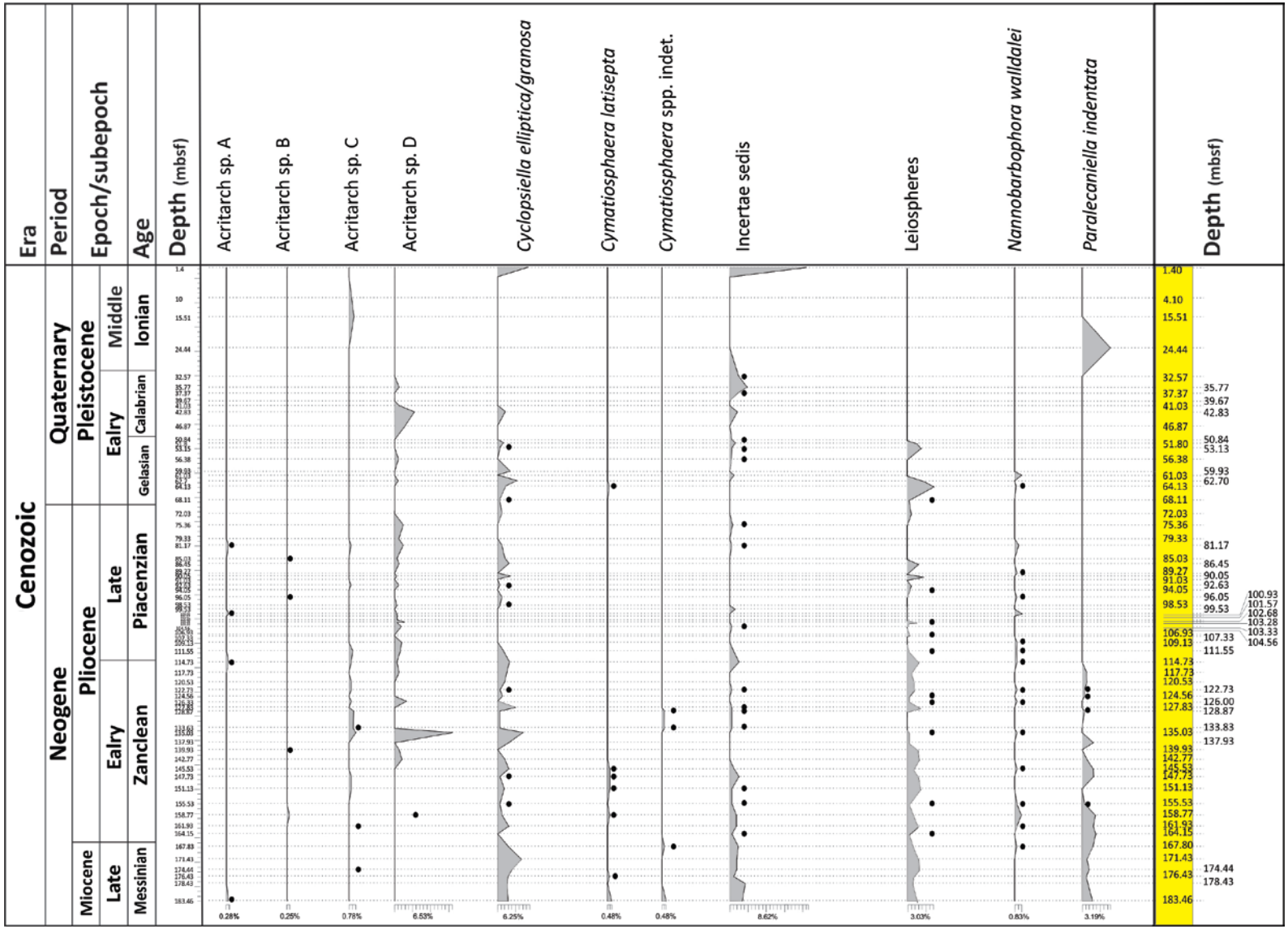


**Figure 28.** Relative abundances of acritarch taxa recovered in this study (based on percentage of total acritarchs). A solid dot indicates taxa recorded in the counts with frequencies below 1%.

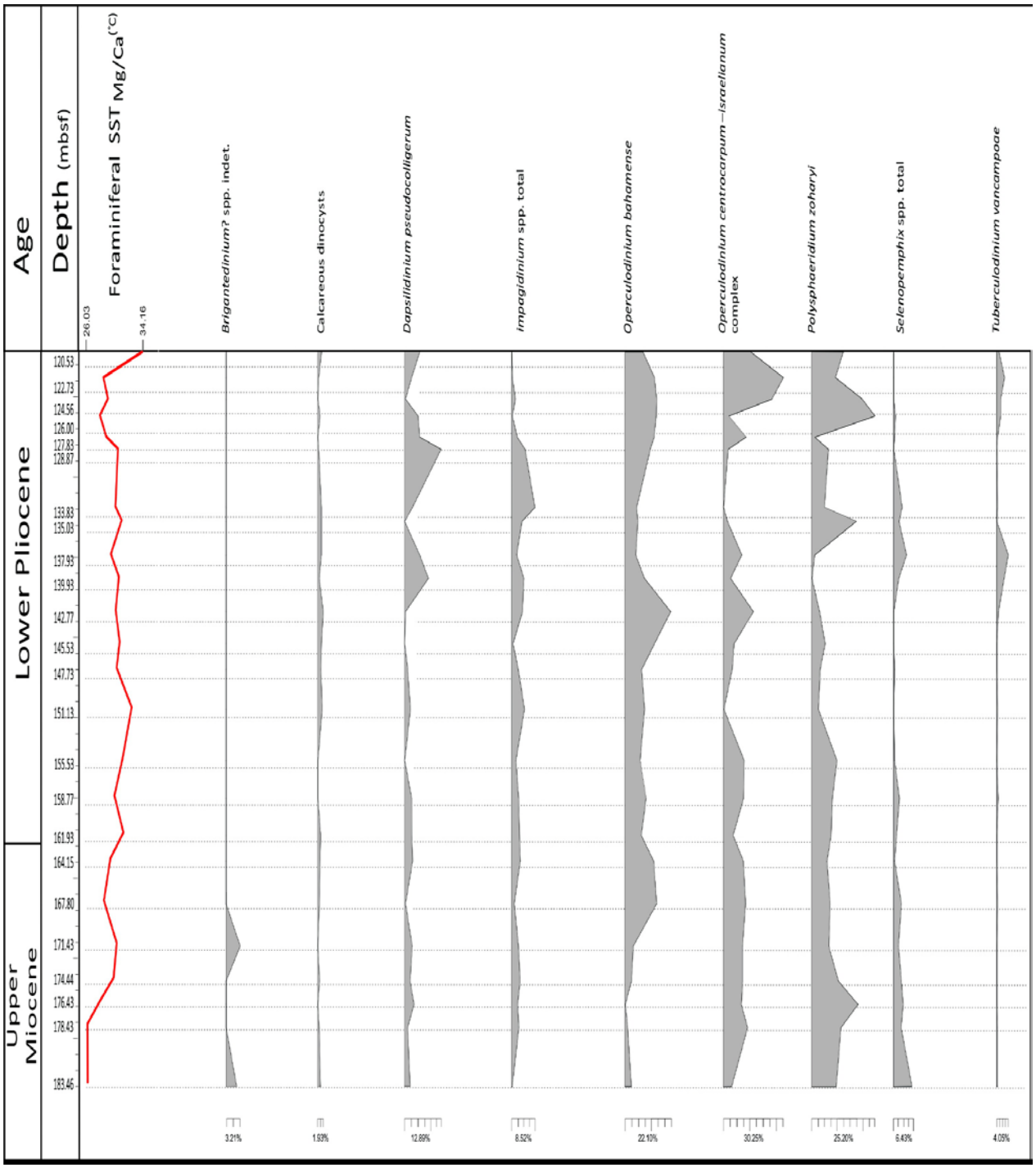


**Figure 29.** Selected dinocyst taxa (as percentage of total palynomorphs) compared with the Mg/Ca-based SST from the Upper Miocene to Lower Pliocene (5.6–3.9 Ma).

## 5.2 Results of statistical analysis

Six main informal dinocyst assemblage biozones (DAZ 1–6) were delineated based on constrained cluster analysis (Figure 30). The two uppermost samples, samples 69 and 70 (Middle Pleistocene), were excluded from the analysis because they yielded too few dinocysts. These two samples are assigned to a separate zone, DAZ 7. The dinocyst assemblage biozones are characterized as follows:

### 5.2.1 Dinocyst assemblage biozonation and constrained cluster analysis

Six main informal dinocyst assemblage biozones (DAZ 1–6) were delineated based on constrained cluster analysis (Figure 35). The two uppermost samples, samples 69 and 70 (Middle Pleistocene), were excluded from the analysis because they yielded too few dinocysts. These two samples are assigned to a separate zone, DAZ 7. The dinocyst assemblage biozones are characterized as follows:

**Dinocyst assemblage biozone 1: samples 1–25, 183.46–117.73 m (5.5–3.8 Ma):**

*Achomosphaera/Spiniferites* spp. indet. (16–34%), *Polysphaeridium zoharyi* (4–31%), *Operculodinium* spp. total (0–26%), *Dapsilidinium pseudocolligerum* (0–14%), *Brigantedinium*? spp. indet. (1–10%), outer neritic–oceanic taxa (0–10%), *Selenopemphix* spp. (0–8%), *Lejeunecysta* spp. indet. (0–5%), *Tuberculodinium vancampoae* (0–5%), *Batiacasphaera* spp. indet. (0–4.5%), *Lingulodinium machaerophorum* (0–4%), cf. *Batiacasphaera hirsuta* (0–3.5%), calcareous dinocysts (0–2%), *Hystrichokolpoma rigaudiae* (0–2%), *Spiniferites* spp. total (0–1%).

**Dinocyst assemblage biozone 2: samples 26–30, 114.73–106.93 m (3.7 –3.4 Ma):**

*Achomosphaera/Spiniferites* spp. indet. (23–47%), *Operculodinium* spp. total (0–40%), *Brigantedinium*? spp., (6–10%), *Lingulodinium machaerophorum* (0–8%), calcareous dinocysts (0.6–4%), *Polysphaeridium zoharyi* (0–3%), *Spiniferites spp.* (0–2%), *Selenopemphix nephroides* (0–2%), oceanic taxa (0–1%), *Tuberculodinium vancampoae* (0–1%), *Lejeunecysta* spp. indet. (0–1%) and *Hystrichokolpoma rigaudiae* (0–0.5 %).

**Dinocyst assemblage biozone 3: samples 31–34, 104.56–102.68 m (3.4–3.3 Ma):**

*Polysphaeridium zoharyi* (31–61%), *Achomosphaera/Spiniferites* spp. indet. (7–31%), *Operculodiniu*m spp. total 0 (13) 28%, calcareous dinocysts (0–9.5%), *Lingulodinium machaerophorum* (0–3%), *Brigantedinium*? spp. (0–2%), oceanic taxa (0–1%), *Dapsilidinium pseudocolligerum* (sample 34, 0.3%), *Selenopemphix nephroides* (0.3%), *Spiniferites mirabilis* (0.3%), and *Tuberculodinium vancampoae* (0.3%).

**Dinocyst assemblage biozone 4: samples 35–57, 101.57–53.13 m (3.3–2.2 Ma):**

*Operculodinium* spp. 0 (25) 50%, *Polysphaeridium zoharyi* 0 (15) 30%, *Achomosphaera/Spiniferites* spp. indet. (22–46%), *Lingulodinium machaerophorum* (0–12%), *Brigantedinium*? spp. (0–8%), *Dapsilidinium pseudocolligerum* (0–8%), *Spiniferites* spp. (0–5%), calcareous dinocysts (0–4%), outer neritic–oceanic taxa (0–3.5%), *Hystrichokolpoma rigaudiae* (0–1%), *Lejeunecysta* spp. indet. (0–1%), *Tuberculodinium vancampoae* (0–1%), and *Selenopemphix nephroides* (0–0.5%).

**Dinocyst assemblage biozone 5: sample 58, 51.8 m (2.2 Ma):**

A significant peak of *Polysphaeridium zoharyi* (62%) *Operculodinium* spp. total (0–16%), *Achomosphaera/Spiniferites* spp. indet. (15%), *Nematosphaeropsis labyrinthus* (2%), *Selenopemphix nephroides* (0.3%) and *Spiniferites mirabilis* (0.3%).

**Dinocyst assemblage biozone 6: samples 59–68, 50.84–15.51 m (2.2–0.4 Ma):**

*Achomosphaera/Spiniferites* spp. indet. (23–65%), *Operculodinium* spp. total 0 (25) 54%, *Polysphaeridium zoharyi* 0 (15) 27%, *Brigantedinium*? spp. (sample 67, significant peak of 22%), *Lingulodinium machaerophorum* (0–5), outer neritic–oceanic taxa (0–3.5), calcareous dinocysts (0–2.5%), *Hystrichokolpoma rigaudiae* (0–2.5%), *Selenopemphix nephroides* (0–1%), *Lejeunecysta* spp. indet. (0–0.5%), and *Spiniferites mirabilis* (0–0.5%).

**Dinocyst assemblage biozone 7: samples 69–70, 4.1–1.4 m (0.2 Ma):**

*Achomosphaera/Spiniferites* spp. indet. (32–66%), *Operculodinium* spp. total (0–25%) and *Impagidinium strialatum* (1–4%).

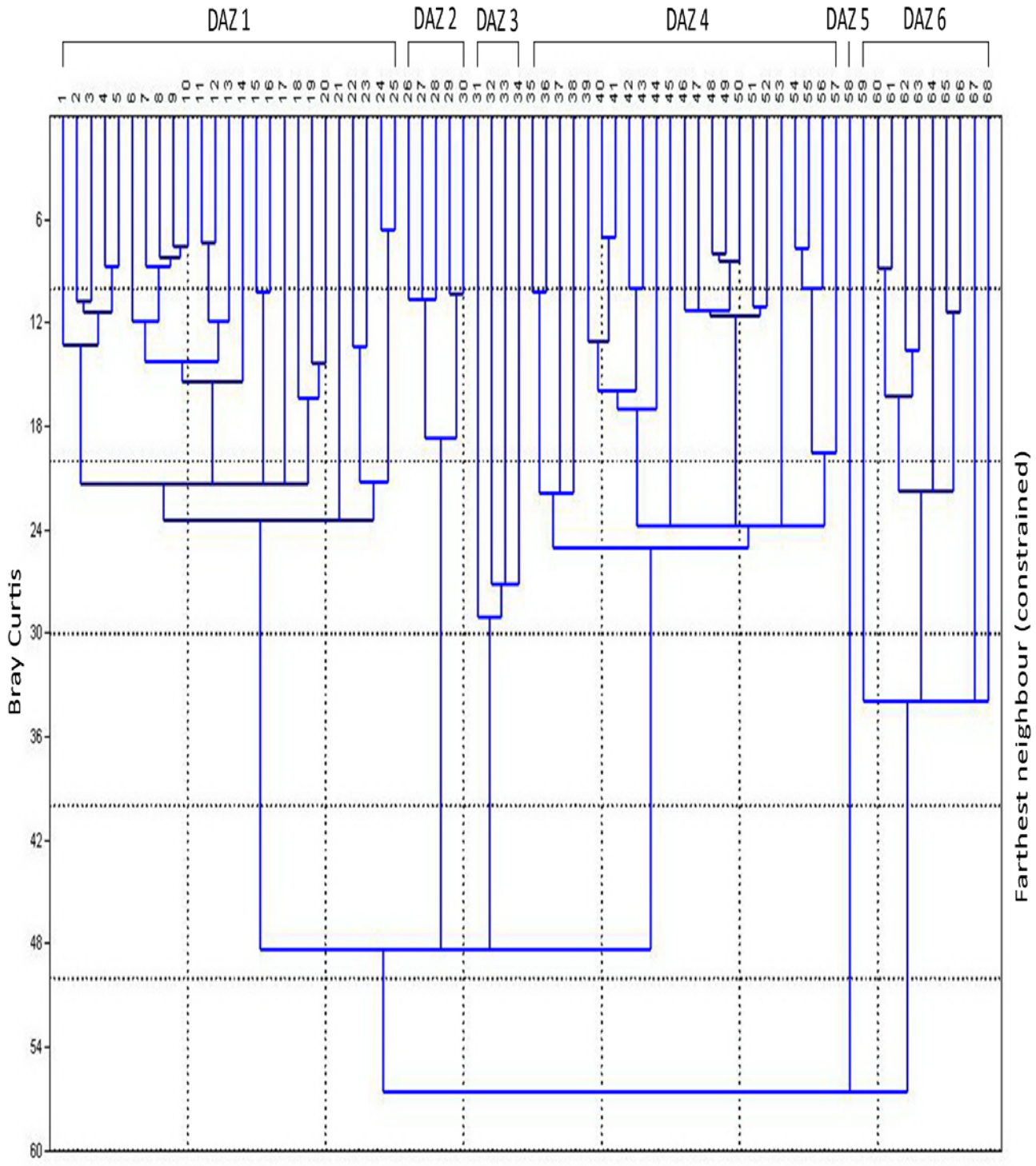


**Figure 31.** Six dinocyst (DAZ 1–6) assemblage biozones identified using constrained cluster analysis (dinocyst taxa only). The two highest samples (samples 69 and 70) were excluded from the analysis owing to low counts, and have been assigned to DAZ 7.

# 6. DISCUSSION

## 6.1 Biostratigraphy

### 6.1.1 Ecostratigraphy

There are no directly comparable studies within the Caribbean region with which to compare the seven dinocyst assemblage biozones recognized at ODP Site 1000, with the exception of a dinocyst study of the Clino Core, Great Bahama Bank. Here, an Upper Zanclean interval (4.1–3.6 Ma) and a Gelasian interval (2.3–2.1 Ma) were described in detail by Head and Westphal (1999). The Upper Zanclean interval was deposited on an open carbonate ramp whereas the Upper Zanclean interval mostly represents sediments exported from the carbonate shelf.

The Upper Zanclean interval is characterized by the co-dominance of *Achomosphaera/Spiniferites* spp. and *Polysphaeridium zoharyi*, with subordinate *Operculodinium* spp., *Lingulodinium machaerophorum*, and protoperidiniaceans, and minor representations of *Operculodinium*? *longispinigerum*, and *Capisocysta lata*. The temporally equivalent interval at ODP Site 1000 is from samples 19–26, which represents the upper part of dinocyst assemblage zone (DAZ) 1 and the lowermost sample of DAZ 2. The assemblages from DAZ 1 are broadly similar to those of the Clino Core, except in having higher abundances of *Operculodinium* spp. (including *O. bahamense*), and an absence of *Capisocysta lata*. The sample from DAZ 2 is unlike the equivalent Clino Core interval in the low abundance of *Polysphaeridium zoharyi.*

The Gelasian interval in the Clino Core is characterized by the dominance of *Spiniferites/Achomosphaera* spp. and subordinate *Lingulodinium machaerophorum* and *Operculodinium* spp., and mostly rare *Polysphaeridium zoharyi* and *Melitasphaeridium choanophorum*. The temporally equivalent interval at ODP Site 1000 is approximately represented by samples 56–59, which belong to the upper part of DAZ 4, DAZ 5, and lowermost DAZ 6. This interval differs from the Clino Core in having generally high abundances of *Polysphaeridium zoharyi*, low abundances *Lingulodinium machaerophorum*, and an absence of *Melitasphaeridium choanophorum*.

### 6.1.2 Traditional biostratigraphy

Most species recorded at Site 1000 have ranges elsewhere in the North Atlantic that extend through the Messinian–Middle Pleistocene, and many have sporadic stratigraphic distributions at Site 1000. Nonetheless, some species have restricted ranges that are relevant to this site.

*Dapsilidinium pseudocolligerum* (Stover, 1977) and *Dapsilidinium pastielsii* (Williams et al., 1966) are closely similar, have overlapping morphologies, and have been grouped in the literature (e.g. de Verteuil and Norris, 1996). Although specimens from Site 1000 are referred to *Dapsilidinium pseudocolligerum* owing to their narrower process bases, they are treated as a single species for the purpose of assessing the stratigraphic literature. It has been reported frequently from the Miocene–Pleistocene of North Atlantic and adjucent seas (e.g. Mudie, 1989; Head et al., 1989c; Edwards, 1984; Norris, 1996; Louwye and Laga 1998; and Louwye et al., 2004; Jiménez-Moreno et al., 2006; Louwye and Laga, 2008; De Schepper et al., 2008, 2011; Fischer, 2011; Schreck et al., 2012 and references therein). It has a highest occurrence (HO) in the Lower Pleistocene of the Gulf of Mexico (e.g., Wrenn and Kokinos, 1986; Aubry, 1993), and was recorded from the Lower Pleistocene (Gelasian, 2.3 Ma) of the Clino Core, Bahamas (Head and Westphal, 1999). It appears to have a slightly higher HO in the eastern Indian Ocean, being reported from the mid-Pleistocene by McMinn (1992). This species has a HO within the Gelasian, which agrees with a Lower Pleistocene HO for this species in the North Atlantic. Mertens et al. (2014) have placed *Dapsilidinium pseudocolligerum* in synonym with *Dapsilidinium pastielsii*, although they note a detailed systematic treatment of *Dapsilidinium* will be published in the future. Pending this more formal study, the present work continuous to use the name *Dapsilidinium pseudocolligerum* as the specimens recorded fit closer to this morphology (Plate 1, Figures 10-12).

*Batiacasphaera hirsuta* was described from the Middle Oligocene of the Blake Plateau on the eastern Atlantic Shelf by Stover (1977). It is documented throughout the Miocene of the North Atlantic and adjacent seas (e.g., Manum et al., 1989; Goll, 1989; Louwye and Laga, 1998; Zevenboom, 1995; de Verteuil, 1996; Munsterman and Brinkhuis, 2004; Dybkjær, 2004; Schreck et al., 2012 and references therein), with a highest HO recorded in the Upper Tortonian of the Netherlands (Munstermann and Brinkhuis, 2004; Schreck et al., 2013). Specimens from Site 1000 are labelled cf. *Batiacasphaera hirsuta* Stover, 1977 because the archeopyle was seldom seen. The specimens from Site 1000 have a highest persistent occurrence at 4.8 Ma (Early Zanclean) with a single specimen at 4.4 Ma (mid-Zanclean). If these specimens indeed belong to *Batiacasphaera hirsuta*, they will increase the North Atlantic range of this species well into the Lower Pleistocene.

*Edwardsiella sexispinosa* Versteegh and Zevenboom *in* Versteegh, 1995, originally reported as Incertae sedis sp. I by Edwards (1984; Head et al., 1989b), is a distinctive oceanic species ranging from Oligocene to Pliocene (Versteegh & Zevenboom, 1995). Although not recorded in high abundances in the North Atlantic, it usually occurs persistently within its range

in oceanic settings. The HO of this species has been recorded at 3.20 Ma in the eastern North Atlantic (De Schepper and Head, 2008), at 3.1 Ma in the Norwegian–Greenland Sea (M. Smelror in De Schepper and Head, 2008), and 2.81 Ma at DSDP Hole 603C in the western North Atlantic (M.J. Head in De Schepper and Head, 2008). It occurs rarely and sporadically at Site 1000, although its HO at 2.9 Ma is close to the western North Atlantic HO of 2.81 Ma.

*Hystrichokolpoma rigaudiae* Deflandre and Cookson, 1955 has a stratigraphic range of Lower Eocene through Pliocene and Pleistocene in the North Atlantic and adjacent seas, although extending into the Pleistocene only in lower latitudes (see Head and Westphal, 1999 for review). The highest recorded HO seems to be the Lower and possibly Middle Pleistocene of the Gulf of Mexico (Wrenn and Kokinos, 1986; de Vernal et al., 1992). At ODP Site 1000 it ranges persistently from the base of the studied section (Messinian) to about 3.5 Ma (Lower Piacenzian), and then occurs sporadically to ca. 1.2 Ma (Calabrian, upper Lower Pleistocene) confirming its high stratigraphic range at low-latitudes. It was curiously not recorded from the Upper Gelasian of the Clino Core, Bahamas (Head and Westphal, 1999), perhaps reflecting the more distal setting of ODP Site 1000.

*Nematosphaeropsis lativittata* Wrenn, 1988 was described from Middle Miocene through Middle Pleistocene oceanic deposits from the Gulf of Mexico (as *Nematosphaeropsis* sp. A in Wrenn and Kokinos, 1986; Wrenn, 1988). In the eastern North Atlantic, it has a persistent occurrence through the Upper Zanclean and Piacenzian, disappearing probably in response to cooling at 2.63 Ma (De Schepper and Head, 2009). Occurences at Site 1000 are sporadic through the Piacenzian–Calabrian, but an HO at 1.6 Ma is consistent with the extension of this species into the Pleistocene at low latitudes.

*Operculodinium bahamense* Head *in* Head and Westphal, 1999 was first recorded from the upper Middle–Upper Miocene of the Norwegian Sea (as *Operculodinium* sp. 3 in Manum et al., 1989) and subsequently recorded from the Zanclean and Gelasian of the Clino Core, Great Bahama Bank (Head and Westphal, 1999). It was reported to occur nearly continuously from the Upper Oligocene through Lower Pleistocene (ca. 1.4 Ma, Calabrian) of ODP Site 1007, toe-of-slope of the present Bahamanian platform margin (Paez-Reyes and Head, 2013). A similar HO is recorded at Site 1000 of the present study, *Operculodinium bahamense* occurring persistently from the base of the examined section in the Messinian to a HO in the Lower Pleistocene (1.6 Ma, Calabrian). *Operculodinium* cf. *bahamense* has been recorded from surface sediment in the Gulf of Mexico (Limoges et al., 2013).

*Operculodinium janduchenei* Head et al., 1989 was first recorded from the Upper Miocene of Spain (as *Operculodinium* sp. in Jan du Chêne, 1997) and formally described from

the Upper Miocene of the Labrador Sea (Head et al., 1989a). It has been recorded frequently from the Upper Miocene of the North Atlantic (e.g., Edwards, 1984b; Mudie, 1987), western Caribbean Sea (Wrenn, 1986), and Gulf of Mexico (Wrenn and Kokinos, 1986). It has a LO within dinocyst zone DN8 (lower to middle Upper Miocene) of the USA Atlantic margin (de Verteuil and Norris, 1996), and a LO in the lower Upper Miocene of the Indian Ocean (McMinn, 1992). It has been documented only infrequently below the Upper Miocene (see Soliman et al., 2012 for discussion) and a Lower Miocene record from the British Southwestern Approaches (Powell, 1988) must be questioned. Its HO is also uncertain but apparently diachronous within the North Atlantic, being recorded at 2.90 Ma in DSDP Hole 610A, 2.34 Ma at DSDP Site 607 (De Schepper and Head, 2008), and about 2.0 Ma in DSDP Hole 603C (Fischer, 2011). Records from modern deposits, as from the Gulf of Mexico (Limoges et al., 2013), are possibly the result of misidentification (M.J. Head, pers. commun., 2014). In the present study, *Operculodinium janduchenei* occurs rarely and sporadically from the base of the section (5.5 Ma, Messinian) to near the top (0.2 Ma, Middle Pleistocene).

*Operculodinium longispinigerum* Matsuoka, 1983 was first documented from the Middle Miocene through Lower Pleistocene of central and northern Japan (Matsuoka, 1983; Matsuoka et al., 1987) and has been reported from modern sediments of the eastern equatorial Indian Ocean and adjacent seas (Zonneveld et al., 2013) and modern sediments of the Gulf of Mexico (Limoges et al., 2013). At ODP Site 1000, it ranges from the Messinian (5.5 Ma) to Lower Gelasian (2.5 Ma), although it is persistent only until about 3.9 Ma in the mid-Zanclean.

*Spiniferites rhizophorus* Head *in* Head and Westphal, 1999 was first recorded from the Lower Pliocene (4.1–3.6 Ma, Upper Zanclean) and Lower Pleistocene (ca. 2.3–2.1 Ma, Gelasian) of the Clino Core, Bahamas (Head and Westphal, 1999), and appears not to have been reported since. At ODP Site 1000, this species was reported rarely, occurring in just three samples within the interval 4.2–3.8 Ma (Zanclean).

Several acritarch species are biostratigraphically significant at ODP Site 1000. *Cyclopsiella elliptica* Drugg and Loeblich, 1967 and *Cyclopsiella granosa* (Matsuoka, 1983) Head et al., 1992 intergrade morphologically at Site 1000 and are therefore referred to "*Cyclopsiella elliptica*/*granosa*". *Cyclopsiella elliptica* has been recorded from the upper Lower Eocene of the Norwegian Sea (Manum, 1976), Lower Miocene of the eastern North Atlantic (Williams, 1978), Middle and Upper Miocene of the Norwegian Sea (as *Cyclopsiella elliptica* in Mudie, 1989), Pliocene and Pleistocene of the Gulf of Mexico (considered reworked, in Wrenn and Kokinos, 1986), Upper Pliocene of the northern North Sea (Louwye and De Shepper, 2010),

and Gelasian of the Bahamas (as *Cyclopsiella* sp. in Head and Westphal, 1999). *Cyclopsiella elliptica* has a highest known range of Upper Miocene–Lower Pliocene (Williams and Brideaux, 1975; Williams and Bujak, 1977; Barss et al., 1979; Drugg and Stover, 1975). *Cyclopsiella* cf. *elliptica* has been reported from the Lower Pleistocene (Gelasian) of southwestern England (Head, 1993), and an isolated specimen was reported from the Lower Pleistocene of the eastern North Atlantic (De Schepper and Head, 2009). In the present study, *Cyclopsiella elliptica/granosa* was recorded throughout the examined sequence, ranging from Messinian (5.5 Ma) through Middle Pleistocene (0.2 Ma).

*Cymatiosphaera latisepta* De Schepper and Head, 2008 was formally described from the eastern North Atlantic DSDP Hole 610A where it ranges from 3.3 Ma to 2.6 Ma within the Piacenzian (De Schepper and Head, 2008). In central North Atlantic DSDP Site 607 it ranges from 2.8 Ma to 2.5 Ma, from Labrador Sea ODP Hole 646B it ranges into the lowermost Gelasian, and in western North Atlantic DSDP Hole 603C it ranges from 3.6 Ma to 2.6 Ma (De Schepper and Head, 2008; M.J. Head, pers. commun.). At ODP Site 1000, it is represented by scattered occurences from the Messinian (5.5 Ma) to Gelasian (2.4 Ma). The present study therefore extends the global stratigraphic ranges both above and below its previously known range.

*Nannobarbophora walldalei* Head, 1996 is a small, distinctive, acanthomorphic acritarch described from the Lower Pleistocene of eastern England (Head, 1996, 1998, 2003). It is a senior synonym of *Impletosphaeridium acropora* Warny and Wrenn, 1997, the holotype of which was described from the Messinian of the Atlantic coast of Morocco, and which apparently has a range in Morocco of Tortonian through Zanclean (Warny and Wrenn, 1997, 2002, Warny et al., 2004). *Nannobarbophora walldalei* has been recorded from numerous site in the North Atlantic region (Head, 2003) including the Upper Miocene through Lower Pleistocene of western North Atlantic DSDP Hole 603C (Head, 2003; Fischer, 2011), the Lower Pliocene through lower Middle Pleistocene of eastern North Atlantic DSDP Hole 610A where it ranges from 3.98 Ma to 0.76 Ma (De Shepper and Head, 2009), Upper Miocene–Pliocene of the northern North Sea (Louwye and De Shepper, 2010), Lower Pliocene and Lower Pleistocene of the Bahamas (Head and Westphal, 1999), Upper Pliocene though Lower Pleistocene of eastern England (Head, 1996a, 1998a), and Upper Pliocene of Belgium (De Schepper et al., 2008). At Site ODP 1000, it has a sporadic range from 5.4 Ma (Messinian) through 2.4 Ma (Gelasian) which is within the reported range for this species.

*Paralecaniella indentata* (Deflandre and Cookson, 1955) Cookson and Eisenack, 1970 emend. Elsik, 1977 was first described from Paleocene through Miocene deposits of Australia (as

*Epicephalopyxis indentata* in Deflandre and Cookson, 1955) and is widely reported from the Paleogene and Lower Neogene globally. It has a HO in the Upper Miocene of the northern North Sea (Louwye and De Schepper, 2010) and Middle–Late Miocene in the southern North Sea (Louwye and Laga, 2008). Possible reworking has obscured the true age of the extinction of this species, and it is uncertain, for example, whether Pliocene specimens from Belgium are reworked (Louwye et al., 2004). At ODP Site 1000, *Paralecaniella indentata* is reported persistently in low numbers in the lower part of the examined sequence from 5.5 Ma to 3.8 Ma (Messinian–Zanclean), although six specimens were recorded from a single isolated sample much higher in the sequence at 0.8 Ma (lower Middle Pleistocene).

### 6.1.3 Biostratigraphic summary

Comparing dinocyst assemblages from the Clino Core of the Great Bahama Bank (Head and Westphal, 1999) with those of the present study reveals a broad similarity for the Upper Zanclean interval (4.1–3.6 Ma) when the Clino Core location was an open carbonate ramp. The Gelasian interval (2.5–2.2 Ma), at a time when Clino Core deposition was mostly influenced by sediment export from the carbonate top, shows broad differences with the present study. This indicates that the dinocyst assemblage zones of the present study are limited in their stratigraphic applicability because they largely reflect environmental changes that may vary laterally as well as vertically.

The relatively low number of species recorded in the present study, and the sporadic occurrences of many, restricts the utility of dinocysts for long-distance biostratigraphic correlation. The low dinocyst diversity is a combination of: 1) the low-latitude position of this site where the cyst-producing strategy for overwintering is less important than at mid- to high latitudes; and 2) the low siliciclastic sediment input which suggests low nutrient levels that will likely have inhibited the production of neritic dinocystss, especially protoperidiniaceans which are poorly represented at ODP Site 1000. This explains why ODP Site 1000 is more comparable to the Clino Core assemblages from the Great Bahama Bank (Head and Westphal, 1999) than to, say, the Gulf of Mexico where presumably greater river (nutrient) influence has led to far higher dinocyst species diversity including diverse protoperidiniaceans (Duffield and Stein, 1986; Wrenn and Kokinos, 1986).

In spite of these limitations, a number of species ranges have been identified as significant within the North Atlantic region.

*Dapsilidinium pseudocolligerum* has a HO within the Gelasian which agrees with a Lower Pleistocene HO for this species in the North Atlantic. The HO of *Edwardsiella sexispinosa* at 2.9 Ma is close to the western North Atlantic HO of 2.81 Ma. The unusually high HO of

*Hystrichokolpoma rigaudiae* at ca. 1.2 Ma (Calabrian, upper Lower Pleistocene) confirms the high stratigraphic range of this thermophilic species at low latitudes. Similarly, the HO of *Nematosphaeropsis lativittata* at ca. 1.6 Ma is consistent with its range extension into the Pleistocene at low latitudes. *Operculodinium bahamense* has an HO in the Lower Pleistocene (ca. 1.6 Ma, Calabrian) which is close to its HO in the Lower Pleistocene (ca. 1.4 Ma, Calabrian) of ODP Site 1007, toe-of-slope of the present Bahamanian platform margin. *Operculodinium janduchenei* extends to near the top of the investigated section at Site 1000 (0.2 Ma, Middle Pleistocene), which represents one of the youngest verified occurrences of this species. The seldom-reported *Spiniferites rhizophorus* occurs three samples within the interval 4.3–3.8 Ma (Zanclean), slightly extending its previously documented LO of 4.1 Ma. The acritarch *Cyclopsiella elliptica/granosa* occurs throughout the examined sequence, from the Messinian (5.5 Ma) through Middle Pleistocene (0.2 Ma), although, as with other sites, it is not clear whether reworking is responsible for the stratigraphically higher specimens. *Cymatiosphaera latisepta* ranges from 5.5 Ma to 2.4 Ma, considerably extending its previously known range of 3.6 Ma to slightly younger than 2.6 Ma.

**6.2 Paleoenvironmental evolution of Site 1000**

The dinocyst assemblages comprise both neritic and oceanic species throughout the studied section. Outer neritic–oceanic taxa, recorded by *Amiculosphaera umbraculum*, *Edwardsiella sexispinosa*, *Nematosphaeropsis labyrinthus* and total *Impagidinium* spp., are rare (0–10%) but their presence throughout the section demonstrates a continuous oceanic influence at Site 1000. Assemblages are dominated, however, by such neritc taxa as *Achomosphaera/Spiniferites* spp., *Operculodinium centrocarpum–israelianum, O. bahamense* and *Polysphaeridium zoharyi*. It is assumed therefore that these neritic cysts represent a substantial transported component from environments on the shelf. Protoperidinioid species are poorly represented (0–21%) and mostly comprise the genera *Brigantedinium*?, *Selenopemphix*, and *Lejeunecysta*. The protoperidinioid/gonyaulacoid ratio (Figure 26), which is often used to measure productivity (e.g., Versteegh, 1995; De Schepper, 2006), implies relatively low nutrient input.

With respect to the palynofacies, the pollen+spores/dinocyst ratio (Figure 26) reflects the degree of transport from the coast, as most pollen and embryophyte spores in marine sediments originate from coastal vegetation and fluvial input (e.g., Chmura et al., 1999; McCarthy et al., 2003), with a smaller airborne component. They may be transported to oceanic sites by ocean currents and downslope processes (e.g., McCarthy and Muid, 1998). It is also true that decreasing sea level over time will cause the coast to migrate increasingly closer to the site at which the

palynomorphs are deposited, and would register a higher influx of pollen or reworked dinocysts. Lowering of sea level also causes erosion of coastal sediments and oceanward redeposition. At Site 1000, the proportion of pollen+spores is never above 8.6%, and indicates the relatively low terrestrial influence throughout the examined section, although the increasing proportion from the late Piacenzian onwards likely reflects low sea level associated with the intensification of NHG starting around 2.7 Ma (e.g., De Shepper et al., 2013).

A paleoenvironmental reconstruction of Site 1000 is given below for each of the dinocysts assemblage biozones recognized (DAZ 1–7).

**DAZ 1 (Messinian–Zanclean).** The oceanic and hence in-situ component of the dinocyst assemblages is represented mostly by the extant *Impagidinium aculeatum, I. patulum, I. paradoxum, I. plicatum,* and *I strialatum*, these each having a temperate to equatorial distribution today (Zonneveld, 2013). The extant cosmopolitan *Nematosphaeropsis labyrinthus* is also frequently recorded in some samples and likewise reflects open-marine conditions, although its modern distribution indicates an affinity for both oligotrophic and eutrophic conditions (Zonneveld, 2013).

The dominance of neritic dinocyst taxa, in particular *Achomosphaera/Spiniferites* spp. indet. (16–34%), *Polysphaeridium zoharyi* (4–31%), *Operculodinium* spp. total (0–26%), and *Dapsilidinium pseudocolligerum*, attest to strong transport processes from shallow marine environments, and elevated frequencies of spores and pollen in the Upper Messinian and lowermost Zanclean suggest that glacio-eustatic fall at this time (Hilgen et al., 2012) was responsible for increased erosion on the shelf.

*Polysphaeridium zoharyi* is an inner-neritic tropical to subtropical extant species and one of the best indicators of very warm surface waters. In a study of the subsurface Pliocene of the Great Bahama Bank, Head and Westphal (1999) reviewed the paleoecological record for *Polysphaeridium zoharyi*. Its modern distribution commonly reflects shallow and restricted marine conditions, including shallow lagoons, with variable but usually elevated salinities, although its has also been associated with low and fluctuating salinities (e.g., Brewster-Wingard et al., 1996; Head and Westphal, 1999; Marret and Zonneveld, 2003; Durugbo at al., 2010; Fischer, 2011; Limoges et al., 2013; Radi et al., 2013). Morover, it has been found in association with mangrove vegetation today (e.g., Head and Westphal, 1999; Durugbo at al., 2010; Usup et al., 2012; Limoges et al., 2013). Edwards and Andrle (1992) recorded high percentages of *Polysphaeridium zoharyi* in shallow areas off Bermuda, with winter sea-surface temperatures above 15°C and summer sea-surface temperatures above 23°C. In accounting for its presence in more open waters of the northern Arabian Sea, Reichart et al. (2004) suggested hyperstratification

due to a lack of winter mixing that led to evaporation and abrupt influxes of *Polysphaeridium zoharyi*. It recorded in the Middle Miocene of the eastern Campine area (Louwye and Laga, 2008) and Porcupine Basin off southwest Ireland (Louwye et. al., 2008). Louwye et al. (2008) noted its disappearance precisely during the onset of the gradual cooling, at approximately 14.1 Ma, that terminated the Middle Miocene Climatic Optimum (e.g., Miller et al. 1991, 1998). High abundances (up to 98%) have been recorded in the Gulf of Mexico and the Banda Sea (off Indonesia) where high upper-water salinities and temperatures exist (see Zonneveld et al., 2012), and it is registered from coastal sediments off southern Korea, the South China Sea, the Gulf off Oman, coastal areas off North Australia and off the NW Iberian peninsula (Marret and Zonneveld, 2003; Ribeiro and Amorim, 2008; Pospelova and Kim, 2010; Usup et al., 2012). Based on both its modern and fossil distributions, this species is here regarded as an indicator of tropical to subtropical conditions on the carbonate platforms adjacent to Site 1000, and that its transport to Site 1000 reflects productivity on these platforms.

*Operculodinium centrocarpum–israelianum* comprises morphotypes with shorter processes (resembling *Operculodinium israelianum*) and those with longer processes (closer to *Operculodinium centrocarpum sensu stricto*), although these morphologies intergraded. The modern distribution of *Operculodinium israelianum* indicates it to be a subtropical to equatorial species with high relative abundances in nearshore areas and where surface salinities are high (Zonneveld et al., 2013). *Operculodinum bahamense* is an extinct species for which there is little paleoenvironmental information, other than its affinity for tropical carbonate environments (Head and Westphal, 1998; Paez-Reyes and Head, 2013).

*Dapsilidinium pseudocolligerum* is an extinct tropical to warm-temperate species based on its fossil distribution (Head and Westphal, 1999). It occurs fairly persistently (0–14%) to the top of DAZ 1, after which it only again becomes persistent in DAZ 4 with no higher records. It has been recorded from the Lower Oligocene–Upper Miocene of the North Atlantic and adjacent seas (e.g., Stover, 1977; Head et al., 1989a; de Verteuil and Norris, 1996), Lower Pliocene of southwestern Florida (Edwards et al., 1998), east-central Florida (Weedman et al., 1995), the Lower Pleistocene? of the Gulf of Mexico (Wrenn and Kokinos, 1986), and Lower Pleistocene (Gelasian) of the Clino Core, Bahamas (Head and Westphal, 1999). Its absence from higher-latitude, Pliocene–Pleistocene records might be related to cooling of the North Atlantic during the latest Miocene and formation of the cold Labrador Current (Head and Westphal, 1999). Cooling has also been attributed to the Middle Miocene disappearance of *Dapsilidinium pseudocolligerum* from the Northwestern Pacific (Bujak and Matsuoka, 1986). It is not clear whether its temporary

disappearance from Site 1000 at the top of DAZ 1 is related to cooling or some other environmental perturbation.

The heterotrophic dinocysts mainly comprise *Brigantedinum* spp. and *Selenopephix quanta*, and are poorly to moderately represented (1–10%). Several studies have linked high surface water productivity with high relative abundances of *Brigantedinium* spp. (e.g., Targarona et al., 1999; Zonneveld et al., 2001a). Nutrient levels are therefore inferred to have been low to moderate.

Of the other palynomorph groups recorded, *Paralecaniella indentata*, recorded in low percentages, suggest transport from shallower waters. Brinkhuis and Schiøler (1996) reported *Paralecaniella indentata* in clayey layers indicating a marginal marine or restricted marine influence. Zaporozhets et al. (2006) found abundant *Paralecaniella indentata* in the Paleogene of Kamchatka and regarded this species as indicative of reduced salinities and shoaling phases of depositional basins.

**DAZ 1** therefore represents warm open waters, with shallow tropical to subtropical restricted-marine environments in the vicinity. Intermittent peak abundances of spores and pollen in the Upper Messinian and lowermost Zanclean might be explained by episodic lowering of sea level causing occasional exposure and erosion of the shelf.

**DAZ 2 (uppermost Zanclean–lowermost Piacenzian)**. Assemblages are somewhat similar to those of DAZ 1, but the characteristic features of this narrow biozone comprising just five samples are the: 1) temporarary disappearance of *Dapsilidinium pseudocolligerum*, 2) increased abundance of *Lingulodinium machaerophorum* (0–8%), 3) decreased numbers of *Operculodinum bahamense* (2–10%), 4) increased numbers of *Operculodinium centrocarpum–israelianum* (33–40%), 5) strongly decreased numbers of *Polysphaeridium zoharyi* (0–3%), and 6) disappearance of *Paralecaniella indentata*.

*Lingulodinium machaerophorum* has a tropical to temperate distribution today, and the physiology, morphology and ecology of the cyst and motile stage have been reviewed by Lewis and Hallett (1997). They observed that the motile cells usually occur in the water column during late summer, which implies late summer temperatures as a controlling factor (e.g., Dale, 1996; Rochon et al., 1999, Head and Westphal, 1999). Their laboratory culture studies confirm a broad salinity tolerance of the motile cells, ranging from 10 to 40 psu. The cysts have been recorded in surface sediments from regions with SSS of at least ca. 10 psu (see Dale, 1996; Persson et al., 2000, Head et al. 2005; Head, 2007). Elevated abundances have been linked to slight increases in nutrient levels, such as caused by diffuse upwelling (Dale, 1996; Head, 1997; Head and Westphal, 1999, Smayda and Trainer, 2010).

The transition to DAZ 2 suggests slight cooling (temporarary disappearance of *Dapsilidinium pseudocolligerum* and decline in *Polysphaeridium zoharyi*) and / or a change to less restricted-marine environments. Increases in *Lingulodinium machaerophorum* and *Operculodinium centrocarpum–israelianum* indeed imply salinities lower than the potentially hypersaline environments of DAZ 1. It is emphasized, however, that these changes are expressed primarily in the allochthonous (neritic) component, which might therefore represent changes in current systems delivering these neritic cysts to the site.

**DAZ 3 (Lower Piacenzian)**. This narrow biozone, comprising just four samples, is recognized by significantly elevated levels of *Polysphaeridium zoharyi* (31–61%), and very low numbers of heterotrophic (0–2%) and oceanic taxa (0–0.7%).

Somewhat elevated numbers of calcareous dinocyst linings (9.5% in sample 31, 3.4 Ma) are recorded in DAZ 3. The organic linings of calcareous dinocysts are often neglected in palynological investigations due to their small size (on average: 16–26 µm in diameter) and indistinct morphology. Consequently, information about their paleoenvironmental significance is limited. However, Dale (1992a, b) noted that dinocysts assemblages of the subtropical to tropical Atlantic and Pacific oceans are intensely dominated by calcareous forms, suggesting that they may play an important role to the oceanic carbon flux.

DAZ 3 (samples 32-34) mostly represents the cold stage MIS M2, which is characterised by the temporary eustatic closure of the CAS and consequent build up of heat and salinity in the Caribbean Sea (the Caribbean Warm Pool). This is reflected in the elevated levels of *Polysphaeridium zoharyi* and reduced numbers of heterotrophic dinocysts, as also observed at ODP Site 999 (De Schepper et al., 2013).

**DAZ 4 (Lower Piacenzian–Upper Gelasian)**. This broad biozone is similar to DAZ 1 in having comparable levels of *Polysphaeridium zoharyi* (0–30%) and heterotrophic taxa (0–8%). However, it contains higher abundances of *Operculodinium* spp. (0–50%) and *Lingulodinium machaerophorum* (0–12%) than to other biozones, and lower percentages of outer neritic–oceanic taxa (0–3.5%). Significantly, *Dapsilidinium pseudocolligerum* returns and is fairly persistent through the middle and upper part of the zone. Other palynomorphs are mostly represented by foraminiferal linings (0–37%), leiospheres (0–3%), *Cyclopsiella elliptica/granosa* (0–2.2%), and angiosperm pollen (0–2.8%).

The pollen+spore/dinocyst ratio is somewhat elevated in DAZ 4, and likely reflects the intensification of NHG from about 2.74 Ma onwards, with successive glaciations lowering sea level and exposing the surrounding carbonate banks to erosion. From the Upper Piacenzian the heterotroph/autotroph ratio also increases, possibly in response to increasing nutrients released

during erosion. While the overall character of DAZ 4 reflects warm, shallow, environments in the vicinity, the relatively low abundances of *Polysphaeridium zoharyi* in the upper part of DAZ 4 may either reflect cooling associated with the onset of NHG or the disappearance of coastal lagoons due to sea-level fall. It should be noted that no cool-water dinocysts are recorded in the interval.

**DAZ 5 (Upper Gelasian)**. This biozone, represented by a single sample, is characterized by high values of *Polysphaeridium zoharyi* (<62.45%) and low species richness. DAZ 5 presumably reflects an interglacial interval within the Upper Gelasian when carbonate platforms in the vicinity were submerged and restricted-marine environments were widespread.

**DAZ 6 (uppermost Gelasian–Middle Pleistocene)**. This biozone is representd by *Achomosphaera/Spiniferites* spp. indet. (23–65%), *Operculodinium* spp. (0–54%), *Polysphaeridium zoharyi* (0–27%), and *Brigantedinium*? spp. (sample 67, significant peak of 21.84%). Notable absences include *Dapsilidinium pseudocolligerum* which has its highest occurrence at the top of DAZ 4, and which presumably represents a cooling event. Nonetheless, sustained moderate to low levels of *Polysphaeridium zoharyi* indicate generally warm surface waters in the vicinity, although by the latter part of DAZ 6, conditions had become less favourable for this species than in earlier biozones. A significant peak in *Brigantidinium* spp. indet. (<21.84%) suggests elevated nutrient availability in the upper part of DAZ 6.

**DAZ 7 (Middle Pleistocene).** The two uppermost samples are assigned to this biozone and are characterized by a scarcity of dinocysts. *Achomosphaera/Spiniferites* spp. indet. (32–66%), *Impagidinium* spp. (1–4%), and *Operculodinium centrocarpum–israelianum* (8–31%), are all present, and the last of these attests to temperatures that were at least temperate. Most notable, however, is the absence of *Polysphaeridium zoharyi*, which might reflect cooling in the Middle Pleistocene. The pollen+spore/dinocyst ratio remains high. This continues a trend that began in the middle of DAZ 4 and may reflect sea-level lowering in response to increasing NHG.

## 7. SITE 1000 COMPARED WITH OTHER PUBLISHED DINOCYST RECORDS

ODP Site 1000, located in the Pedro Channel in the Caribbean Sea and surrounded by shallow carbonate banks, represents a very specific tropical environment that is reflected in a reduced species diversity compared with sites at higher latitudes in the North Atlantic. Even the low-latitude Gulf of Mexico contains different assemblages and higher diversity, presumably reflecting river input and higher nutrient levels.

The following species typically recorded in Pliocene–Pleistocene assemblages in the North Atlantic were *not* found at Site 1000:

*Achomosphaera andalousiensis, Ataxiodinium confusum, Ataxiodinium zevenboomii, Barssidinium graminosum, Batiacasphaera minuta/micropapillata, Bitectatodinium raedwaldii, Bitectatodinium tepikiense, Capisocysta lata, Corrudinium devernaliae, Dalella chathamense, Desotodinium wrennii, Filisphaera species, Geonettia waltonensis, Impagidinium solidum, I. cantabrigiense, I. multiplexum, I. sphaericum, Invertocysta lacrymosa, Leffingwellia costata, Leiosphaeridia rockhallensis, Lejeunecysta marieae, Melitasphaeridinium choanophorum, Operculodinium*? *eirikianum* var. *cerebrum, Operculodinium giganteum, Operculodinium tegillatum, Protoperidinium stellatum, Pyxidinopsis tuberculata, Pyxidinopsis vesiculata, Tectatodinium pellitum,* acritarchs *Lavradosphaera crista* and *Lavradosphaera lucifera*. Their absence from Site 1000 is likely related to various environmental factors due to the complexity of marine environments, but relatively low nutrient levels owing to the absence of large nearby river outflows, and low seasonality will have an important impact on cyst diversity.

## 8. REGIONAL AND GLOBAL CONTEXT

The present study is the first to provide a detailed record of environmental change using dinocysts within the Caribbean Sea area. The CAS has regularly been considered a major participant in climate change from the Pliocene onwards. From fully open conditions to shoaling and closure around 4.5–2.7 Ma, the history of the CAS coincides with a remarkable modification of the ocean circulation, changes in heat and moisture advection to higher latitudes, and the development of NHG (e.g., Driscoll and Haug, 1998; Haug and Tiedemann, 1998; Haug et al., 2001; Bartoli et al., 2005; Groeneveld et al. 2008; De Schepper et al., 2013). Even though Site 1000 was drilled north of the CAS, some influence of its shoaling and closure might be expected. Furthermore, given the predominance of carbonate-platform-sourced sediment at Site 1000, the effects of global sea level change on carbonate platforms surrounding Site 1000 are likely to have influenced sediment supply to Site 1000 itself. Nonetheless, changes in the palynology are expected to be subtle because: 1) there is little change in the lithology throughout the examined interval, with a persistent dominance (>80%) of carbonates (Figure 23); and 2) the Caribbean has not been subjected to the extreme temperature changes during the Late Cenozoic that characterize the higher northern latitudes.

DAZ 1 (5.5–3.8 Ma) has a dominant restricted-marine element within the dinocyst record that, along with sporadic acmes of terrestrial palynomorphs in the uppermost Miocene and lowermost Zanclean, might reflect globally low sea levels (Haq et al, 1987) and recurrent shelfal exposure and erosion. DAZ 1 includes at 4.5 Ma the start of an increase in SST and SSS (based on foraminiferal geochemistry) due to the progressive plate tectonic closure of CAS that resticted

the exchange of water masses between the Pacific and Atlantic oceans (Groeneveld et al., 2008). Prior to 4.5 Ma, heterotrophic dinocysts are relatively abundant and diverse, particularly in the Miocene, and after 4.5 Ma, they become less so, suggesting somewhat reduced nutrient levels. In addition, cf. *Batiacasphaera hirsuta*, is much less common after 4.5 Ma, although the paleoautecology of this species is poorly known. After 4.5 Ma, the thermophilic dinocyst *Dapsilidinium psedocolligerum* increased moderately with increasing $SST_{Mg/Ca}$ at this time, perhaps reflecting shoaling of the CAS.

Significant changes in dinocyst assemblages inevitably occur at boundaries separating the seven dinocyst assemblage biozones. The oldest of these is the DAZ 1/2 boundary at 3.8–3.6 Ma in the latest Zanclean. This boundary suggests a slight cooling or perhaps a change to less restricted-marine environments based on a decrease in *Dapsilidinium psedocolligerum* and *Polysphaeridium zoharyi* and increase in *Lingulodinium machaerophorum* and *Operculodinium centrocarpum–israelianum*. Head and Westphal (1999) in their study of the the Plio-Pleistocene of the Bahamas also noted the anticorrelation between *Polysphaeridium zoharyi* and *Lingulodinium machaerophorum* and attributed this to more open marine conditions favouring *Lingulodinium machaerophorum*. Globally, the latest Zanclean is marked by two significant glacial stages, MIS Gi4 and Gi2 (Lisiecki and Raymo, 2005). It therefore seems possible that the DAZ 1/2 boundary does indeed represent a slight cooling event, or a readjustment in ocean circulation as a result of this global cooling phase.

The three highest samples of DAZ 3 and the two lowest samples of DAZ 4 (103.33–100.93 mbsf) at around 3.3 Ma in the Early Piacenzian represent the pronounced cold stage MIS M2 (3.31–3.26 Ma). A noticeable rise in abundance of *Polysphaeridium zoharyi* and a reduction in *Brigantedinium*? spp. indet. together characterize this interval and indeed all of DAZ 3. MIS M2 and its adjacent interglacials have been analysed for dinocysts and foraminiferal geochemistry at ODP Site 999 just south of Site 1000 in the Caribbean Sea (De Schepper et al., 2013). The dinocyst signal at ODP Site 999 (De Schepper et al., 2013, Figure 5) paradoxically shows an increase in *Polysphaeridium zoharyi* and a decrease in *Brigantedinium* spp. during MIS M2. This has been interpreted to represent the eustatic closure of the CAS during this cold stage, resulting in the development of the Caribbean warm pool with increasing temperature and salinity and a reduction in productivity explained by the resulting absence of nutrient-rich Pacific waters (De Schepper et al., 2013). The decrease in *Brigantedinium* spp. is therefore a reflection of this reduction in productivity. These same characteristics are found at Site 1000, although the abundances of *Brigantedinium*? spp. indet. before and after MIS M2 are lower than at Site 999 presumably because Site 1000 is further from the CAS and therefore less affected by the inflow

of Pacific waters. Nonetheless the basic and distinctive signature of MIS M2 in the Caribbean is confirmed by the present study.

The DAZ 3/4 boundary at 3.3 Ma is marked by a decline in *Polysphaeridium zoharyi* although values are still greater than for most samples higher in DAZ 4. DAZ 4 continues to 2.2 Ma in the Mid-Gelasian. Less abundant *Polysphaeridium zoharyi* during all but the two lowest samples in DAZ 4 together with an increase in *Lingulodinium machareophorum* and moderate values of *Brigantedinium*? spp. indet. might indicate somewhat more open marine environments than for DAZ 3, with a return to an open CAS immediately following MIS M2. The important global climatic transition from the Mid-Piancenzian Warm Period (3.6–3.0 Ma) to the onset of NHG (2.7–2.6 Ma) and less severe glaciations following MIS 96 in the Early Gelasian are all encompassed by DAZ 4. Research mainly focused on foraminiferal geochemical records from the Caribbean and Pacific (Groeneveld, 2005; Steph et al., 2006) shows major changes took place at around 2.7 Ma. The response based on the dinocyst record is subdued, however, indicating the resilience of the Caribean Sea to climatic and oceanographic changes that were profoundly affecting the more northerly North Atlantic. Nonetheless, the lower abundances of *Polysphaeridium zoharyi* in the upper part of DAZ 4 may reflect global cooling or possibly a disappearance of restricted marine environments due to global sea-level fall. Some evidence for the latter comes from somewhat increased proportions of terrestrial palynomorphs and heterotrophic dinocysts, consistent with lowered sea level and increasing nutrients. Nonetheless, no cool-water dinocysts are found in this DAZ 4, and the thermophilic *Dapsilidinium pseudocolligerum* is fairly persistent throughout.

DAZ 5 is represented by a single sample, and seems to reflect a relatively warm interval within the Upper Gelasian, but the DAZ 4/5 boundary at 2.2 Ma (Upper Gelasian) is marked by the final disappearance of *Dapsilidinium pseudocolligerum*, which presumably represents a cooling event perhaps related to glacial MIS 82. At higher latitudes of the North Atlantic this species disappears earlier, as for example in the Late Miocene of the Norwegian Sea (Mudie, 1989; Manum et al., 1989) and Iceland Sea (Schreck et al., 2012). Its persistence into the Upper Gelasian at Site 1000 accords with its similar disappearance in the Upper Pliocene or Lower Pleistocene of the Gulf of Mexico (as *Dapsilidinium* sp. A in Wrenn and Kokinos, 1986) and attests to the relatively warm conditions in the Caribbean Sea even during the extensive NHG of the latest Piacenzian.

DAZ 7 is represented by the two highest samples in the examined interval, and the DAZ 6/7 boundary occurs at between approximately 400 and 200 ka. The age control is not precise in this part of the hole, but DAZ 7 seems to reflect cooling associated with the severe glacial stages

of the Middle Pleistocene. The absence of *Polysphaeridium zoharyi*, already in significant decline from the middle of DAZ 6, may represent a combination of cooling and habitat loss resulting from sea-level fall. Increased magnetic susceptibility of the sediments in Hole 1000A from about 30 mbsf and upwards (Figure 26), as well as increasing levels of pollen and spores, all attest to increasing erosion caused by reduced sea level during the Middle Pleistocene glaciations.

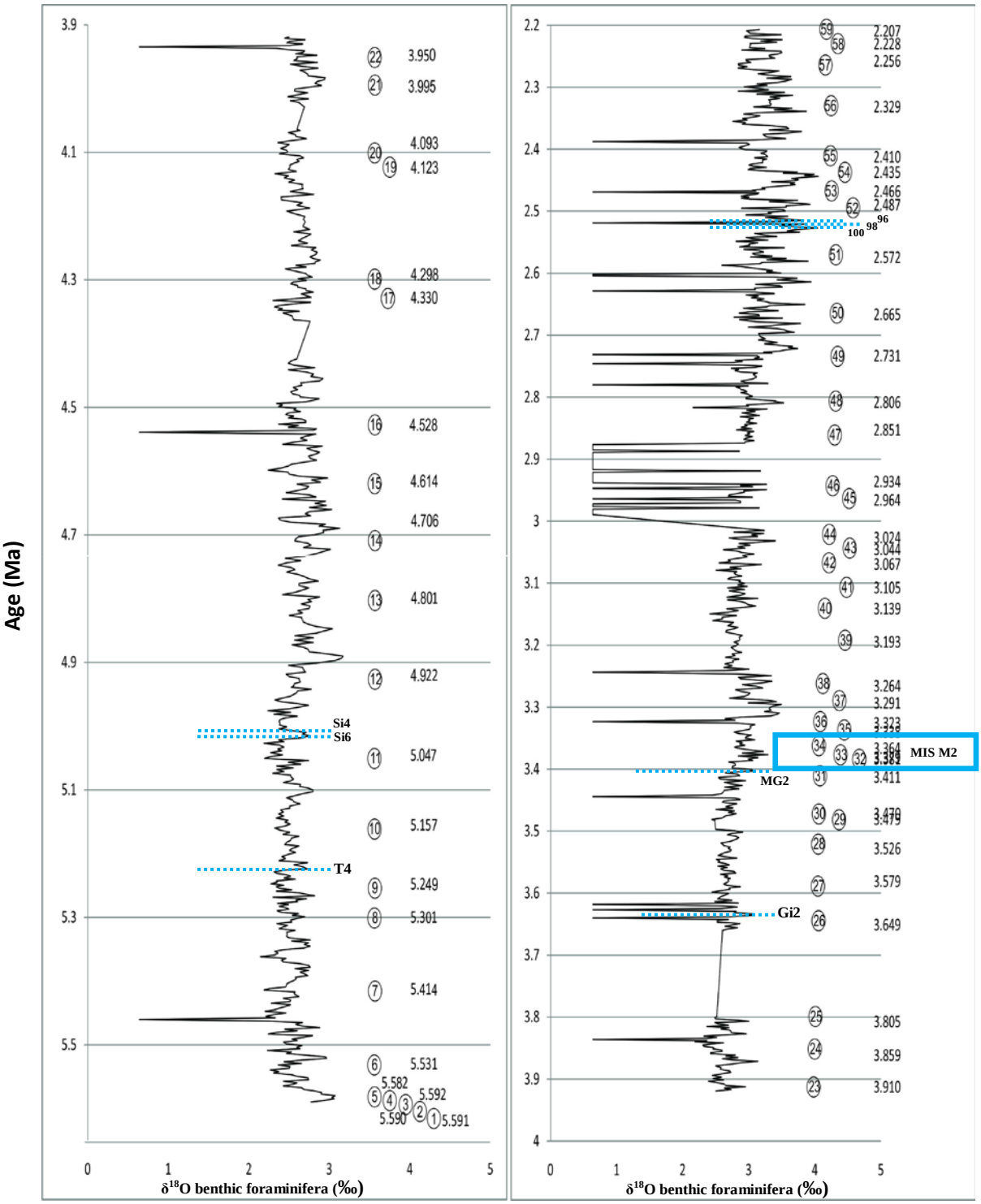


**Figure 31.** Correlation between the marine isotope stages (Steph et al., 2006) and samples (this study) from Site 1000 for the interval 5.5–2.2 Ma. Circled numbers show sample codes (Table 3) and are followed by the age of each samples.

## 9. SUMMARY AND CONCLUSIONS

The present study of dinocysts, acritarchs and other palynomorphs, comprising 70 samples from the Late Miocene (5.5 Ma) to Middle Pleistocene (0.2 Ma), at ODP Site 1000 in the Caribbean Sea, represents the first detailed and continuous record of marine palynomorphs for this interval from the Caribbean Sea. The record is constrained by marine isotope stratigraphy between 5.5 and 2.2 Ma (Steph et al., 2006), and upper (1.8–0.2 Ma) parts of the section are constrained by nannofossil biostratigraphy (Kameo and Sato, 2000; Raffi et al., 2008). It is also augmented by planktonic foraminiferal $SST_{Mg/Ca}$ for the interval 5.5–3.8 Ma (Groeneveld et al., 2008).

Dinocysts are abundant and well-preserved thoughout the section. A total of 49 dinocyst taxa were recorded, which is of lower diversity than for assemblages of comparable age in the Gulf of Mexico (Wrenn and Kokinos, 1986). Assemblages consist of a dominant neritic allochthonous component sourced from nearby carbonate platforms, and a sparse oceanic component. Heterotrophic dinocysts are distinctly subordinate. Seven dinocyst assemblage biozones (DAZ 1–7) have been identified statistically and reflect paleoenvironmental shifts in the Caribbean. These include: 1) a subtle change in assemblage composition at around 4.6 Ma when shoaling of the CAS caused a temperature rise in the Caribbean; 2) slight cooling or perhaps a change to less restricted-marine environments at around 3.8–3.6 Ma in the latest Zanclean; 3) pronounced warming during the cold MIS M2, explained by isostatic closure of the CAS and build-up of the Caribbean Warm Pool (De Schepper et al., 2013), 4) possible weak expression of cooling at around 2.7 Ma in connection with the onset of NHG, and 5) a pronounced change in assemblages in the Middle Pleistocene presumably caused by a combination of global cooling and sea-level fall.

Several biostratigraphic datums are notable, including the highest occurrences of *Edwardsiella sexispinosa* at 2.9 Ma, *Dapsilidinium pseudocolligerum* at ca. 2.2 Ma, *Nematosphaeropsis lativittata* at ca. 1.6 Ma, *Operculodinium bahamense* at ca. 1.6 Ma, *Hystrichokolpoma rigaudiae* at ca. 1.2 Ma, and *Operculodinium janduchenei* at ca. 0.2 Ma. *Spiniferites rhizophorus* occurs within the interval 4.3–3.8 Ma (Zanclean), slightly extending its previously documented LO of 4.1 Ma, and the acritarch *Cymatiosphaera latisepta* was recorded at 5.5 Ma, considerably extending is previously known range of 3.6 Ma to slightly younger than 2.6 Ma.

**REFERENCES**

Arden, D.D., 1975. Geology of Jamaica and the Nicaraguan Rise. In: Stehli FG, editor. The ocean basins
and margins: the Gulf of Mexico and the Carribbean. New York. Plenum Press: 617–61.

Aubry, M.P., 1993. Neogene allostratigraphya nd depositionalh istory of the De Soto Canyon area, northern Gulf of Mexico. Micropale-ontology, 39:327–366.

Barss, M.S., Bujak J.P., Williams G.L., 1979. Palynological zonation and correlation of sixty-seven wells,
eastern Canada. Geological Survey of Canada, Paper 78–24:1–117.

Bartoli, G., Sarnthein, M., Weinelt, M., Erlenkeuser, H., Garbe-Schönberg, D., Lea, D.W., 2005. Final closure of Panama and the onset of Northern Hemisphere Glaciation. Earth and Planetary Science Letters 237: 33–44.

Batten, D.J., 1996. Palynofacies and palaeoenvironmental interpretation. In: Jansonius, J., MacGregor, D.C.
(Eds.), Palynology: Principles and Applications. American Association of Stratigraphic Palynologists
Foundation, Dallas, TX, pp. 1011–1064.

Batten, D.J., Stead, D.T., 2005. Palynofacies analysis and its stratigraphic application. Applied Stratigraphy, pp. 203–226.

Bemis, B.E., Spero, H.J., Bijma, J., Lea, D.W., 19. Reevaluation of the oxygen isotopic composition of
planktonic foraminifera: Experimental results and revised paleotemperature equations. Paleoceanography, 13: 150–160.

Berger, A., 1988. Milankovitch theory and climate. Review of Geophysics 26: 624–657.

Berger, W.H., Wefer, G., 1996. Central themes of South Atlantic circulation, in The South Atlantic: Present
and Past Circulation, edited by G. Wefer et al., Springer-Verlag Berlin: 1–11.

Berggren, W.A., 1977. Late Neogene planktonic foraminiferal biostratigraphy of the Rio Grande Rise
(South Atlantic). Marine Micropaleontology, 2: 265–313.

Berggren, W.A., Hollister, C.D., 1974. Paleogeography, paleobiogeography, and the history of circulation

of the Atlantic Ocean, in Studies in Paleoceanography, edited by W.W. Hay, Spec. Publ.–Soc. Econ. Paleontol. Mineral., 20: 126–186.

Berggren, W.A., Hollister, C.D., 1977. Plate tectonics and paleocirculation: commotion in the ocean. In Bonin, J., and Dietz, R.S. (Eds.), The Present State of Plate Tectonics. Tectonophysics, 38:11–48.

Bickert, T., Curry, W.B., Wefer, G., 1997. Late Pliocene to Holocene (2.6–0 Ma) western equatorial Atlantic deep-water circulation: Inferences from benthic stable isotopes. Leg 154, Proc. Ocean Drill. Program Sci. Results, 154: 239–254.

Billups, K., Ravelo, A.C., Zachos, J.C., Norris, R.D., 1999. Link between oceanic heat transport, thermohaline circulation, and the Intertropical Convergence Zone in the Early Pliocene Atlantic. Geology, 27: 319 –322.

Bradford, M.R., Wall, A., 1984. The distribution of recent organic-walled dinoflagellate cysts in the Persian Gulf, Gulf of Oman, and North-western Arabian Sea. Palaeontographica, Abteilung B, 192:16–84.

Brewster–Wingard, G.L., Ishman S.E., Edwards L.E., Willard D.A., 1996. Preliminary report on the distribution of modern fauna and flora at selected sites in north–central and north–eastern Florida Bay. U.S. Geological Survey Open-File Report, 96–732.

Brinkhuis, H., Munsterman, D.K., Sengers, S., Sluijs, A., Warnaar, J., Williams, G.L., 2003. Late Eocene–Quaternary dinoflagellate cysts from ODP Site 1168, Off Western Tasmania. In: Exon, N.F., Kennett, J.P., Malone, M.J. Eds., Proceedings of the Ocean Drilling Program, Scientific Results, 189, 1–36. College Station, Texas: Ocean Drilling Program.doi:10.2973/odp.proc.sr.189.105.2003.

Broecker, W.S., 1991. The Great Ocean Conveyor. Oceanography 4: 79–89.

Broecker, W.S., Denton G.H., 1989. The role of ocean–atmoshpere reorganizations in glacial cycles. Geochimica et Cosmochimica Acta 53: 2465-2501.

Bujak, J.P., 1984. Cenozoic dinoflagellate cysts and acritarchs from the Bering Sea and northern North Pacific, DSDP Leg 19. Micropaleontology, 30(2):180–212.

Bujak, J.P., Matsuoka K., 1986. Late Cenozoic dinoflagellate cysts zonation in the Western and Northern Pacific. In J. H. Wrenn, S.L. Duffield, and J.A. Stein (eds.), Papers from the First Symposium on Neogene dinoflagellate cysts Biostratigraphy. American Association of Stratigraphic Palynologists Contributions Series, 17: 7–25

Burke, K., 1988. Tectonic evolution of the Caribbean. Annual Review of Earth and Planetary Sciences 16: 201-230.

Burton, K.W., Fei Ling, H., O'Nions R. k., 1997. Closure of the Central American Isthmus and its effect on deep–water formation in the North Atlantic. Nature, 386: 382–385.

Cane, M.A., Molnar, P., 2001. Closing of the Indonesian seaway as a precursor to east African aridification around 3-4 million years ago. Nature 411:157–162.

Chaisson, W.P., Ravelo, A.C., 2000. Pliocene development of the east-west hydrographic gradient in the equatorial Pacific. Palaeoceanography, 15: 497-505.

Chandler, M., Dowsett, H., Haywood, A., 2008. The PRISM model-data cooperative: Mid–Pliocene data–model comparisons. PAGES News 16: 24–25.

Chezem, M.A., 2012, Foraminiferal paleoecology across the Early to Middle Eocene transition (emet) of the Western Caribbean. Ball State Department of Geological Sciences, 142 pp.

Chmura, G.L. Smirnov, A., Campbell, I.D. 1999. Pollen transport through distributaries and depositional patterns in coastal waters. Palaeogeography, Palaeoclimatology, Palaeoecology, 149: 257–270.

Clark, R.L., 1985. Effects on charcoal of pollen preparation procedures; Pollen et Spores 26: 559–576.

Coates, A.G., Collins, L.S., Aubry, M.P., Berggren, W.A., 2004. The Geology of the Darien, Panama, and the Late Miocene-Pliocene collision of the Panama arc with the northwestern South America. Geological Society of America Bulletin 116: 1327–1344.

Coates, A.G., Obando, J.A., 1996. The geological evolution of the Central American Isthmus. In Jackson, J. B.C., Budd, A.F., Coates, A.G. (eds). Evolution and environment in tropical America. Univ. of Chicago Press, Chicago, Illinois, 21–56.

Cohen, A.C., Morin J.G., 1993. The cypridinid copulatory limb and a new genus Kornickeria (Ostracoda: Myodocopoida) with four new species of bioluminescent ostracodes from the Caribbean. Zoological journal of the Linnean society, 108: 23–84.

Collins, L.S., Coates, A.G., Berggren, W.A., Aubry, M.P., Zhang, J., 1996. The Late Miocene Panama isthmiam strait. Geology, 24: 687–690.

Collins, L.S., Coates, A.G., Jackson, J.B. C., Obando, J.A., 1995. Timing and rates of emergence of the Limón and Bocas del Toro basins: Caribbean effects of Cocos Ridge subduction? In: Geologic and Tectonic Development of the Caribbean Plate Boundary in Combaz, A., 1964. Les palynofacie `s. Revue de Micropaleontologie 7: 205–218.

Combaz, A., 1980. Les Kérogenès vus au microscope, in kerogen: Insoluble organic matter from sedimentary rocks (ed. B. Durand), Éditions Technip, Paris, pp. 55–111.

Cookson I., Eisenack A., 1970. Die Familie der lecaniellaceae n. famfossile Chlorophyta, Volvocales? Neues jahrbuch für Geologie und Palaöntologie, Monatshefte 6: 321 –325.

Corrigan, J., Mann, P., and Ingle Jr., J. C., 1990. Forearc response to subduction of the Cocos Ridge, Panama-Costa Rica. Geological Society of America Bulletin 102: 628–652.

Dale, B., Dale, A. 2002a. Application of ecologically based statistical treatments to micropaplaeontology, p. 259–286. In: S. K. Haslett (Editor), Quaternary Environmental Micropalaeontology, Arnold, London.

Dale, B., Dale, A. 2002b. Environmental application of dinoflagellate cysts and acritarchs, p. 207–239. In: S. K. Haslett (Editor), Quaternary Environmental Micropalaeontology, Arnold, London.

Dale, B., 1976. Cyst formation, sedimentation, and preservation: factors affecting dinoflagellate cysts assemblages in recent sediments from Trondheimsfjord, Norway. Rev. Palaeobot. Palynol. 22: 39–60.

Dale, B., 1996. Dinoflagellate cysts ecology: modeling and geological applications. In: Jansonius, J., McGregor, D.C. (Eds.), Palynology: Principles and Applications, vol. 3. AASP Foundation, Salt Lake City, UT, 1249–1275.

Davey, R.J., 1971. Palynology and palaeo-environmental studies, with special reference to the continental shelf sediments of SouthAfrica. In: Farinacci, A., Matteucci, R. (Eds.), Proceedings of the Second Planktonic Conference, Roma 1970, vol. 1. Technoscienza, Rome, pp. 331–347.

de Boer, J.Z., Drummond, M.S., Bordelon, M.J., Defant, M.J., Bellon, H., Maury R.C., 1995. Cenozoic magmatic phases of the Costa Rican island arc (Cordillera de Talamanca). In: Geologic and Tectonic Development of the Caribbean Plate Boundary in Southern Central America (P. Mann, ed.). Special Paper Geological Society of America 295: 35–55.

De Schepper, S., Fischer, E.I., Groeneveld, J., Head, M.J., Matthiessen, J., 2011. Deciphering the palaeoecology of Late Pliocene and Early Pleistocene dinoflagellate cysts. Palaeogeography, Palaeoclimatology, Palaeoecology 309: 17–32.

De Schepper, S., Groeneveld J, Naafs B.A.D., Van Renterghem C., Hennissen J., et al., 2013. Northern Hemisphere Glaciation during the Globally Warm early Late Pliocene. PLoS ONE 8 (12): e81508. doi:10.1371/journal.pone.0081508.

De Schepper, S., 2006. Plio-Pleistocene dinoflagellate cysts biostratigraphy and palaeoecology from the eastern North Atlantic and southern North Sea Basin. Unpublished PhD thesis: University of Cambridge, 327 pp.

De Schepper, S., Head, M. J. 2009. Pliocene and Pleistocene Dinoflagellate cysts and Acritarch Zonation of Dsdp Hole 610A, Eastern North Atlantic. Palynology, 33: 179–218.

De Schepper, S., Head, M.J. 2008. New dinoflagellate cysts and acritarch taxa from the Pliocene and Pleistocene of the eastern North Atlantic (DSDP Site 610). Journal of systematic Palaeontology, 6 (1): 101–117.

De Schepper, S., Head, M.J., 2014. New late Cenozoic acritarchs: evolution, palaeoecology and correlation potential in high latitude oceans. Journal of Systemati Palaeontology. doi:10.1080/14772019.2013.783883.

De Schepper, S., Head, M.J., 2008. Age calibration of dinoflagellate cysts and acritarch events in the Pliocene-Pleistocene of the eastern North Atlantic (DSDP Hole 610A). Stratigraphy 5(2): 137–61.

De Schepper, S., Head, M.J., and Groeneveld, J., 2009. North Atlantic Current variability through MIS M2 (circa 3.3 Ma) during the mid-Pliocene. Palaeoceanography, 24 PA4206, doi: 10.1029/2008PA001725.

De Schepper, S., Head, M.J. , Louwye, S. 2004. New dinoflagellate cysts and incertae sedis taxa from the Pliocene of northern Belgium, southern North Sea Basin. Journal of Paleontology, 78 (4): 625–644.

De Schepper, S., Head, M.J., 2009. Pliocene and Pleistocene dinoflagellate cysts and acritarch zonation of DSDP Hole 610A, eastern North Atlantic. Palynology 33: 179–218.

De Schepper, S., Head, M.J., Groeneveld, J., 2009. North Atlantic Current variability through marine isotope stage M2 (circa 3.3 Ma) during the mid-Pliocene. Paleoceanography 24: PA4206.

De Schepper, S., Head, M.J., Louwye, S., 2008. Pliocene dinocysts stratigraphy, palaeoecology and sequence stratigraphy of the Tunnel-Canal Dock, Belgium. Geological Magazine 146: 92–112.

de Vernal, A., Eynaud, F., Henry, M., Hillaire-Marcel, C., Londeix, L., Mangin, S., Matthiessen, J., Marret, F., Radi, T., Rochon, A., Solignac, S., Turon, J.L., 2005. Reconstruction of sea-surface conditions at middle to high latitudes of the Northern Hemisphere during the last glacial maximum (LGM) based on dinoflagellate cysts assemblages. Quaternary Science Reviews 24: 897–924.

de Vernal, A., Londeix, L., Harland, R., Morzadec-Kerfourn, M.-T., Mudie, P.J., Turon, J.L., Wrenn, J., 1992. The Quaternary organic walled dinoflagellate cysts of the North Atlantic Ocean and adjacent seas: ecostratigraphic and biostratigraphic records. In: Head, M.J., Wrenn, J.H. (Eds.), Neogene and Quaternary Dinoflagellate Cysts and Acritarchs. American Association of Stratigraphic Palynologists Foundation, Dallas, Texas, pp. 289–328.

de Vernal, A., Mudie, P.J., 1989. Pliocene and Pleistocene palynostratigraphy at ODP Sites 646 and 647, eastern and southern Labrador Sea. In: Srivastava, S.P., Arthur, M., Clement, B., et al. (Eds.), Proceedings of the Ocean Drilling Program, Scientific Results 105: 401–422 College Station, TX.

de Vernal, A., Turon, L., Guiot, J., 1994, Dinocysts distribution in high-latitude marine environments and quantitative reconstruction of sea-surface salinity, temperature and seasonality. Can. J. EarthSci. 31: 48–62.
de Vernal, L., Norris G., 1996a. Middle to Upper Miocene Geonettiaclineae, an opportunistic coastal embayment dinocysts of the Homotryblium Complex. Micropaleontology, 42:263–284.

de Verteuil, L., 1996. Data report: Upper Cenozoic dinocysts from the continental slope and rise off New Jersey. In: Mountain, G.S., Miller, K.G., Blum, P., Poag, C.W., Twichell, D.C. (Eds.), Proceedings of the Ocean Drilling Program, Scientific Results 150: 439–454 College Station, TX.

de Verteuil, L., Norris, G., 1996. Miocene dinocysts stratigraphy and systematics of Maryland and Virginia. Micropaleontology 42:1–172 (supplement).

Deflandre, G., Cookson I., 1955. Fossil microplankton from Australian late Mesozoic and Tertiary sediments, Australian Journal of Marine and Freshwater Research 6: 242–313.

Dekens, P. S., Lea, D. W., Pak, D. K., and Spero, H. J., 2002. Core top calibration of Mg/Ca in tropical foraminifera: Refining paleotemperature estimation. Geochemistry Geophysics Geosystems 3: 1–29.

Dengo, G., 1985. Tectonic setting for the Pacific margin from southern Mexico to Northwestern Columbia. In Nairn, A. E., Stehli, F. G., and Uyeda, S. (eds), The Pacific Ocean: The ocean basins and margins, 7A. Plenum Press, New York, 123–180.

Devillers, R., deVernal, A., 2000. Distribution of dinoflagellate Cysts in Surface Sediments of the Northern North Atlantic in Relation to Nutrient Content and Productivity in Surface Waters. Mar. Geo. 166:103–124.

Donnelly, T.W., 1994. The Caribbean Sea Floor: in Donovan, S. K. and Jackson, T. A., Caribbean Geology: an Introduction, p. 41–65.

Downie, C., Singh, G., 1969. Dinoflagellate cystsfrom estuarine and raised beachdeposits at Woodgrange, Co. Down, N. Ireland. Grana 9: 1–3.

Dowsett, H. J., Poore, R.Z., 1991. Pliocene sea surface temperatures of the North Atlantic Ocean at 3.0 Ma. Quat. Sci. Rev. 10, 189–204, doi: 10.1016/0277-3791(91) 90018.

Dowsett, H. J., Robinson, M. M., 2007. Mid-Pliocene planktonic foraminiferal assemblage of the North Atlantic Ocean. Micropaleontology 53: 105–126.

Dowsett, H. J., Wiggs, L.B., 1992. Planktonic foraminiferal assemblage of the Yorktown Formation, Virginia, USA. Micropaleontology 38: 75-86.

Dowsett, H.J., Barron, J.A., Poore, R.Z., Thompson, R.S., Cronin, T.M., Ishman, S.E., Willard, D. A., 1999. Middle Pliocene paleoenvironmental reconstruction: PRISM2. United States Geological Survey, Open File Report, no. 99–535.

Dowsett, H.J., Chandler M.A., Robinson M.M., 2009. Surface temperatures of the Mid-Pliocene North Atlantic Ocean: Implications for future climate, Philos. Trans. R. Soc. Ser. A, 367: 69–84, doi: 10.1098/ rsta.2008.0213.

Draper, G., Jackson, T. A., Donovan, S. K., 1994, Geologic Provinces of the Caribbean Region: in Donovan, S. K. and Jackson, T. A., Caribbean Geology: an Introduction, p. 3–12.

Driscoll, N.W., Haug, G.H., 1998. A short circuit in thermohaline circulation: A cause for Northern Hemisphere Glaciation? Science, 282: 436–438.

Drugg, W.S., Loeblich A. R., 1967. Some Eocene and Oligocene phytoplankton from the Gulf Coast, U.S.A. Tulane Studies in Geology, 5: 181–194.

Drugg, W.S., Stover L. E., 1975. Stratigraphic range charts, selected Cenozoic dinocysts and plates illustrating Cenozoic species. American Association of Stratigraphic Palynologists, Contributions Series, 4: 73–76.

Duffield S.L., Stein J.A. ,1986. Peridinacean-dominated dinoflagellate cysts assemblage from the Miocene of the Gulf of Mexico Shelf, offshore Louisiana. American Association of Stratigraphy Palynologists Contribution Series, 17:27–45.

Duncan D., Hine A.C, Droxler A.W., 1999. Tectonic controls on carbonate sequence formation in an active strike-slip setting: Serranilla Basin, northern Nicaraguan Rise, and Carribbean Sea. Mar Geol: 355–82.

Duque–Caro, H., 1990. Neogene stratigraphy, paleoceanography and paleobiogeography in northwest SouthAmerica and the evolution of the Panama seaway. Paleogeogr. Paleoclimatol. Paleoecol. 77: 203–234.

Durugbo, E., Ogundipe, O.T. Kaluulu, O., 2011. Preliminary reports on Middle Miocene-Early Pleistocene dinoflagellate cysts from the Western Niger Delta, Nigeria, Ozean Journal of Applied Sciences 4(4): ISSN 1943–2429.

Dwyer, G.S., and Chandler, M.A., 2009. Mid-Pliocene sea level and continental ice volume based on coupled benthic Mg/Ca palaeotemperatures and oxygen isotopes. Phil. Trans. R. Soc. A 367: 157–168.

Dybkjær, K., 2004. Dinocyst stratigraphy and palynofacies studies used for refining a sequence stratigraphic model– uppermost Oligocene to Lower Miocene, Jylland, Denmark. Review of Palaeobotany and Palynology 131: 201–249.

Edwards, L.E., 1986. Late Cenozoic dinoflagellate cysts from South Carolina, U.S.A. U.S. Geological Survey: AASP Contribution Series, 17: 47–51.

Edwards, L.E., 1992. New semiquantitative (paleo) temperature estimates using dinoflagellate cysts, an example from the North Atlantic Ocean, p. 69–87. In: Head, M. J., and Wrenn, J. H. (Eds.), Neogene and Quaternary Dinoflagellate Cysts and Acritarchs: American Association of Stratigraphic Palynologists Foundation, Dallas.

Edwards, L.E., Mudie, P.J., de Vernal, A., 1991. Pliocene paleoclimatic reconstruction using dinocysts: comparison of methods. Quaternary Science Reviews, 10: 259–274.

Edwards, L., Andrle V., 1992. Distribution of selected dinoflagellate cysts in modern marine sediments. In Neogene and Quaternary Dinoflagellate Cysts and Acritarchs, Head M.J., Wrenn J.H. (eds), American Association of Stratigraphic Palynologists Foundation: Utah: 259–288.

Edwards, L.E., 1984. Miocene dinocysts from Deep Sea Drilling Project Leg 81, Rockall Plateau, eastern North Atlantic. In: Roberts, D.G., Schnitker, D., et al. (Eds.), Initial Reports of the Deep Sea Drilling Project, 81. U.S. Government Printing Office, Washington, D.C., pp. 581–594.

Ellegaard, M., 2000. Variations in dinoflagellate cysts morphology under conditions of changing salinity during the last 2000 years in the Limfjord, Denmark. Rev. Palaeobot. Palynol. 109: 65-81.

Elsik W., 1977. Paralecaniella indentata (Deflandre and Cookson 1955) Cookson and Eisenack, 1970 and allied dinocysts, Palynology, 1: 95–103.

Erez, J., Luz, B., 1983. Experimental paleotemperature equation for planktonic foraminifera. Geochim. Cosmochim. Acta, 47: 1025–1031.

Evitt, W. R., 1985. Sporopollenin Dinoflagellate Cysts. Their Morphology and Interpretation. American Association of Stratigraphic Palynologists Foundation, Dallas, Texas, 333 pp.

Evitt, W.R., 1963. A discussion and proposals concerning fossil dinocysts, hystrichospheres and acritarchs. Proc.Nat. Acad. Sci. USA 49: 158–164, 298–302.

Evitt, W.R., Davidson, S.E., 1964. Dinocysts studies. I. Dinoflagellate cystsand thecae. Stanford Univ. Publ. Geol. Sci. 10: 3–12.

Hilgen, F.J. Lourens, L.J., Van Dam, J.A., Beu, A.G., Boyes A.F., Cooper, R.A., Krijgsman, W. Ogg J.G., Piller W.E., Wilson, D.S. 2012. The Geologic Time Scale, 2012, Pages 923–978.

Fensome R.A., Williams G.L., Barss M.S., Freeman J.M., Hill J.M., 1990. Acritarchs and fossil prasinophytes: an index to genera, species and intraspecific taxa, American Assoication of Stratigraphic Palynologists Foundation, Contributions Series Number, 25: 1–771.

Fensome, R.A., MacRea, R.A., Moldowan, J.M., Taylor, F.J.R., Williams, G.L., 1996a. The Early Mesozoic radiation of dinocysts. Paleobiology 22: 329 –338.

Fensome, R.A., Riding, J.B., Taylor, F.J.R., 1996b. Dinocysts. In: Jansonius, J., McGregor, D.C. (Eds.), Palynology: Principles and Applications, vol. 1. AASP Foundation, Salt Lake City, UT, pp. 107–169.

Fensome, R.A., Saldarriaga, J.F., Taylor, F.J.R., 1999. Dinocysts phylogeny revisited: reconciling morphological and molecular based phylogenies. Grana 38: 66 –80.

Fensome, R.A., Taylor, F.J.R., Norris, G., Sarjeant, W.A.S., Wharton, D.I., Williams, G.L., 1993. Micropaleontology, Special Publication, 7: A Classi ¢ cation of Modern and Fossil Dinocysts. Sheridan Press, Hanover, NH, 351 pp.

Fischer, E.,I., 2011. Palynology and foraminiferal geochemistry of the Lower Pleistocene Olduvai Subchron (ca. 1.8 Ma) in DSDP Hole 603C, western North Atlantic. Faculty of Mathematics and Science, Brock University, 169 pp.

Foster, G.L., Lunt, D.J., Parrish R.R., 2009. Mountain uplift and the threshold for sustained Northern Hemisphere Glaciation. Climate of the Past Discussions 5: 2439–2464.

Garrison, T., 2008, Essentials of Oceanography, Thomson learning. 361. Geological Journal 43, 75–94 Geosystems 3, 1–29.

Gibbard, P.L., Head, M.J., Walker, M.J.C. and the Subcommission on Quaternary Stratigraphy, 2010. Formal ratification of the Quaternary System/Period and the Pleistocene Series/Epoch with a base at 2.58 Ma. J. Quaternary Sci., Vol. 25 pp. 96–102. ISSN 0267–8179.

Gibbard, P.L, Head, M.J., 2009a. The definition of the Quaternary System/Era and the Pleistocene Series/Epoch. Quaternaire, 20(2): 125–133.

Gibbard, P.L., Head, M.J., 2009b. IUGS ratification of the Quaternary System/Period and the Pleistocene Series/Epoch with a base at 2.58 Ma. Quaternaire, 20(4): 411–412.

Gibbard, P.L., Head, M.J., 2010. The newly-ratified definition of the Quaternary System/Period and redefinition of the Pleistocene Series/Epoch, and comparison of proposals advanced prior to formal ratification. Episodes, 33: 152–158.

Gibbard, P.L., Head, M.J., Walker, M.J.C. and The Subcommission on Quaternary Stratigraphy, 2010. Formal ratification of the Quaternary System/Period and the Pleistocene Series/Epoch with a base at 2.58 Ma. Journal of Quaternary Science, 25(2): 96–102.

Gladenkov, A. Y., Oleinik, A.E., Marincovich, L.J., Konstantin B.B., 2002. A refined age for the earliest opening of Bering Strait. Palaeogeography, Palaeoclimatology, Palaeoecology, 183: 321–328.

Goll, R.M., 1989. A synthesis of Norwegian Sea biostratigraphies: ODP Leg 104 on the Vøring Plateau. In: Eldholm, O., Thiede, J., Taylor, E., et al. (Eds.), Proceedings of the Ocean Drilling Program, Scientific Results 104: 777–826 College Station, TX.

Gradstein, F.M., Srivastava, S.P., 1980. Aspects of Cenozoic stratigraphy and paleoceanography of the Labrador Sea and Baffin Bay. Palaeogeogr., Palaeoclimatol., Palaeoecol., 30:261–295.

Groeneveld, J., 2005. Effect of the Pliocene closure of the Panamanian Gateway on Caribbean and east Pacific sea surface temperatures and salinities by applying combined Mg/Ca and $\delta^{18}O$ measurements (5.6-2.2 Ma), Ph.D. thesis, 327 pp.

Groeneveld, J., Nürnberg, D., Tiedemann, R., Reichart G.J., Steph, S., Reuning, L., Crudeli D., Mason P., 2008. Foraminiferal Mg/Ca increase in the Caribbean during the Pliocene: Western Atlantic Warm Pool formation, salinity influence, or diagenetic overprint? Geochemistry, Geophysics, Geosystems, 9 (1) Q01P23, doi: 10.1029/2006GC001564, ISSN: 1525–2027.

Gussone, N., Eisenhauer, A., Tiedemann, R., Haug, G.H., Heuser, A., Bock, B., Th. F., Nägler, Mqllera, A., 2004. Reconstruction of Caribbean Sea surface temperature and salinity fluctuations in response to the Pliocene closure of the Central American Gateway and radiative forcing, using $\delta^{44/4}0Ca$, $\delta^{18}O$ and Mg/Ca ratios, Earth and Planetary Science Letters, 227: 201–214.

Hallett, R.I., 1999. Consequences of Environmental Change on the Growth and Morphology of Lingulodinium polyedrum (Dinophyceae) in Culture. Ph.D. Dissertation, University of Westminster, London, 109 pp.

Hansen, B., Østerhus S., 2000. North Atlantic-Nordic Seas exchanges, Prog. Oceanography, 45: 109 –208, doi: 10.1016/S0079-6611(99)00052-X.

Haq, B.U., Hardenbol J., Vail P.R., 1987. Chronology of fluctuating sea levels since the Triassic. Science 235:156–1,167, http://dx.doi.org/10.1126/science.235.4793.1156.

Harland, R., 1979. Dinocysts biostratigraphy of Neogene and Quaternary sediments at holes 400/400A in the Bay of Biscay (Deep Sea Drilling Project Leg 48), p. 531–45. In Montadert, L.

Roberts, D. G. et al. (Eds.) Initial Reports of the Deep Sea Drilling Project, 48. Washington D.C.: U.S. Government Printing Office.

Haug, G.H., Ganopolski, A., Sigman, D.M., Rosell-Mele, A., Swann, G.A., Tiedemann, R., Jaccard, S.L., Bollmann, J., Maslin, M.A., Leng, M.J., Eglinton, G., 2005. North Pacific seasonality and the glaciation of North America 2.7 million years ago. Nature, 433: 821–825.

Haug, G.H., Tiedemann, R., 1998. Effect of the formation of the Isthmus of Panama on Atlantic Ocean thermohaline circulation. Nature, 393: 673–676.

Haug, G.H., Tiedemann, R., Keigwin, L.D., 2004. How the Isthmus of Panama Put Ice in the Arctic. Oceanus, 42: 94–97.

Haug, G.H., Tiedemann, R., Zahn, R., Ravelo, A.C., 2001. Role of Panama uplift on Oceanic freshwater balance. Geology, 29: 207–210.

Haywood, A.M., Valdes, P.J., Sellwood, B.W., 2002. Magnitude of climate variability during Middle Pliocene warmth: history (16–71 Ma) of the Galápagos hotspot: Implications for the tectonic and biological evolution of the Americas. Geology, 30: 795–798.

Head, M.J., 1993. Dinoflagellate cysts, sporomorphs, and other palynomorphs from the Upper Pliocene St. Erth Beds of Cornwall, southwestern England. Paleontological Society Memoir 31 (Journal of Paleontology, 67 Supplement), 62 p.

Head, M.J., 1994. Morphologya nd paleoenvironmenta silgnificance of the Cenozoic dinocysts genera *Habibacysta* and *Tectatodinium*. Micropaleontology, 40:289–321.

Head, M.J., 1996. Late Cenozoic dinocysts from the Royal Society borehole at Ludham, Norfolk, Eastern England. Journal of Paleontology, 70 (4): 543–570.

Head, M.J., 1996. Paleoecological and taxonomic revision of Late Cenozoic dinocysts from the Royal Society borehole at Ludham, eastern England. Journal of Paleontology, 70: 543–70.

Head, M.J., 1997. Thermophilic dinocyst assemblages from the mid Pliocene of Eastern England. Journal of Paleontology, 71 (2): 165–193.

Head, M.J., 1998. Marine environmental change in the Pliocene and Early Pleistocene of eastern England: the dinocysts evidence reviewed. In The Dawn of the Quaternary (eds. T. Van Kolfschoten and P. L. Gibbard). Mededelingen Nederlands Instituut voor Toegepaste Geowetenschappen TNO, 60: 199–226.

Head, M.J., 2003a. Neogene occurrences of the marine acritarch genus Nannobarbophora Habib and Knapp, 1982 emend, and the new species N. gedlii. Journal of Paleontology, 77: 382–385.

Head, M.J., 2007. Last Interglacial (Eemian) hydrographic conditions in the southwestern Baltic Sea based on dinoflagellate cysts from Ristinge Klint, Denmark. Geological Magazine, 144 (6): 987–1013.

Head, M.J., Norris, G. 2003. New species of dinoflagellate cysts and other palynomorphs from the latest Miocene and Pliocene of DSDP Hole 603C, western North Atlantic. Journal of Paleontology, 77 (1): 1–15.

Head, M.J., 1997. Thermophilic dinocysts assemblages from the Mid–Pliocene of eastern England. Journal of Paleontology, 71: 165–93.

Head, M.J., Norris G., Mudie, P., 1989. Palynology and dinocyst stratigraphy of the Miocene in ODP Leg 105, Hole 645E, Baffin Bay. In Proceedings of the Ocean Drilling Program, Scientific Results, Vol. 105, Srivastava S.P., Arthur M.A., Clement B. College Station, Texas, 467–514.

Head, M.J., Norris, G., Mudie, P.J., 1989. Palynology and dinocyst stratigraphy of the Upper Miocene and lowermost Pliocene, ODP Leg 105, Site 646, Labrador Sea. In S.P. Srivastava, M.A. Arthur, B. Clement, et al. (Eds.), Proceedings of the Ocean Drilling Program, Scientific Results, 105. Ocean Drilling Program, College Station, Texas, 423–451.

Head, M.J., Westphal, H., 1999. Palynology and paleoenvironments of a Pliocene carbonate platform: the Clino Core, Bahamas. Journal of Paleontology 73(1): 1–25.

Head, M.J., Pillans, B., and Farquhar, S., 2008b. The Early–Middle Pleistocene Transition: characterization and proposed guide for the defining boundary. Episodes, 31(2): 255–259.

Hellweger, F.L., and Gordon A.L., 2002, Tracing Amazon River water into the Caribbean Sea, J. Mar. Res., 60(4): 537–549.

Hodell, D.A., Warnke D.A., 1991. Climate evolution of the Southern Ocean during the Pliocene epoch from 4.8 to 2.6 million years ago, Quat. Sci. Rev., 10: 205–214.

Hoernle, K., Bogaard, P.V.D., Werner, R., Lissinna, B., Hauff, F., Alverado, G., Garbe-Schönberg, D., 2002. Missing Inferences from benthic stable isotopes, Leg 154, Proc. Ocean Drill. Program Sci. Results, 154: 239–254.

Hopkins, J.A., McCarthy, F.M.G., 2002. A laboratory experiment studying the effects of progressive oxidation on Quaternary palynological assemblages in marine sediments. Palynology 26: 167–184.

Imbrie, J., Kipp, N.G., 1971. A new micropaleontological method for quantitative paleoclimatology: Application to a late Pleistocene Caribbean core, in K.K. Turekian (ed.), The Late Cenozoic Glacial Ages, Yale Univ. Press, New Haven, C.T.: 1-81. impact on Atlantic hurricanes. Geophysical Research Letters 34, 1-5 in tropical foraminifera: Refining

paleotemperature estimation. Geochemistry, Geophysics, J., Taylor, E., et al. (Eds.), Proceedings of the Ocean Drilling Program, Scientific Results Jacobs, C., Birgl, H., Conley, D. L., 1963. Am. Assoc. Petrol. Geologists Mem. 2: 62–72.

Jan du Chêne, R. 1977. Etude palynologique du Miocene superieur An-dalou (Espagne). Revista Espafiola de Micropaleontologia, 9: 97–114.

Jiang, D., et al., 2005. Modeling the Pliocene climate with a global atmospheric general circulation model. J. Geophys. Res., 110, D14107, doi: 10.1029/2004JD005639.

Jiménez-Moreno, G., Head, M.J., Harzhauser, M., 2006. Early and Middle Miocene dinoflagellate cysts stratigraphy of the Central Paratethys, Central Europe. Journal of Micropalaeontology 25: 113–119.

Johns, W.E., T.L., Townsend, D.M., Fratantoni, W. D. Wilson, 2002. On the Atlantic inflow to the Caribbean Sea, Deep Sea Res., Part I, 49: 211 –243.

Johnson, H.L. Marshall, D.P., 2002. A Theory for the Surface Atlantic Response to Thermohaline Variability, J. Phys. Oceanogr., 32: 1121–1132, doi:10.1175/1520–0485.

Kameo, K., Sato, T., 2000. Biogeography of Neogene calcareous nannofossils in the Caribbean and the eastern equatorial Pacific: Floral response to the emergence of the Isthmus of Panama. Marine Micropaleontology 39: 201–218.

Keller, G., Zenker, C.E., Stone, S.M., 1989. Late Neogene history of the Pacific-Caribbean Gateway. J. South Am. Earth Sci., 2, 73–108.

Kleiven, H.F., Jansen, E., Fronval, T., Smith, T.M., 2002. Intensification of Northern Hemisphere Glaciations in the circum Atlantic region (3.5–2.4 Ma). Ice-rafted detritus evidence, Palaeogeogr. Palaeoclimatol., Palaeoecol., 184: 213–223, doi:10.1016/S0031- 0182(01)00407–2.

Klemenk, K.W., 1964. Armoured dinocysts of the Gulf of California. Bull. Scripps Inst. Ocean, Univ. Calif. La Jolla 8: 347–372.

Klocker A., Prange M., Schulz M., 2005. Testing the influence of the Central American seaway on orbitally forced Northern Hemisphere Glaciation. Geophysical Research Letters 32: 1–4.

Laskar, J., Robutel, P., J., F., Gastineau, M., Correia, A.C.M., Levrard, B., 2004. A long-term numerical solution for the insolation last 8 million years (sites 657–661), Proc. Ocean Drill. Program Sci. Results, 108: 241–277.

Lea, D.W., 2003. Elemental and isotopic proxies of past ocean temperatures. in H. Elderfield (ed), The oceans and marine geochemistry, Elsevier-Pergamon, Oxford: 365–390.

Lenoir, E.A., Hart, G.F., 1986. In: Wrenn, J.H., Duffield, S.L., Stein, J.A. (Eds.), Burdigalian (Early Miocene) Dinocysts from Offshore Louisiana: AASP Contribution Series Papers, 17: 59–81.

Lepš, J. and Šmilauer, P., 1999. Multivariate Analysis of Ecological Data.. Faculty of Biological Sciences,
University of South Bohemia, 110 pp.

Levitus, S., Boyer, T.P., 1994b. World Ocean Atlas 1994 (Vol. 4): Temperature. NOAA Atlas NESDIS 4, United States Governmental Printing Office, Washington D. C., 117 pp.

Lewis, J., Dodge, J.D., Powell, A.J., 1990. Quaternary dinoflagellate cysts from the upwelling system onshore Peru, hole 686B, ODP Leg 112. Proc. ODP Sci. Results, 112: 323–327.

Lewis, J., Hallett, R., 1997. *Lingulodinium polyedrum* (*Gonyaulax polyedra*) a blooming dinocysts. Oceanogr. Mar. Biol. Annu. Rev., 35: 97–161.

Audrey, L., Londeix, L., de Vernal A., 2013. Organic-walled dinoflagellate cysts distribution in the Gulf of Mexico. Marine Micropaleontology, 102: 51–68.

Lisiecki, L.E., Raymo, M.E. 2005. A Pliocene–Pleistocene stack of 57 globally distributed benthic $\delta^{18}O$ records, Paleoceanography, 20: PA1003, doi:10.1029/2004PA001071.

Lister, J.K., Batten, D.J., 1988. Stratigraphic paleoenvironmental distribution of Early Cretaceous dinoflagellate cysts in the Hurlands Farm Borehole, West Sussex, England. Palaeontographica B210, 9-89.
Lloyd J. J., 1963. Am. Assoc. Petrol. Geologists Mem., 2: 88–100.

Locarnini, R.A., Mishonov, A.V., Antonov, J.I., Boyer, T.P., Garcia, H.E.., 2006. World Ocean Atlas 2005, Volume 1: Temperature. In: Levitus S., editor. NOAA Atlas NESDIS 61. Washington, D.C.: U.S. Gov. Printing Office. p. 182. Available: http://www.nodc.noaa.gov/OC5/indprod.html.

Lourens, L., Hilgen, F., Shackleton, N.J., Laskar, J., Wilson, D., 2005. The Neogene. In: Gradstein, F.M., Ogg, J.G., and Smith, A.G., Eds., A Geological Time Scale 2004, 409–430. Cambridge, U.K.: Cambridge University Press.

Louwye, S., De Schepper S., Laga, P., Vandenberghe, N., 2007. The Upper Miocene at the southern North Sea Basin: a palaeoenvironmental and stratigraphic reconstruction with dinoflagellate cysts. Geological Magazine 144(1): 33–52.

Louwye, S., Laga, P., 2008. Dinoflagellate cysts stratigraphy and palaeoenvironment of the marginal marine Middle and Upper Miocene of the eastern Campine area, northern Belgium (southern North Sea Basin). Geological Journal 43: 75–94.

Louwye, S. and Laga, P., 1998. Dinoflagellate cysts of the shallow marine Neogene succession in the Kalmthout well, northern Belgium Bull. geol. Soc. Denmark, 45(1): 73–86.

Louwye, S., De Schepper, S., 2010. The Miocene–Pliocene hiatus in the southern North Sea Basin (northern Belgium) revealed by dinoflagellate cysts. Geological Magazine, 147: 760–776.

Louwye, S., Head, M.J. , De Schepper, S., 2004. Dinoflagellate cyst stratigraphy and palaeoecology of the Pliocene in northern Belgium, southern North Sea Basin. Geological Magazine, 141 (3): 353–378.

Lunt, D.J., Foster, G.L., Haywood, A.M., Stone, E.J., 2008. Late Pliocene Greenland glaciation controlled by a decline in atmospheric CO2 levels. Nature, 454: 1102–1105, doi: 10.

Maher, Jr., L.J., 1981. Statistics for microfossil concentration measurements employing samples spiked with marker grains. Review of Paleobotany and Palynology, 32: 153–191.

Maier-Reimer, E., Mikolajewicz, U., Crowley, T., 1990. Ocean general circulation model sensitivity experiment with an open Central American isthmus. Palaeoceanography, 5: 349 –366.

Manabe, S., Stauffer, R.J., 1988. Two stable equilibria of a coupled ocean-atmosphere model. Journal of Climatology, 1: 841–866.

Manum, S., 1976. Dinocysts in Tertiary Norwegian-Greenland Sea sediments (Deep Sea Drilling Project Leg 38), with observations on palynomorphs and palynodebris in relation to environment. In Talwani, M., Udintsev, G., et al., Init. Repts. DSDP, 38: Washington (U.S. Govt. Printing Office), 897–919.

Manum, S.B., Boulter, M.C., Gunnarsdottir, H., Rangnes, K., Scholze, A., 1989. Eocene to Miocene palynology of the Norwegian Sea (ODP Leg 104). In: Eldholm, O., Thiede, J., Taylor, E., et al. (Eds.), Proceedings of the Ocean Drilling Program, Scientific Results, 104: 611–662 College Station, TX.

Marret, F., Zonneveld, K.A.F., 2003. Atlas of modern organic-walled dinoflagellate cysts distribution. Review of Palaeobotany and Palynology, 125 (1–2): 1–200.

Marret, F., 1994. Distribution of dinoflagellate cysts in recent marine sediments from the east Equatorial Atlantic (Gulf of Guinea). Rev. Palaeobot. Palynol. 84: 1–22.

Marshall, L.G., 1988. Land Mammals and the Great American Interchange. American Scientist 76: 380–388.

Marshall, L.G., Webb, S.D., Sepkosko Jr., J.J., Raup, D.M., 1982. Mammalian evolution and the great American interchange. Science, 215: 1351–1357.

Maslin, M.A., Li, X.S., Loutre, M.F., Berger, A., 1998. The contribution of orbital forcing to the progressive intensification of Northern Hemisphere Glaciation. Quat. Sci. Rev., 17: 411–426.

Matsuoka, K., 1983. Late Cenozoic dinocysts and acritarchs in the Niigata district, central Japan. Palaeontogr. Abt. B, 187:89–154.

Matsuoka, K., Bujak, J.P., Shimazaki, T., 1987. Late Cenozoic dinoflagellate cysts biostratigraphy from the west coast of northern Japan. Micropaleontology, 33: 214–229.

Matthiessen, J., Brenner, W., 1996. Dinoflagellate cysts ecostratigraphy of Plio-Pleistocene sediments from the Yermak Plateau (Arctic Ocean, Hole 911A), p.243–253. In: Thiede, J., Myhre, A.M., Firth, J.V., Johndon, G.L. and Ruddiman, W.F. (Eds.) Proceedings of the Ocean Drilling Program Scientific Results, 151: College Station, Texas (Ocean Drilling Program).

Matthiessen, J., 1991. GEOMAR Report, 7: Dinocystsn-Zysten im Spätquartär des europäischen Nordmeeres: Palökologie und Palaö Ozeanographie. GEOMAR, Kiel, 115 pp.

Matthiessen, J., 1994a. Distribution patterns of dinoflagellate cysts and other organic walled microfossils in recent Norwegian-Greenland Sea sediments. Mar. Micropaleontol. 24: 307–334.

Mertens, K.N., Takano, Y., Head, M.J., and Matsuoka, K. 2014. Living fossils in the Indo-Pacific warm pool: A refuge for thermophilic dinocysts during glaciations. Geology, doi:10.1130/G35456.1. GSA data repository item 2014187 (for online supplementary data). Also featured in Research Highlights, Nature, vol. 508, 24 April, 2014.

McCarthy, F.M.G., Mudie, P.J., 1996. Palynology and dinocysts biostratigraphy of Upper Cenozoic sediments from sites 898 and 900, Iberia Abyssal Plain, p. 241–265. In: Whitmarsh, R. B., Saywyer, D. S., Klaus, A. and Masson, D. G. (Eds.) Proceedings of the Ocean Drilliing Program, Scientific Results, 149: College Station, Texas, (Ocean Drilling Program).

McCarthy, F.M.G., Mudie, P.J., 1998. Oceanic pollen transport and pollen: dinocyst ratios as markers of late Cenozoic sea level change and sediment transport. Palaeogeography, Palaeoclimatology, Palaeoecology, 138: 187–206.

McCarthy, F.M.G., Gostlin, K.E., Mudie, P.J., Hopkins, J.A., 2003. Terrestrial and marine palynomorphs as sea-level proxies: an example from Quaternary sediments on the New Jersey margin, U.S.A, p. 119–129. In Olson, H.C., Leckie, R.M. (Eds.). Micropaleontologic proxies for sea-level change and stratigraphic discontinuities. Society for Sedimentary Geology, Special Publication No. 75.Tulsa, Oklahama, U.S.A.

McDougall, K., 1996. Benthic foraminiferal response to the emergence of the Isthmus of Panama and coincident paleoceanographic changes. Marine Micropaleontology, 28: 133–169.

McMinn, A., 1992. Pliocene through Holocene dinocysts distribution cyst biostratigraphy of the Gippsland Basin, Australia, p. 147–161. In M. J. Head and J. H. Wrenn (Eds.), Neogene and Quaternary Dinoflagellate Cysts and Acritarchs. American Association of Stratigraphic Palynologists Foundation, Dallas, Texas.

McMinn, A., 1992a. Neogene dinocysts distribution in the eastern Indian Ocean from Leg 123, Site 765, p. 429–441. In E M. Gradstein, J. N. Ludden, A. C. Adamson, et al., Proceedings of the Ocean Drilling Program, Scientific Results, 123. Ocean Drilling Program, College Station, Texas.

McMinn, A., 1993a. Neogene dinoflagellate cysts biostratigraphy from sites 815 and 823, Leg 133, northeastern Australian margin, p. 97–105. In J. A. McKenzie, P. J. Davies, A. Palmer-Julson, et al., Proceedings of the Ocean Drilling Program, Scientific Results, 123. Ocean Drilling Pro-gram, College Station, Texas.

Meinen, C.S., Johns, W.E, Garzoli, S.L., van Sebille, E., Rayner, D, Kanzow, T., Baringer, M.O., 2013.Variability of the Deep Western Boundary Currentat 26.51N during 2004–2009, Deep-Sea Research II, 85: 154–168.

Meinen, C.S., Luther, D.S., Baringer, M.O., 2009. Structure, transport and potential vorticity of the Gulf Stream at 68°W: Revisiting older data sets with new techniques. Deep-Sea Research I, 56: 41-60.

Mertens, K.N., Verhoeven, K., Verleye, T., Louwye, S., Amorim, A., Ribeiro, S., Deaf A.S., Harding I.C., De Schepper S., González C., Kodrans-Nsiah M., De Vernal, A., Henry, M., Radi, T., Dybkjaer, K., Poulsen, N.E., Feist-Burkhardt, S., Chitolie, J., Heilmann-Clausen, C., et al., 2009. Determining the absolute abundance of dinoflagellate cysts in recent marine sediments: The *Lycopodium* marker-grain method put to the test. Review of Palaeobotany and Palynology, 157: 238–252.

Mikolajewicz, U., Crowley, T.J., 1997. Response of a coupled ocean/energy balance model to restricted flow through the Central American Isthmus. Palaeoceanography, 12: 429–441.

Mitchell, T.P., Wallace, J.M., 1992. The annual cycle of equatorial convection and sea surface temperature. Journal of Climate, 5: 1140–1156.

Milsom, J., 2009. The Caribbean: an oroclinal basin?: The Origin and Evolution of the Caribbean Plate, in James, K. H., Lorenter, M. A., and Pindell, J. L. eds., The Geological Society of London Special, 328: 139–154.

Molnar, P., 2008. Closing of the Central American Seaway and the Ice Age: A critical review. Paleoceanography, 23: 1–15.

Montes, C., Bayona, G., Cardona, A., Buchs, D.M., Silva, C.A., Morón, S., Hoyos, N., Ramirez, D.A., Jaramillo, C.A., Valencia, V., 2012a. Arc-Continent Collision and Orocline Formation: Closing of the Central American Seaway. Journal of Geophysical Research, 117, 1–25.

Montes, C., Cardona, A., McFadden, R., Morón, S.E., Silva, C.A., Restrepo-Moreno, S., Ramírez, D.A., Hoyos, N., Wilson, J., Farris, D., Bayona, G.A., Jaramillo, C.A., Valencia, V., Bryan, J., Flores, J.A., 2012b. Evidence for Middle Eocene and younger land emergence in central Panama: Implications for Isthmus closure. Geological Society of America Bulletin, 1–20.

Morzadec-Kerfourn, M.T., 1977. Les kystes dinoflagellets dansles sédiments récents le long des côtes bretonnes. Rev. Micropaléontol., 20: 157–166.

Mozardec-Kerfourn, M.T., 1992. Estuarine dinoflagellate cysts among Oceanic assemblages of Pleistocene deep-sea sediments from the West African Margin and their paleonenivronental significance. In: Head, M.J. and Wrenn, J.H. (eds). Neogene and Quartenary Dinocysts and Acritarchs; American Association of Stratigraphic Palynologists Foundation, Dallas. pp. 133–146.

Mudie, P.J., 1987. Palynology and dinocysts biostratigraphy of Deep Sea Drilling Project Leg 94, Sites 607 and 611, North Atlantic Ocean, p. 785–812. In Ruddiman, W.F., Kidd, R.B., Thomas, E., et al. Initial Reports of the Deep Sea Drilling Project, 94. Washington (U.S. Government Printing Office).

Mudie, P.J., 1989. Palynology and dinocyst biostratigraphy of the Late Miocene to Pleistocene, Norwegian Sea: ODP Leg 104, Sites 642 to 644. In: Eldholm, O., Thiede, J., Taylor, E., et al. (Eds.), Proceedings of the Ocean Drilling Program, Scientific Results, 104: 587–610 College Station, TX.

Mudie, P.J., 1992. Circum-Arctic Quaternary and Neogene marine palynofloras: paleoecology and statistical analysis, In: Head, M.J., Wrenn, J.H., eds., Neocene and Quatemary Dinoflagellate Cysts, American Association of Stratigraphic Palynologists Foundation, pp. 347–390.

Müller, C., 1979. Calcareous nannofossils from the North Atlantic (Leg 48). In: Montadert, L., Roberts, D.G., et al. (Eds.), Initial Reports of the Deep Sea Drilling Project, 48. U.S. Government Printing Office, Washington, D.C., pp. 589–639.

Müller, P. J., Kirst, G., Ruhland, G., von Stroch, I., Rosell-Mele, A., 1998. Calibration of the alkenonepaleotemperature index UK based on core-tops from the eastern South Atlantic and the global ocean (608N-608S). Geochim. Cosmochim. Acta, 62: 1757–1772.

Munsterman, D.K., Brinkhuis, H., 2004. A southern North Sea Miocene dinocyst zonation. Geologie en Mijnbouw, 83: 267–285.

Naafs, B.D.A., Stein, R., Hefter, J., Khèlifi, N., De Schepper, S., Haug, G.H., 2010. Late Pliocene changes in the North Atlantic Current. Earth and Planetary Science Letters, 298: 434–442.

Nisancioglu, K.H., Raymo, M.E., Stone, P.H., 2003. Reorganization of Miocene deep water circulation in response to the shoaling of the Central American Seaway. Palaeoceanography, 18, doi: 10.1029/2002PA000767.

Nürnberg, D., 2000. Taking the temperature of past ocean surfaces. Science, 289: 1698–1699.

Oboh-Ikuenobe, F.E., Obi, C.G., Jaramillo, C.A., Miropyle, A., 2005. Lithofacies, palynofacies, and sequence stratigraphy of Palaeogene strata in southeastern Nigeria. Journal of African Earth Sciences 41: 79–102.

Paez-Reyez, M., Head, M.J., 2013. The Cenozoic gonyaulacacean dinocysts genera Wall, 1967 and *Protoceratium* Bergh, 1881 and their phylogenetic relationships. Journal of Paleontology, 87: 786–803.

Persson, A., Godhe, A., Karlson, B., 2000. Dinocysts in recent sediments from the West Coast of Sweden. Bot. Mar., 43: 69–79.

Pflaumann, U., et al., 2003. Glacial North Atlantic: Sea-surface conditions reconstructed by GLAMAP (2000), Palaeoceanography, 18: 1065, doi: 10.1029/2002PA000774.

Piasecki, S., 2003. Neogene dinocysts from Davis Strait, offshore West Greenland. Marine and Petroleum Geology, 20: 1075–1088.

Piasecki, S., Gregerson, U., Johannessen, P.N., 2002. Lower Pliocene dinocysts from cored Utsira Formation in the Viking Graben, northern North Sea, Marine and Petroleum Geology, 19: 55–67.

Poore, H.R., Samworth, R., White, N.J., Jones, S. M., McCave, I. N., 2006. Neogene overflow of Northern Component Water at the Greenland-Scotland Ridge. Geochemistry, Geophysic,s Geosystems, 7: 1–24.

Powell, A.J., 1988. A preliminary in vestigation into the Neogene dinocysts biostratigraphy of the British Southwestern Approaches. Bulletin des Centres de Recherches Exploration-Production Elf-Aquitaine, 12 (1): 277-311. pp. 263–289.

Prahl, F.G., Wakeham, S.G., 1987. Calibration of unsaturation patterns in long-chain ketone compositions for palaeotemperature assessment. Nature, 330: 367–369.

Prange, M., Schulz, M., 2004. A coastal upwelling seesaw in the Atlantic Ocean as a result of the closure of the Central American Seaway, Geophys. Res. Lett., 31, L17207, doi: 10.1029/2004GL020073.

Prentice, M.L., Matthews, R.K., 1991. Tertiary Ice Sheet Dynamics: the snow gun hypothesis. Journal of Geophysical Research, 96: 6811–6827.

Raffi, I., Backman, J., Fornaciari, E., Pälike, Domenico R.H., Lourens, L., and Hilgen, F., 2006. A review of calcareous nannofossil astrobiochronology encompassing the past 25 million years: Quaternary Science Reviews, 25: 3113–3137.

Rahmstorf, S., 2002. Ocean circulation and climate during the past 120,000 years, Nature, 419: 207–214.

Ravelo, A.C., Andreasen, D.H., Lyle, M., Lyle, A.O., Wara, M.W., 2004. Regional climate shifts caused by gradual global cooling in the Pliocene epoch, Nature, 429: 263–267.

Raymo, M.E., Ruddiman, W.F., 1992. Tectonic forcing of Late Cenozoic climate. Nature, 359: 117–122.

Raymo, M.E., Grant, B., Horowitz, M., Rau, G.H., 1996. Mid–Pliocene warmth: stronger greenhouse and stronger conveyor. Mar. Micropaleontol., 27: 313–326, doi: 10.1016/0377–8398(95)000488.

Raymo, M.E., Ruddiman, W.F., Froelich, P.N., 1988. Influence of Late Cenozoic mountain building on ocean geochemical cycles. Geology, 16: 649–653.

Rayner, D., Hirschi, J.J.M., Kanzow, T., Johns, W.E., Wright, P.G., Frajka-Williams, E., Bryden, H.L., Meinen, C.S., Baringer, M.O., Marotzke, J., Beal, L.M., Cunningham, S.A., 2011. Monitoring the Atlantic meridional overturning circulation. Deep-Sea Res. II, 48: 1744–1753.

Reichart, G.J., Brinkhuis, H., Huiskamp, F., Zachariasse, W.J., 2004. Hyper-stratification following glacial overturning events in the northern Arabian Sea. Paleoceanography, 19 (2): PA2013, doi:10.1029/2003PA000900.

Renterghem, C.V., 2012. Pliocene Panamanian Gateway tectonics and climate change at 3.3 Ma: palynological and Mg/Ca analysis of MIS M2 at Caribbean ODP Site 999. Scriptie voorgelegd tot het behalen van de grad van Master in de Geologie, 186 pp.

Rivers, T.J., Morin J.G., 2008, Complex sexual courtship displays by luminescent male marine ostracods, The Journal of Experimental Biology, 211: 2252–2262. Published by The Company of Biologists 2008 doi:10.1242/jeb.011130.

Roberts, C.D., LeGrande, A.N., Tripati A.K., 2009, Climate sensitivity to Arctic seaway restriction Early Paleogene: Geology, 286: 575–585.

Rochon, A., de Vernal, A., Turon, J.L., Matthiessen, J., Head, M.J., 1999. Distribution of Recent Dinocysts in surface sediments from the North Atlantic Ocean and adjacent seas in relation to sea-surface parameters. AASP Contr. Ser, 35: 1–150.

Rosell-Mélé, A., Bard, E., Emeis, K..C., Farrimond, P., Grimalt, J., Müller, P.J., Schneider, R., 1998. Project takes a new look at past sea surface temperatures, EOS, Transactions AGU, 79 (33): 393–394.

Rossby, T., 1996. The North Atlantic Current and surrounding waters: At the crossroads, Rev. Geophys., 34 (4): 463–481.

Rossignol, M., 1964. Hystrichosphères du Quaternaire en Méditerranée orientale, dans les sédiments pléistocènes etles boues marine's actuelles. Rev. Micropaléontol., 7: 83–99.

Ruddiman, W.F., 2008. Earth's Climate, Past and Future (Second Edition). W. H. Freeman and Company, New York, 388 pp.

Ruddiman, W.F., Kutzbach, J.E., 1989. Forcing of Late Cenozoic Northern Hemisphere climate by plateau uplift in southern Asia and the American West. J. Geophys. Res., 94: 18409–18427.

Sarnthein, M., Fenner, J., 1988. Global wind-induced change of deep-sea sediment budgets, new ocean production and $CO_2$ reservoirs ca. 3.3–2.35 Ma BP., Phil., Trans., R., Soc., B., 318: 487–504, doi: 10.1098/rstb.1988.0020.

Savin, S.M., Douglas, R.G., 1985. Sea level, climate, and the Central American land bridge. In: The Great American Biotic Interchange (F. G. Stehli, and S. D. Webb, eds.). Plenum., 303–324.

Schnepf, E., Elbrächter, M., 1992. Nutritional strategies in dinocysts. A review withemph asis on cell biological aspects. Eur., J., Protistol., 28: 3–24.

Schnitker, D., 1980. North Atlantic oceanography as possible cause of Antarctic Glaciation and eutrophication, Nature, 284.

Schreck, M., Méheust, M., Stein, R., Matthiessen, J., 2013. Response of marine palynomorphs to Neogene climate cooling in the Iceland Sea (ODP Hole 907A). Marine Micropaleontology, doi: 10.1016/j., marmicro., 2013.03.003.

Schreck, M., Matthiessen, J., Head, M.J., 2012. A magnetostratigraphic calibration of Mid-Miocene to Pliocene dinocyst and acritarch events in the Iceland Sea (ODP Hole 907A). Review of Palaeobotany and Palynology, 187: 66–94. Sea Research, I: 56, 41-60.

Shackleton, N.J., Hall, M.A., 1997. The Late Miocene stable isotope record, Site 926, Proc. Ocean Drill. Program Sci., Results, 154: 367–373.

Shackleton, N.J., Hall, M.A., Pate, D., 1995. Pliocene stable isotope stratigraphy of Site 846. Proc., ODP Sci., Res., 138: 337–357.

Sigurdsson, H., Leckie, R.M., Acton, G.D., et al., 1997. Proceedings of the Ocean Drilling Program, Initial Reports, 165, 100 pp.

Sluijs, A., Pross, J., Brinkhuis, H., 2005. From greenhouse to icehouse; organic–walled dinocyst as paleoenvironmental indicators in the Paleogene. Earth-Science Reviews, 68: 281–315.

Soliman, A., Ćorić, S., Head, M.J., Piller, W., El Beialy, S.Y., 2012. Lower and Middle Miocene biostratigraphy, Gulf of Suez, Egypt based on dinocysts and calcareous nannofossils. Palynology, 36: 1–42.

Stancliffe, R.P.W., 1989. Microforaminiferal linings: their classification, biostratigraphy and paleoecology, with special reference to specimens from British Oxfordian sediments, Micropaleontology, 35: 337–352.

Stehli, F.G., Webb, S.D., eds., 1985. The Great American Biotic Interchange. Plenum Press, New York: 523 pp.

Stein, R., Kanamatsu, T., Alvarez-Zarikian C., Higgins S.M., Channell, J.E.T., Aboud, E., Ohno, M., Acton, G.D., Akimoto, K., Bailey I., Jørklund K.R.B, Evans, H., Nielsen, S.H.H., Fang N., Ferretti, P., Gruetzner, J., Guyodo, Y.J.B., Hagino, K., Harris R., Hatakeda, K., Hefter, J., Judge, S.A., Kulhanek, D. K., Nanayama, F.H., Sierro Sanchez, F.J., Voelker, A., Zhai, Q., 2006. North Atlantic Palaeoceanography: The Last Five Million Years Eos, 87 (13): 129–133.

Steph, S., 2005. Pliocene stratigraphy and the impact of Panama uplift on changes in Caribbean and tropical east Pacific upper ocean stratification (6-2.5 Ma). Ph.D. thesis. University of Kiel, Germany, 158 pp.

Steph, S., Tiedemann R.,J., Groeneveld, Sturm A., Nürnberg D., 2006. Pliocene changes in tropical East Pacific upper ocean stratification: Response to tropical gateways?, Proc. Ocean Drilling Program Sci. Results, 202: 1–51.

Stockmarr, J., 1971. Tablets with spores used in absolute pollen analysis. Pollen Spores, 13: 615–621.

Stover, L.E., 1977. Oligocene and Early Miocene dinocysts from Atlantic corehole 5/5B, Blake Plateau. AASP Contributions Series, 5A. American Association of Stratigraphic Palynologists Foundation, Dallas, Texas, pp. 66–89.

Stover, L.E., Brinkhuis, H., Damassa, S.P., De Verteuil, L., Helby, R.J., Monteil, E., Partridge, A.D., Powell, A.J., Riding, J.B., Smelror, M., Williams, G.L., 1996. Mesozoic–Tertiary dinocysts, acritarchs and prasynophytes. In: Jansonius, J., McGregor, D.C. (Eds.), Palynology: Principles and Applications, vol. 2. AASP Foundation, Salt Lake City, UT, 641–750.

Swift, J.H., 1986. The Arctic waters, in The Nordic Seas, edited by B.G. Hurdle, Springer, New York,
pp. 129–153.

Taylor, F.J.R., 1987. The Biology of Dinocysts. Blackwell Scientific, Oxford, Botanical Monographs, 21: 785 pp.

Tiedemann R., Sturm A., Steph S., Lund S.P., Stoner J.S., et al., 2006. Astronomically calibrated timescales from 6 to 2.5 Ma and benthic isotope stratigraphies, Sites 1236, 1237, 1239, and 1241. Proc ODP Sci Res., 202: 1–69. doi:10.2973/odp.proc.sr.202.210.2007.

Tiedemann, R., Franz S.O., 1997. Deep water circulation, chemistry, and terrigenous sediment supply in the equatorial Atlantic during the Pliocene, 3.3–2.6 Ma and 5–4.5 Ma. In Shackleton, N.J., Curry, W.B., and Bralower, T.J. (Eds). Proc. ODP, Sci. Results, 154: 299–318. College Station, TX (Ocean Drilling Program),

Tiedemann, R., Sarnthein M., Shackleton N.J., 1994. Astronomic timescale for the Pliocene Atlantic $\delta^{18}O$ and dust flux records of Ocean Drilling Program Site 659. Palaeoceanography, 9 (4): 619–638.

Tiedemann, R., Sarnthein M., Stein R., 1989. Climatic changes in the Western Sahara: Paleo–marine sediment record of the last 8 million years (Sites 657-661). In Ruddiman, W., Sarnthein, M., et al. (Eds) Proc. ODP, Sci. Results, 108: 241–277. College Station, TX (Ocean Drilling Program).

Tomczak, M., Godefrrey, J.S., 1994. Regional Oceanography: an introduction, Pergamon, 422 pp.

Traverse, A., Ginsburg R.N., 1966. Palynology of the surface sediments of Great Bahama Bank, as related to water movement and sedimentation. Marine Geology, 4: 417–459.

Tyson, R.V., 1996. Sequence-stratigraphical interpretation of organic facies variations in marine siliciclastic systems; general principles and application to the onshore Kimmeridge Clay Formation, UK. In: Hesselbo S.P., Parkinson D.N. (Eds.), Sequence Stratigraphy in British Geology. Geological Society Special Publication, 103: 75–96.

van der Zwan, C.J., 1990. Palynostratigraphy and palynofacies reconstruction of the Upper Jurrassic to lowermost Cretaceous of the Draugen Field, offshore mid Norway. Review of Palaeobotany and Palynology, 62: 157–86.

Verleye, T., Louwye, S., 2010. Organic-walled dinocysts in the southeast Pacific (25–53°S) and their relation to the prevailing hydrographical conditions. Palaeogeography, Palaeoclimatology, Palaeoecology, 298 (3–4): 319–340, doi:10.1016/j.palaeo.2010.10.006.

Versteegh, G.J.M. 1995. Palaeoenvironmental changes in the Mediterranean and North Atlantic in relation to the onset of Northern Hemisphere Glaciations (2.5 Ma B. P.) University of Utrecht, 134 pp.

Versteegh, G.J.M., Zonneveld, K.A.E., 1994. Determination of palaeoecological preferences of dinocysts by applying detrended and canonical correspondence analysis to Late Pliocene dinocysts assemblages of the south Italian Singa section. Review of Palaeobotany and Palynology, 84: 181–199.

Versteegh, G.J.M., 1997. The onset of major Northern Hemisphere Glaciations and their impact on dinocysts and acritarchs from the Singa section, Calabria (southern Italy) and DSDP Holes 607/607A (North Atlantic). Marine Micropaleontology, 30: 319–343.

Versteegh, G.J.M., Zevenboom, D., 1995. New genera and species of dinoflaagellate cysts from the Mediterranean Neogene. Rev. Palaeobot. Palynol., 85: 213–229.

von der Heydt, A., Dijkstra, H.A., 2008. The effect of gateways on ocean circulation patterns in the Cenozoic, Global Planet Change, 62: 132–146.

Walker, N.D., 1996. Satellite assessment of Mississippi River plume variability: causes and predictability. Remote Sensing of Environment 58 (1): 21–35.

Wall D., Dale B., Lohman G.P., Smith W.K., 1977. The environmental and climatic distribution of dinocysts in modern marine sediments from regions in the North and South Atlantic oceans and adjacent seas, Marine Micropaleontology, 2: 121-200.

Wall, D., 1962. Evidence from Recent plankton regarding the biological affinities of Tasmanites Newton 1875 and Leiosphaeridea–Eisenack 1958. Geol. Mag., 99: 353–363.

Wall, D., 1965. Modern Hystrichosphaeres and dinocysts from the Woods Hole region. Grana Palynol., 6: 297–314.

Wall, D., Dale, B., 1967. The resting cysts of modern marine dinocysts and their paleontological significance. Rev.Palaeobot. Palynol. 2: 349–354.

Wang, C., Enfield, D.B., 2001. The tropical Western Hemisphere warm pool. Geophysical Research Letters, 28: 1635–1638.

Wang, C., Lee, S., 2007. Atlantic warm pool, Caribbean low–level jet, and their potential impact on Atlantic hurricanes. Geophysical Research Letters, 34: 1–5.

Wara, M.W., Ravelo, A.C., Delaney, M.L., 2005. Permanent El Niño-like conditions during the Pliocene warm period, Science, 309: 758–761.

Warny, S.A., Wrenn, J.H., 1997. New species of dinocysts from the Bou Regreg Core: a Miocene-Pliocene boundary section on the Atlantic Coast of Morocco. Review of Palaeobotany and Palynology, 96:281–304.

Warny, S.A, Bart, P.J., Suc, J.P., 2003. Timing and progression of climatic, tectonic and glacioeustatic influences on the Messinian Salinity Crisis. Palaeogeography Palaeoclimatology Palaeoecology, 202 (1–2): 59–66.

Warny, S.A., Wrenn, J.H., 2002. Upper Neogene dinocysts ecostratigraphy of the Atlantic coast of Morocco. Micropaleontology, 48: 257–272.

Webb, S.D., 1976. Mammalian faunal dynamics of the Great American Interchange. Paleobiology, 2: 216–234.

Webb, S.D., 1997. The great American faunal interchange. In: Coates, A.G. (ed). Central America: A natural and cultural history, New Haven, Connecticut, Yale Univ, 97–122.

Weiler H., 1985. Die Grünalge Pediastrum Meyen in tertiären Sedimenten Südwestdeutschlands. Meinzer geowissenschaftliche Mitteilungen, 14: 307–343.

Weyl, P.K., 1968. The Role of the Oceans in Climatic Change: A Theory of the Ice Ages. Meteorological Monographs, 8: 37–62.

Williams, D.B., 1971. The distribution of marine dinocysts in relation to physical and chemical conditions. In: Funnell, B.M., Riedel, W.R. (Eds.), the Micropalaeontology of Oceans. Cambridge University Press, Cambridge, 91–95 pp.

Williams, G.L., Brideaux, W.W., 1975. Palynologic analyses of Upper Mesozoic and Cenozoic rocks of the Grand Banks, Atlantic Continental Margin. Geol. Surv. Canada Bull., 236: 1–163.

Williams, G.L., 1978. Palynologicalb iostratigraphy, Deep Sea Drill-ing Project, Site 367 and 370, p. 783–815. In Y. Lancelot, E. Seibold, et al., Initial Reports of the Deep Sea Drilling Project, 41, Supplement to volumes 38–41. U.S. Government Printing Office, Washington, D.C.

Williams, G.L., 1975. Dinocysts and spore stratigraphy of the Mesozoic–Cenozoic offshore Canada. Geological Survey of Canada Paper, 30: 107–163.

Williams, G.L., Bujak, J.P., 1977 Cenozoic palynostratigraphy of offshore eastern Canada. American Association of Stratigraphic Palynologists Contributions Series, 5A: 14–47.

Williams, G.L., Brinkhuis, H., Pearce, M.A., Fensome, R.A., Weegink, J.W., 2004. Southern Ocean and global dinocyst events compared: index events for the Late Cretaceous–Neogene. In: Exon, N.F., Kennett, J.P., Malone, M.J. (Eds.), Proceedings of the Ocean Drilling Program, Scientific Results, 189: 1–98 College Station, TX.

Williams, M., Haywood, A.M., Harper, E.M., Johnson, A.L.A., Knowles, T., Leng, M.J., Lunt, D.J., Okamura, B., Taylor, P.D., Zalasiewicz, J. , 2008. Pliocene climate and seasonality in North Atlantic shelf seas. Philosophical Transactions of the Royal Society A, 367: 85–108.

Wrenn, J.H., 1988. Differentiating species of the dinocysts genus Nematosphaeropsis Deflandre & Cookson 1955. Palynology, 12: 129–150.

Wrenn, J.H., Suc, J.P., Leroy, S.A.G., with other contributors, 1999. Comparative regional charts of Pliocene events. In: The Pliocene: Time of change (J.H., Wrenn, J.P., Suc, S.A.G., Leroy, eds.). American Association of Stratigraphic Palynologists Foundation, Dallas, Texas, pp. 13–47.

Wrenn, J.H., Kokinos J.P., 1986. Preliminary comments on Miocene through Pleistocene dinocysts from De Soto Canyon, Gulf of Mexico, p. 169–225. In J.H.Wrenn, S.L.Duffield, and J. A.Stein (eds.), Papers from the First Symposium on Neogene Dinocysts Biostratigraphy. American Association of Stratigraphic Palynologists Contributions Series, 17.

Wright, J.D., Miller, K.G., 1996. Control of North Atlantic Deep Water circulation by the Greenland-Scotland Ridge. Paleoceanography, 11: 157–170.

Wright, J.D., Miller, K.G., Fairbanks, R.G., 1992. Early and Middle Miocene stable isotopes: implications for deepwater circulation and climate. Palaeoceanography, 7(3): 357–389.

Wüst, G., 1964. Stratification and Circulation in the Antillean-Caribbean Basins, Part 1: Spreading and Mixing of the Water Types With an Oceanographic Atlas, Columbia Univ. Press, New York, 201 pp.

Zachos, J.C., Dickens, G.R., Zeebe, R.E., 2008. An Early Cenozoic perspective on greenhouse warming and carbon-cycle dynamics, Nature, 451: 279–283.

Zahn, R., Mix, A.C., 1987. Benthic foraminiferal $\delta^{18}O$ in the ocean's temperature salinity-density field: Constraints on ice age thermohaline circulation. Paleoceanography, 6: 1–20.δ

Zaporozhets N.I., SineĺNikova V.N, Akhmeťev M.A., 2006. Organic-walled phytoplankton from Paleogene sections of Kamchatka, Stratigraphy and Geological correlation, 14: 668–689.

Zevenboom, D., 1995. Dinocysts from the Mediterranean Late Oligocene and Miocene. CIP-Gegevens Koninklijke Bibliotheek, Den Haag, Published Ph.D. thesis, Biology Faculty, State University of Utrecht, Netherlands, 221 pp.

Zhang, Z., Nisancioglu K.H., Flatøy F., Bentsen M., Bethke I., Wang H., 2011. Tropical seaways played a more important role than high latitude seaways in Cenozoic cooling. Clim. Past, 7: 801–81.

Zonneveld, K.A.F., Hoek, R., Brinkhuis, H., Willems, H., 2001a. Lateral distribution of organic walled dinocysts in surface sediments of the Benguela upwelling Region. Prog. Oceanogr., 48: 25–72.

Zonneveld, K.A.F., Marret, F., Versteegh, G.J.M., Bonnet, S., Bouimetarhan, I., Crouch, E., de Vernal, A., Elshanawany, R., Edwards, L., Esper, O., Forke, S., Grøsfjeld, K., Henry, M., Holzwarth, U., Kielt, J.-F., Kim, S.-Y., Ladouceur, S., Ledu, D., Chen, L., Limoges, A., Londeix, L., Lu, S.H., Mahmoud, M.S., Marino, G., Matsuoka, K., Matthiessen, J., Mildenhal, D.C., Mudie, P., Neil, H.L., Pospelova, V., Qi, Y., Radi, T., Richerol, T., Rochon, A., Sangiorgi, F., Solignac, S., Turon, J.-L., Verleye, T., Wang, Y., Wang, Z., Young, M., 2013. Atlas of modern dinocyst distribution based on 2405 datapoints. Review of Palaeobotany and Palynology, 191: 1–197.

Zonneveld, K.A.F., Versteegh, G.J.M., de Lange, G.J., 1997. Preservation of organic-walled dinocysts in different oxygen regimes: a 10,000 year natural experiment. Marine Micropaleontol., 29: 393–405.

Zonneveld, K.A.F., Versteegh, G.J.M., De Lange, G.J., 2001b. Palaeoproductivity and post-depositional aerobic organic matter decay reflected by dinocysts assemblages of the Eastern Mediterranean S1 sapropel. Mar. Geol., 172: 181–195.

Zonneveld, K.A.F., Versteegh, G.J.M., Kasten, S., Eglinton, T.I., Emeis, K.C., Huguet, C., Koch, B.P., de Lange, G.J., de Leeuw, J.W., Middelburg, J. J., Mollenhauer, G., Prahl, F., Rethemeyer, J., Wakeham, S., 2010. Selective preservation of organic matter in marine environments; processes and impact on the fossil record. Biogeosciences, 7: 1–29.

## APPENDICES

### Appendix 1. List of recorded dinocyst taxa from ODP Site 1000

*Achomosphaera/Spiniferites* spp.

*Achomosphaera* cf. *ramulifera* Deflandre, 1937

*Amiculosphaera umbraculum* Harland, 1979

*Ataxiodinium choane* Reid, 1974

cf. *Ataxiodinium*? sp.

*Batiacasphaera* cf. *hirsuta* Stover, 1977

*Batiacasphaera* spp. total

cf. *Blysmatodinium* sp. McMinn, 1992

*Brigantedinium*? spp. indet.

Calcareous dinocysts

cf. *Corrudinium harlandii* Matsuoka, 1983

*Cyclopsiella elliptica/granosa* Drugg and Loeblich Jr., 1967

*Cymatiosphaera* sp. cf. *C. latisepta* De Schepper and Head, 2008

*Dapsidinium pseudocolligerum* (Stover, 1977) Bujak et al., 1980

Dinocyst sp. A

Dinocyst sp. B

*Edwardsiella sexispinosa*Versteegh and Zevenboom (1995)

*Habibacysta tectata* Head et al., 1989

cf. *Homotryblium*? sp.

*Hystrichokolpoma rigaudiae* Deflandre and Cookson, 1955

*Impagidinium aculeatum* (Wall, 1967) Lentin and Williams, 1981

*Impagidinium paradoxum* (Wall, 1967) Stover and Evitt, 1978

*Impagidinium patulum* (Wall, 1967) Stover and Evitt, 1978

*Impagidinium plicatum* Versteegh and Zevenboom in Versteegh, 1995

*Impagidinium strialatum* (Wall, 1967) Stover and Evitt, 1978

*Impagidinium* sp. A

*Impagidinium* sp. B

*Impagidinium velorum* Bujak, 1984

*Lejeunecysta* spp. total

*Lingulodinium machaerophorum* (Deflandre and Cookson, 1955) Wall, 1967

*Nannobarbophora walldalei* Head, 1996

*Nematosphaeropsis labyrinthus* (Ostenfeld, 1903) Reid, 1974

*Nematosphaeropsis* cf. *rigida* Wrenn, 1988

*Operculodinium bahamense* Head and Westphal, 1999

*Operculodinium centrocarpum–israelianum*

*Operculodinium janduchenei* Head et al., 1989

*Operculodinium lomgispinigerum* Matsuoka, 1983

*Operculodinium* sp. A

*Operculodinium* sp. B

*Paralecaniella indentata* Cookson and Eisenack, 1970

*Polysphaeridium zoharyi* (Rossignol, 1962) Bujak et al., 1980

Cyst of *Pentapharsodinium dalei* Indelicato & Loeblich III, 1986

*Pyxidinopsis reticulata* McMinn and Sun Xuekun, 1994

*Pyxidinopsis* sp.

*Selenopemphix nephroides* Benedek, 1972 emend. Bujak in Bujak et al., 1980

*Selenopemphix quanta* Bradford, 1975

*Selenopemphix* cf. *undulata* Verleye et al., 2011

*Spiniferites* cf. *bentorii* Rossignol, 1964

*Spiniferites mirabilis* Rossignol, 1964

*Spiniferites* cf. *ramosus* Ehrenberg, 1838

*Spiniferites rhizophorus* Head and Westphal, 1999

*Tuberculodinium vancampoae* (Rossignol, 1962) Wall, 1967

## Appendix 2. Taxonomy of new dinocysts and acritarchs

This appendix informally describes nine new species of dinocysts and four new species of acritarch taxa encountered in the present study. Descriptions are based exclusively on light microscope observations.

### Dinocysts

**cf. *Ataxiodinium*? sp.** (Plate 6, Figures 1–3)
**Description:** A small sized species with a spherical to subsphaerical central body; central body wall is solid with a smooth surface; the outer wall is solid with a faintly microgranulate surface and consisted of irregular blisters (1µm). Archeopyle is broken and it looks precingular and there are no clear indications of tabulation.
**Dimensions:** Central body length, 30 µm.
**Remarks:** only one specimen has been found throughout the studied samples in the Upper Miocene. It differs from *Ataxadinium* by not having a loose outer layer and funnel-shaped invaginations.

***Batiacasphaera* cf. *hirsuta*** (Plate 6, Figures 4–6)
Gonyaulacacean, proximate cysts, subspheroidal. Acavate, surface atabular, smooth or with low ornamentation including fine, short, hair-like processes and a surface reticulum. It is difficult to recognize the apical archeopyle.
**Dimensions:** Central body length, 28 µm.

**cf. *Blysmatodinium* sp.** (Plate 6, Figures 7–9)
**Description:** Small cavate cyst composed of an endophragm and periphragm. Periphragm forms into numerous nontabular blisters (2µm). The archeopyle is precingular and has smooth margins.
**Dimensions:** Central body length, 35µm.
**Remarks:** Sparse occurrences of this species have been found in the Upper Miocene and Lower Pliocene. It differs from *Blysmatodinium* by having a precingular archeopyle.

**Dinocyst sp. A** (Plate 6, Figures 10–12)
**Description:** Acavate, small, subspheroidal to subovoidal central body bearing variable an irregular, nontabular reticulation. The archeopyle is apical.
**Dimensions:** Diameter, 15-35µm.
**Remarks:** It is distinguished from *Pyxidinopsis* sp. in having an apical archeopyle.

**Dinocyst sp. B** (Plate 6, Figures 13–15)
**Description:** A small colorless cyst with sphaerical and microgranulate central body. Acavate, with numerous and variable short to long, but delicate processes which might be bifid or finely aculeate tips which hard to see except under high magnification. The archeopyle is precingular.
**Dimensions:** Central body diameter (excluding processes), 22µm.
**Remarks:** It differs from *P. dalei* by having microgranulate central body and structure of finely aculeate process tips.

**cf. *Homotryblium*? sp.** (Plate 6, Figures 16–18).
**Description:** This species has a morphological similarity to genus *Homotryblium* (Davey and Williams in Davey et al., 1966). Processes are short, intratabular and vary in size. Archeopyle is broken and appears epicystal.
**Dimensions:** Central body length 42µm.
**Remarks:** Only one specimen has been found in the Early Pliocene.

***Impagidinium* sp. A** (Plate 7, Figures 1–3)
**Description:** A species with a spherical central body and faintly microgranular surface. Crest height more or less constant over cyst surface. Archeopyle formed by loss of precingular plate 3".
**Dimensions:** Length excluding crest 35 µm.
**Remarks:** It differs from *I. sphaericum* in its smaller size and less spherical central body and not having a pronounced apical protuberance.

***Impagidinium* sp. B** (Plate 7, Figures 4–6)
**Description:** A small to medium sized species with without an apical horn. Surface paratabular, parasutures indicated by ridges or crests (5 µm), commonly and microgranular plate surfaces. The Archeopyle is precingular.
**Dimensions:** Central body length 40µm.
**Remarks:** It differs from *I. plicatum* by having less wrinkled sutures.

***Operculodinium* sp. A** (Plate 7, Figures 7–9)
**Description:** A very large, polyhedral species that are chorate, with subspheroidal to rarely subovoidal and granular central body. Acavate, Processes short, nontabular, solid, with conical bases and finely aculeate tips, usually uniform in size and shape. The spines have conical bases and capitate tips.
**Dimensions:** Central body length 40–44µm (processes length 3 µm).
**Remarks:** It differs from *O. bahamense* in not possessing narrow equatorial girdle, traces of tabulation and shape of processes and differs from *O. israelianum* in not having acuminate processes and its larger size.

***Operculodinium* sp. B** (Plate 7, Figures 10–12)
**Description:** A small and sphaerical cyst with microgranulate wall that has short, sparse, delicate and evexate processes.
**Dimensions:** Central body length 30µm and process length less than 1.0 µm.
**Remarks:** The minute spines, smaller size and thiner cyst wall distinguish this species from *O. israelianum.*

***Pyxidinopsis* sp.** (Plate 7, Figures 13–15)
**Description:** A small sphaerical to subsphaerical cysts with muricate surface. Acavate. Surface atabular, with microreticulate ornamentation.
**Dimensions:** Central body length 30µm.
**Remarks:** It differs from *P. reticulata* by having less microreticulate ornamentation.

**Acritarch sp. A** (Plate 8, Figures 1–3)
**Description:** Small, colorless with spherical central body and numerous solid, delicate and short processes that may be branched or unbanched; both type usually being present onn a single specimen. Processes are often minutely branched at their tips. The central body wall is thin (less than 0.5 µm) and has a microreticulate surface.
**Dimensions:** Central body length 10 µm.
**Remarks:** This species had sporadic occurrences in the Upper Miocene and Pliocene.

**Acritarch sp. B** (Plate 8, Figures 4–6)
**Description:** Subsphaerical central body. Processes nontabular, generally solid and uniform in size and shape. Autophragm wrinkled and microreticulate. The central body is surrounded by approximately thick crest (5 µm).
**Dimensions:** Central body length 10 µm.
**Remarks:** Only one specimen of this species was found in the Upper Miocene.

**Acritarch sp. C** (Plate 8, Figures 7–9)
**Description:** spherical to egg-shaped central body. The central body wall is solid with a faintly microgranulate surface. A loose outer layer is connected to the central body by irregularly distributed funnel-shaped invaginations.
**Dimensions:** Central body length 5 µm.
**Remarks:** It resembles *Ataxidinium* but is smaller.

**Acritarch sp. D** (Plate 8, Figures 10–12)
**Description:** Small spherical to sub spherical central body indicated by ridge or crests (5 µm). Surface paratabular and microgranulate.
**Dimensions:** Central body length 10 µm without crest.
**Remarks:** This was the most abundant undescribed acritarch species found in the present study. Higher numbers are found in the Lower Pliocene. It differs from *I. plicatum* by a significantly smaller size and no showing any evidence of an archeopyle.

**Appendix 3. Plates**

**Plate code:** species name, sample number, England finder, lower focus, middle focus, upper focus, centrral body length.

**Plate 1**

1–3. *Amiculosphaera umbraculum*, 23 (2), U39/1, 59µm.
4–6. *Ataxiodinium choane*, 45 (1), S39/1, 25µm.
7–9. *Brigantedinium*? sp., 13 (2) Y46/1, 25µm.
10–12. *Dapsilidinium pseudocolligerum*, 13 (1), 30µm.
13–15. *Edwardsiella sexispinosa*, 22 (3), P44/1, 30µm.
16–21. *Habibacysta tectata*, 22 (4), J50/1, 10µm.

**Plate 2**

1–3. *Hystrichokolpoma rigaudiae*, 14 (1), R43/4, 45µm.
4–6. *Impagidinium aculeatum*, 18 (2), M60/4, 30 µm.
7–9. *Impagidinium paradoxum*, 21 (2), T34/2, 25 µm.
10–12. *Impagidinium patulum*, 20 (2), G68, 27µm.
13–15. *Impagidinium plicatum*, 24 (1), J46/2, 20µm.
16–18. *Impagidinium strialatum*, 19 (3), N57, 35µm.
19–20. *Impagidinium velorum*, 37 (1), R47/3**,** 30µm.

**Plate 3**

1–3. *Lingulodinium machaeropharum*, 14 (1), L65/4, 25 µm.
4–6. *Nematosphaeropsis labyrinthus*, 15 (4), T38, 32µm.
7–8. *Operculodinium bahamense*, 19 (2), J 50, 52µm.
9–11. *Operculodinium longispinigerum*, 14 (5), T71/4, 15 µm.
12–14. *Pentapharsodinium dalei*, 30 (3), J40/1, 21µm.
15–18. *Polysphaeridium zoharyi*, 13 (1),J59/2, 50µm.
19–22. *Pyxidinopsis reticulata*, 31(1), F44/2, 31µm.

**Plate 4**

1–3. *Selenopemphix nephroides*, 25 (2), S62/2, 35µm.
4–6. *Selenopemphix quanta*, 13 (3), N34/4, 17µm.
7–9. *Spiniferites mirabilis*, 37 (4), N37/2, 25µm.
10–13.*Spiniferites rhizophorus*, 37 (3), M56/2, 28µm.
14–16. *Tuberculodinium vancampoae*, 23 (2), J60/4, 80µm.

**Plate 5**

1–3. *Cyclopsiella elliptica/granosa*, 14 (4), M71/3, 57µm.
4–6. *Cymatiosphaera latisepta*, 13 (2), K33/2, 10µm.
7–9. *Nannobarbophora walldalei*, 24 (5), D55/2, 10µm.
10–12. *Paralecaniella indentata*, 17 (1), B32/1, 38µm.

**Plate 6**

1–3. cf. *Ataxiodinium*? spp. 20 (2), M26/3, 30µm.
4–6. *Baticasphaera* cf. *hirsuta*, 13 (1), N65, 28µm.
7–9. cf. *Blysmatodinium* sp. 18 (4), B25/2, 25µm.
10–12. cf. *Corrudinium harlandii* , 56 (2), R17/2, 20µm.
13–15. Dinocyst sp. A, 48 (1), M 43/3, 30µm.
16–18. Dinocyst sp. B, 24 (3), H10/2,10µm.
19–21. cf. *Homotryblium*? sp., 29 (5), F21/1, 42µm.

**Plate 7**

1–3. *Impagidinium* sp. A, 46 (1), L32/2, 33µm.
4–6. *Impagidinium* sp. B , 53 (2), E32, 25µm.
7–9. *Operculodinium* sp. A, 14 (3), G10/1, 50µm.
10–12. *Operculodinium* sp. B, 21 (1), S 32, 10µm.
13–15. *Pyxidinopsis* sp. A., 56 (4), P28//3, 30µm.

**Plate 8**

1–3. Acritarch sp. A, 47 (1), M21, 5µm.
4–6. Acritarch sp. B, 21 (2), N 40/2, 15µm.
7–9. Acritarch sp. C, 56 (1), O65/4, 5µm.
10–12. Acritarch sp. D, 69 (33), T12/3, 6µm.

**Plate 1**

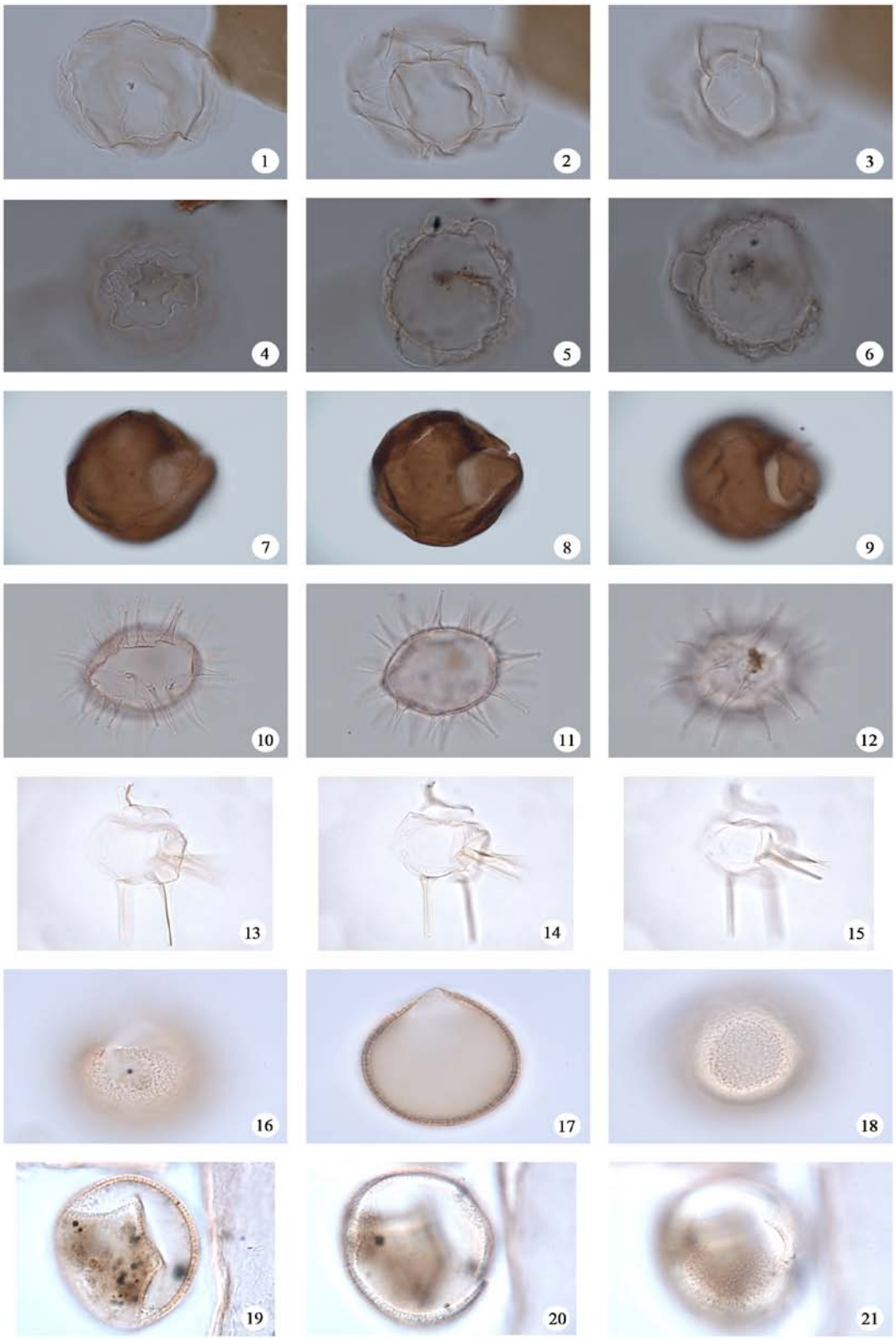

**Plate 2**

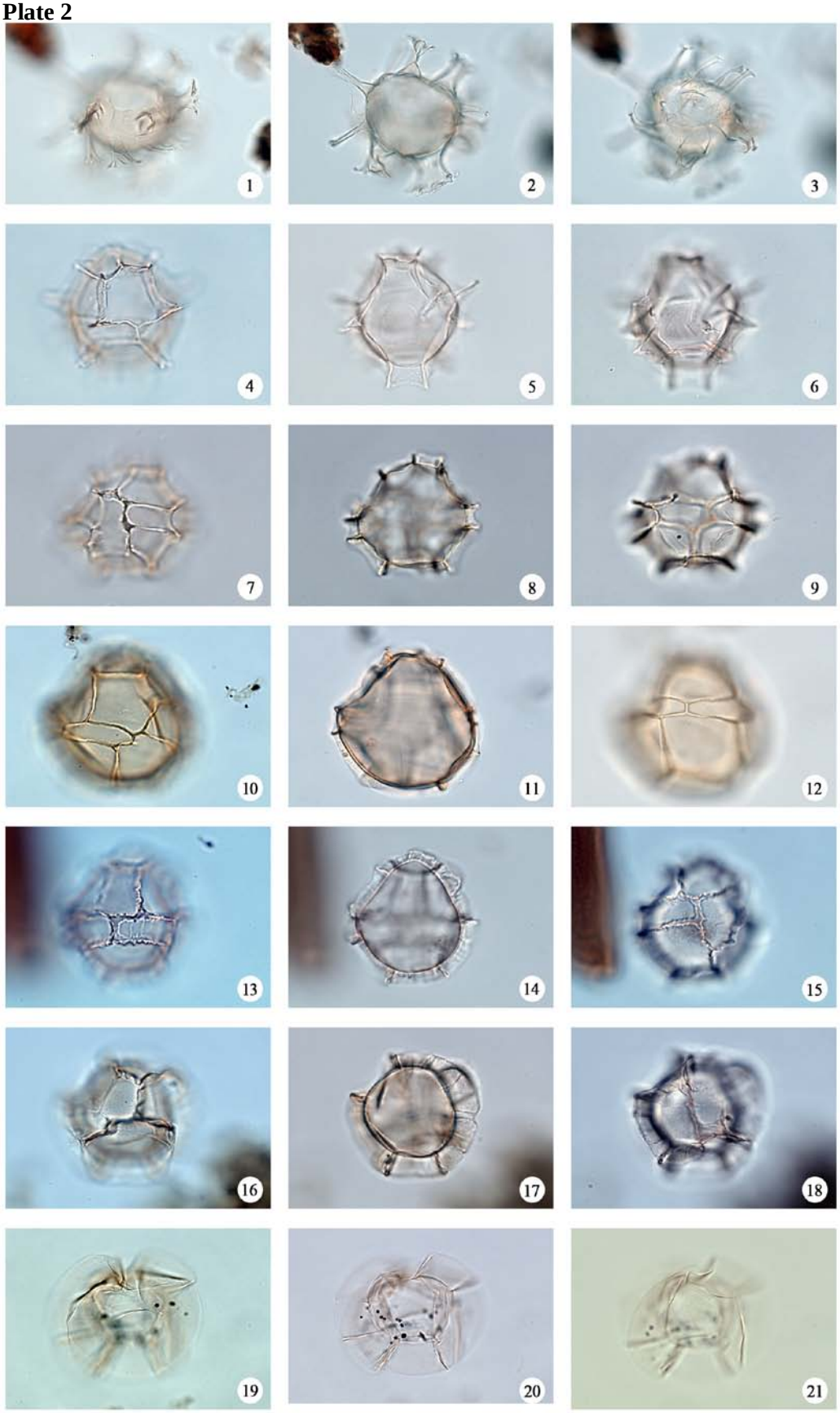

**Plate 3**

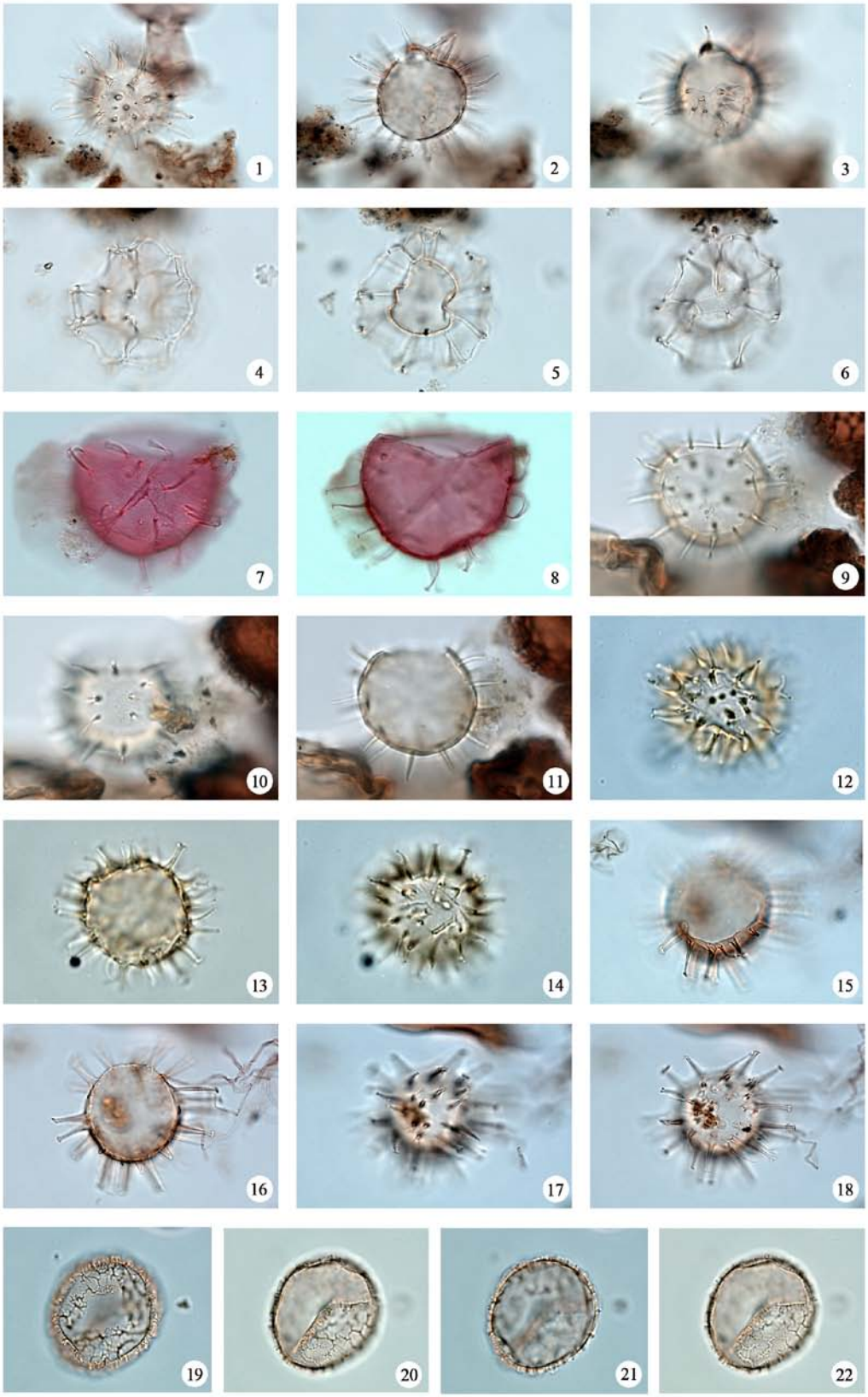

**Plate 4**

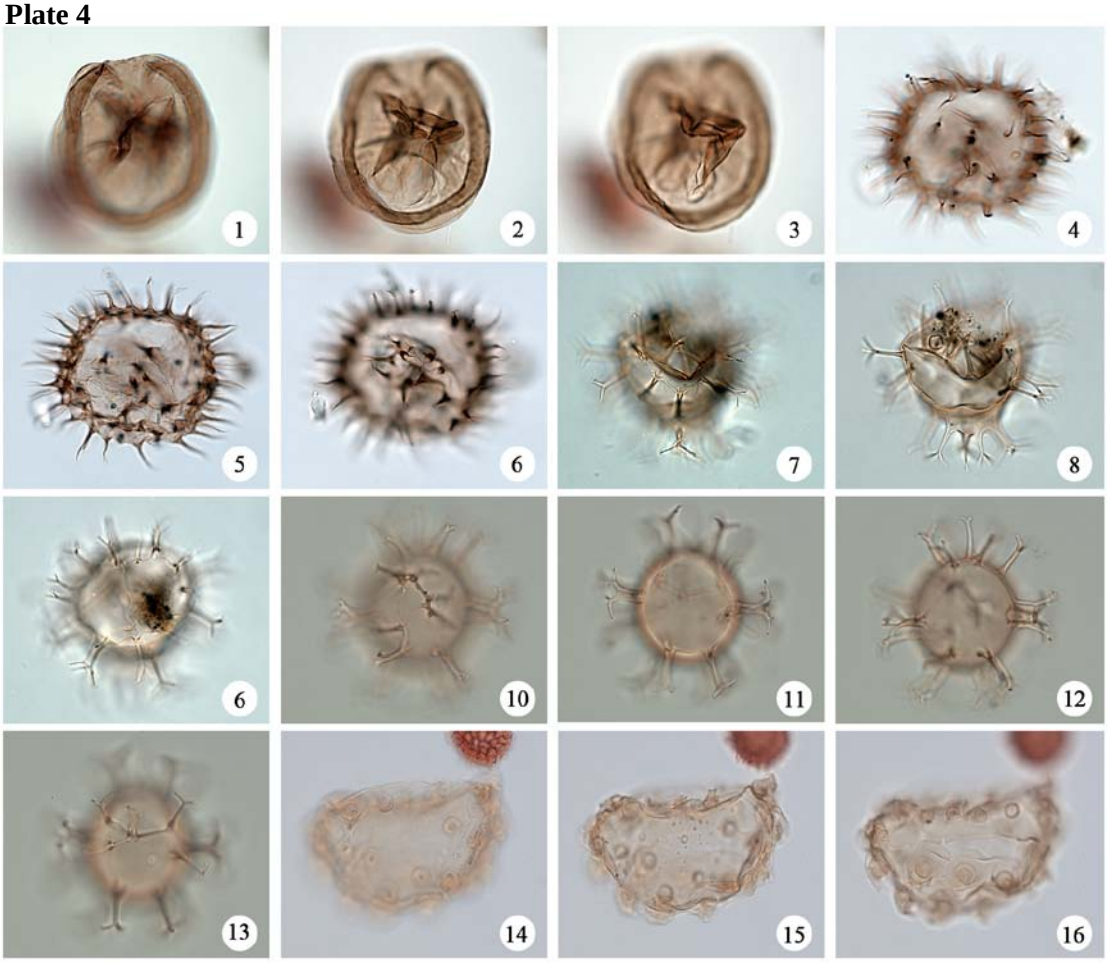

**Plate 5**

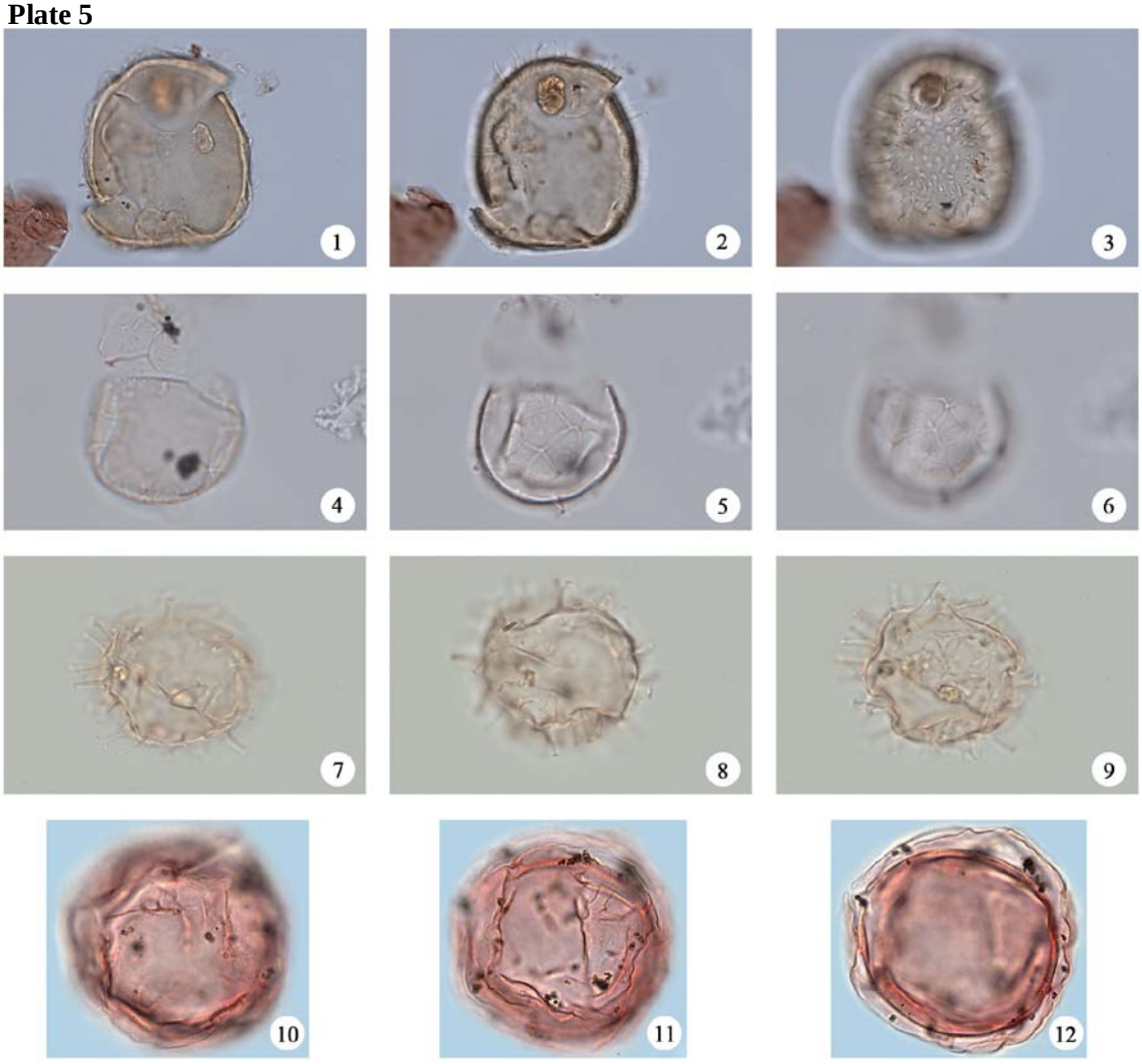

**Plate 6**

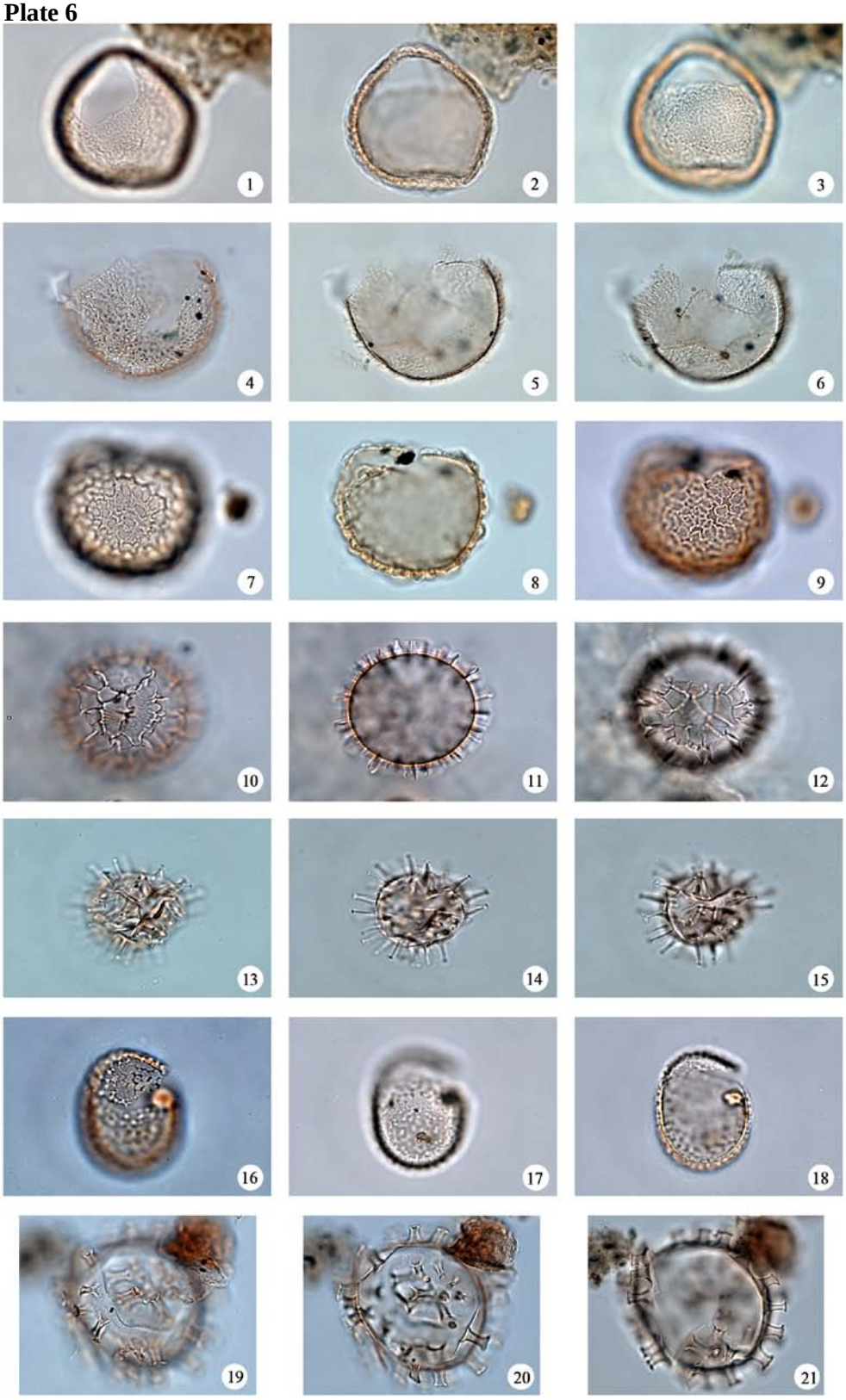

**Plate 7**

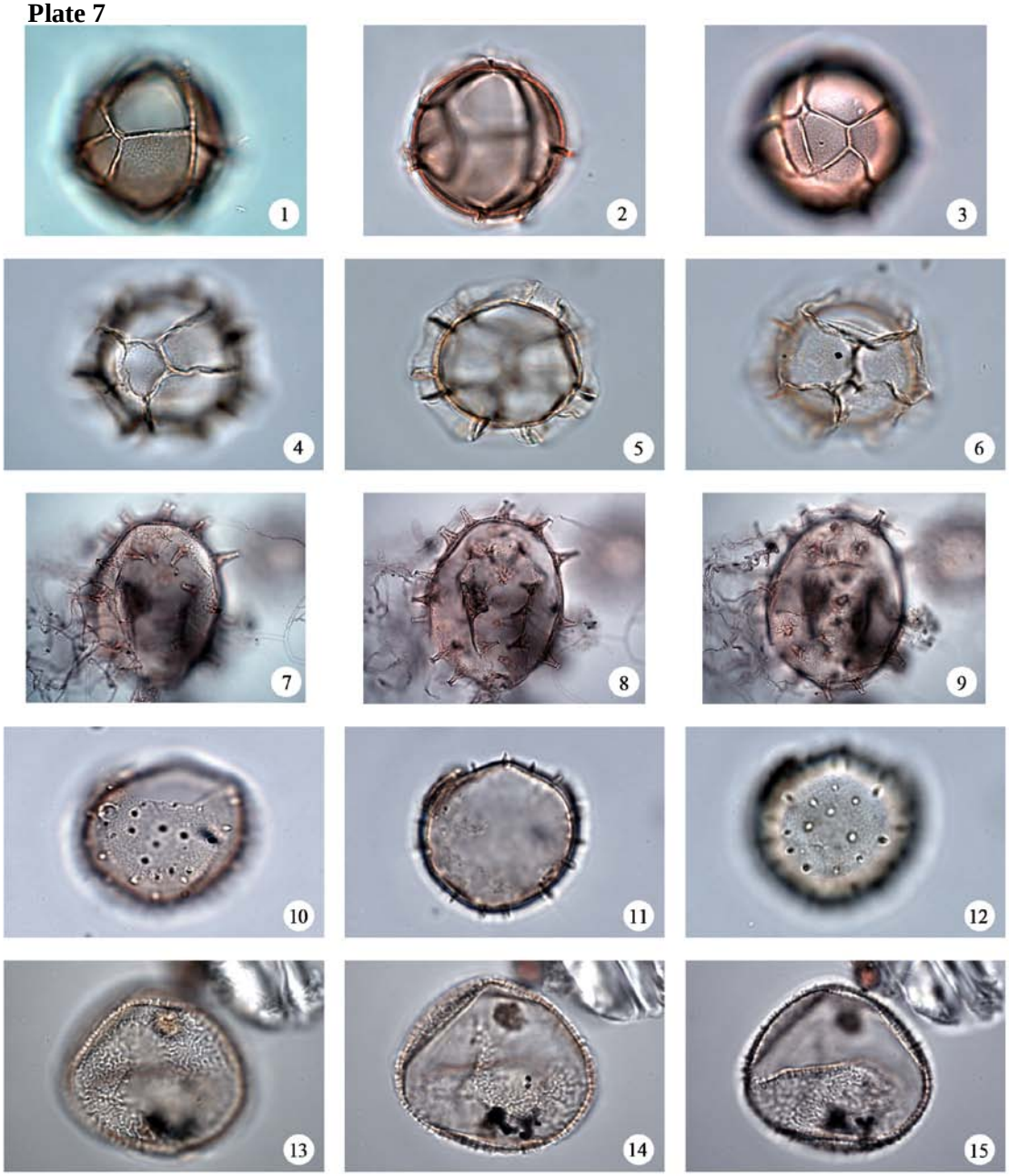

**Plate 8**

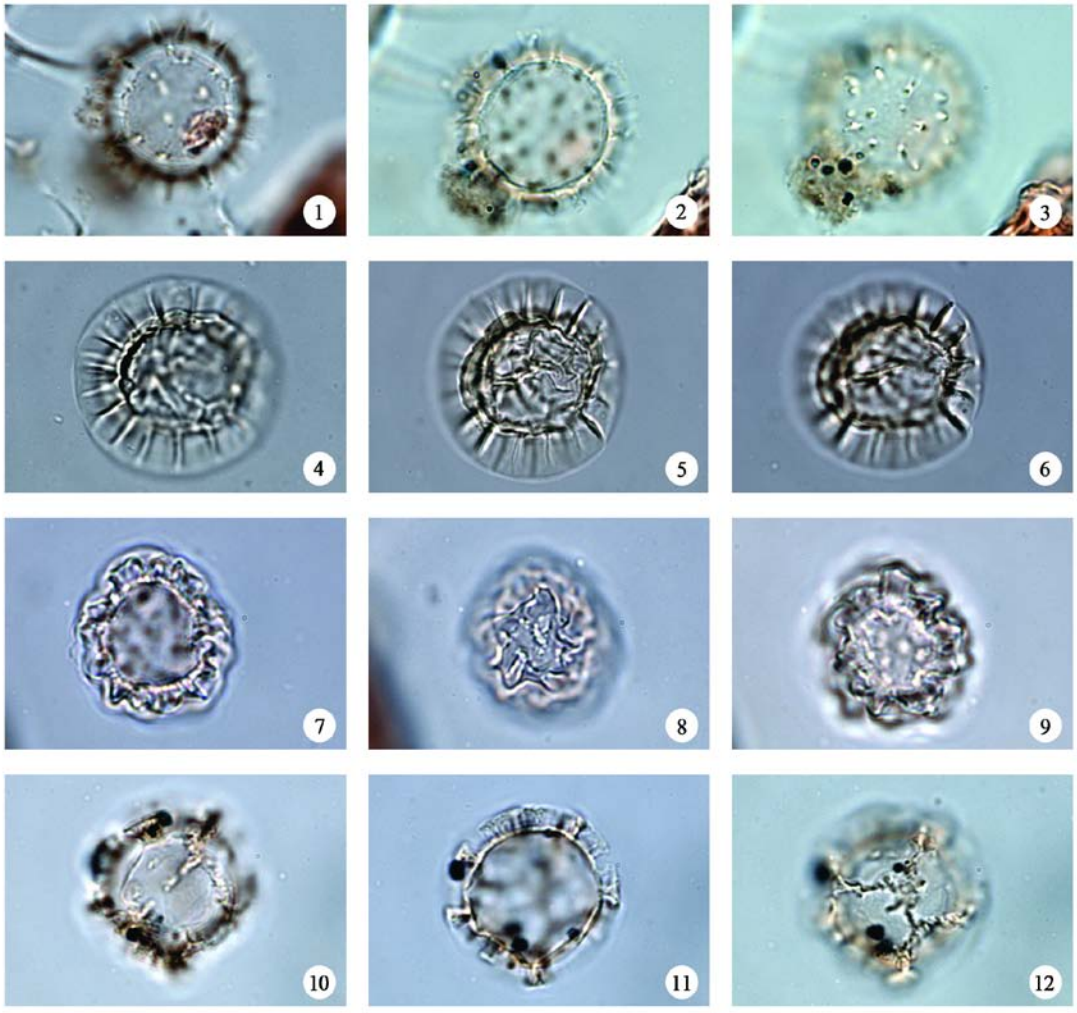

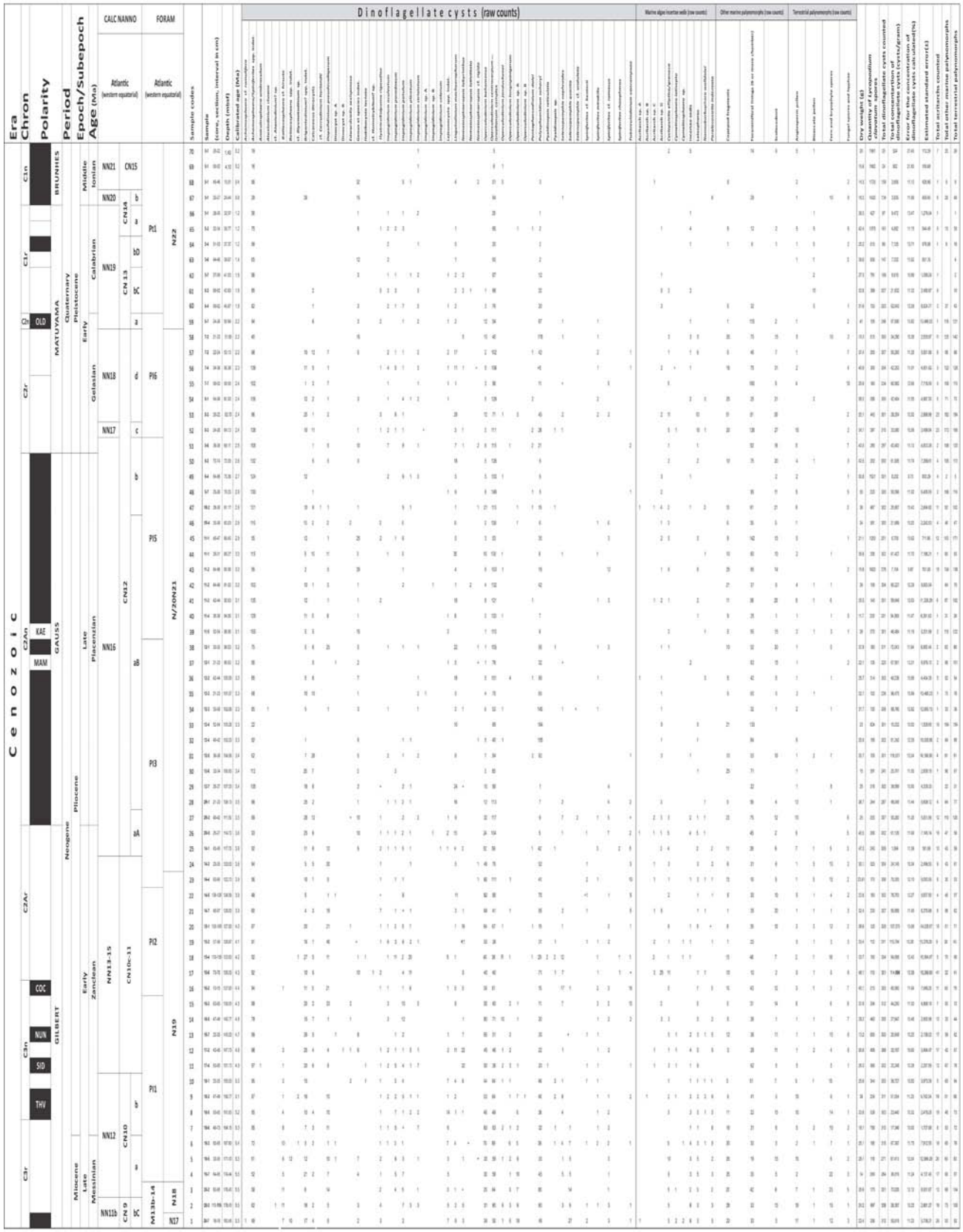

**Table 3.** Stratigraphic distributions of dinocysts, acritarchs and other palynomorphs recorded in the ODP Site 1000 from the latest Miocene–Middle Pleistocene.